Electronic Supplementary Material (ESI) for Inorganic Chemistry Frontiers.

Supporting Information for

Investigation of redox-switchable titanium and zirconium catalysts for the ring-opening polymerization of cyclic esters and epoxides

*Miranda Y. Lowe, Sisheng Shu, Stephanie M. Quan, and Paula L. Diaconescu**

Department of Chemistry and Biochemistry, University of California, Los Angeles, 607 Charles E. Young Drive East, Los Angeles, CA 90095

Table of Contents

Table S1. Control reactions between $^{Ac}FcBAr^{F}$ with L-lactide (LA), ε-caprolactone (CL), and valerolactone (VL).[a]

Entry	Catalyst	Monomer	Time (h)	Temperature (°C)	Conversion (%) [b]	M_n (10^3)	Đ
1	$^{Ac}FcBAr^{F}$	LA	60	100	<5	-	-
2	$^{Ac}FcBAr^{F}$	CL	3	100	80	40	1.19
3	$^{Ac}FcBAr^{F}$	VL	21	100	53	20	1.13
4	N/A	CL	3	100	<1	-	-
5	N/A	VL	20	100	<1	-	-

[a] Conditions: monomer (0.5 mmol), oxidant ($^{Ac}FcBAr^{F}$, 0.005 mmol, 5.5 mg), solvent (4:1 benzene-d_6:1,2-difluorobenzene), hexamethylbenzene (0.025 mmol) as an internal standard.

[b] Conversion was calculated by integration of polymer peaks versus internal standard.

Table S2. Redox switch experiments with (thiolfan*)Ti(O^iPr)$_2$ and L-lactide.[a]

Entry	Monomer	catalyst	Time (h) [b]	Conversion (%) [c]
1	LA	reduced	36	80
		oxidized	4	80

[a] Conditions: monomer (0.5 mmol), catalyst (0.005 mmol), solvent (0.5 mL benzene-d_6), hexamethylbenzene (0.025 mmol) as an internal standard. LA = L-lactide.

[b] Conversion was calculated by integration of polymer peaks versus internal standard.

Table S3. Molecular weight data of one-pot copolymerizations with (thiolfan*)Ti(O^iPr)$_2$ (Ti^{red}) and in situ generated [(thiolfan*)Ti(O^iPr)$_2$][BAr^F] (Ti^{ox}). [a]

Entry[d]	Catalyst	Polymer[c]	Time (h)	Temperature (°C)	Conversion (%) [b]	M_n (10^{-3})	Đ
1a	Ti^{red}	*PLA*	36	100	30	3.7	1.10
1b	Ti^{ox}	PLA-*PCL*	2	100	30 - 10	4.6	1.09
1c	Ti^{red}	PLA-PCL-*PLA*	2	100	30 - 10 - 10	6.1	1.02
2a	Ti^{red}	*PLA*	16	100	78	15.7	1.06
2b	Ti^{ox}	PLA-*PCHO*	2	25	78 - 88	23.1	1.18
3a	Ti^{ox}	*PCHO*	3	25	90	26.2	1.06
3b	Ti^{red}	PCHO-*PLA*	24	100	90 - 87	45.4	1.24

[a] Conditions: monomer (0.15 mmol), oxidant ($^{Ac}FcBAr^F$, 0.005 mmol, 5.5 mg), solvent (4:1 benzene-d_6:1,2-difluorobenzene, 2 mL), hexamethylbenzene (0.05 mmol) as an internal standard.

[b] Conversion was calculated by integration of polymer peaks versus internal standard.

[c] Reaction times and catalyst oxidation states correspond with the italicized polymers for each step in the experiment.

[d] Entry numbers represent separate experiments, whereas the letters represent different oxidation states within the individual experiments.

NMR SPECTROSCOPY

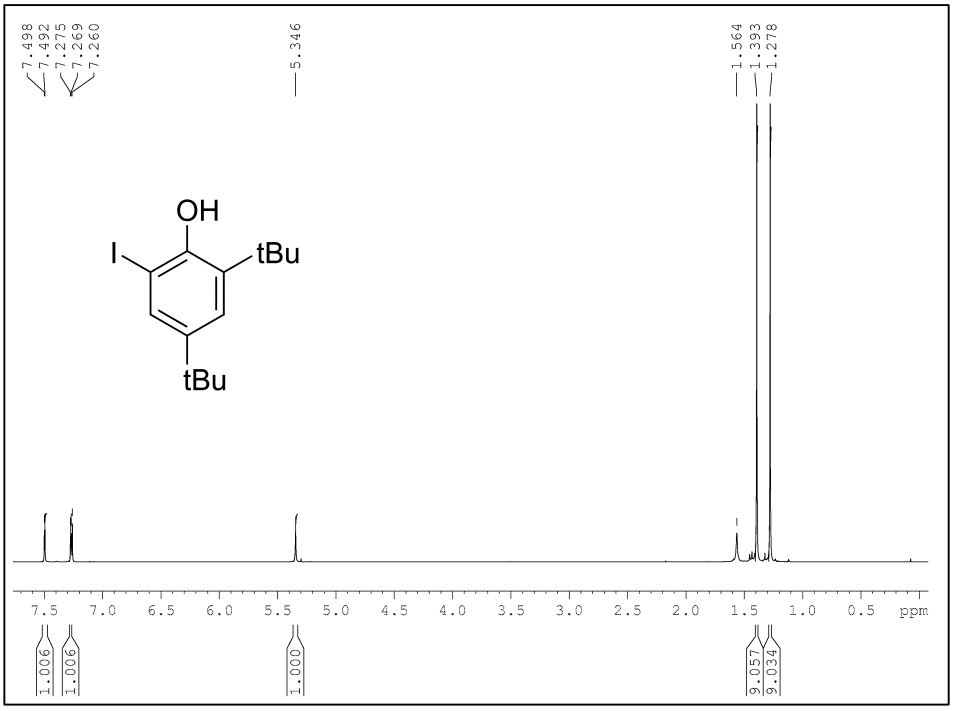

Figure S1. ^{1}H NMR spectrum (300 MHz, $CDCl_3$) of 2,4-di-tert-butyl-6-iodo-phenol, δ (ppm): 1.278 (s, 9H, C(C*H*$_3$)$_3$), 1.393 (s, 9H, C(C*H*$_3$)$_3$), 5.346 (s, 1H, O*H*), 7.260-7.275 (t, 1H, aromatic), 7.492-7.498 (d, 1H, aromatic).

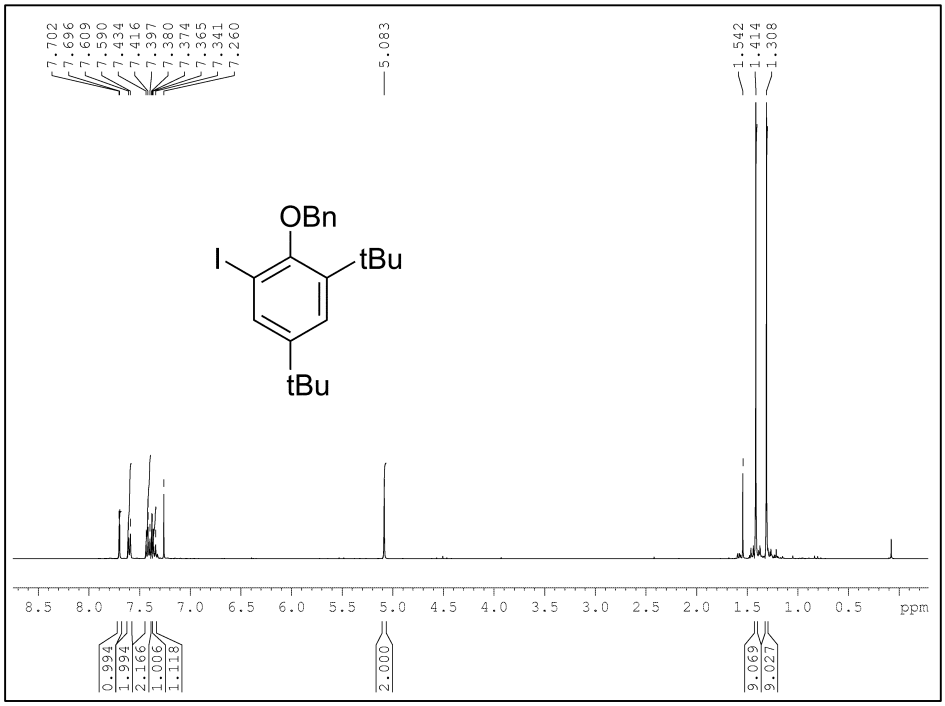

Figure S2. ^{1}H NMR spectrum (300 MHz, $CDCl_3$) of 2,4-di-tert-butyl-6-iodo-phenoxy benzyl ether, δ (ppm): 1.308 (s, 9H, C(C*H*$_3$)$_3$), 1.414 (s, 9H, C(C*H*$_3$)$_3$), 5.083 (s, 2H, OC*H*$_2$Ph), 7.341-7.365 (m, 1H, Ph*H*), 7.374-7.380 (d, 1H, Ph*H*), 7.397-7.434 (t, 2H, Ph*H*), 7.590-7.609 (d, 2H, Ph*H*), 7.696-7.702 (d, 1H, Ph*H*).

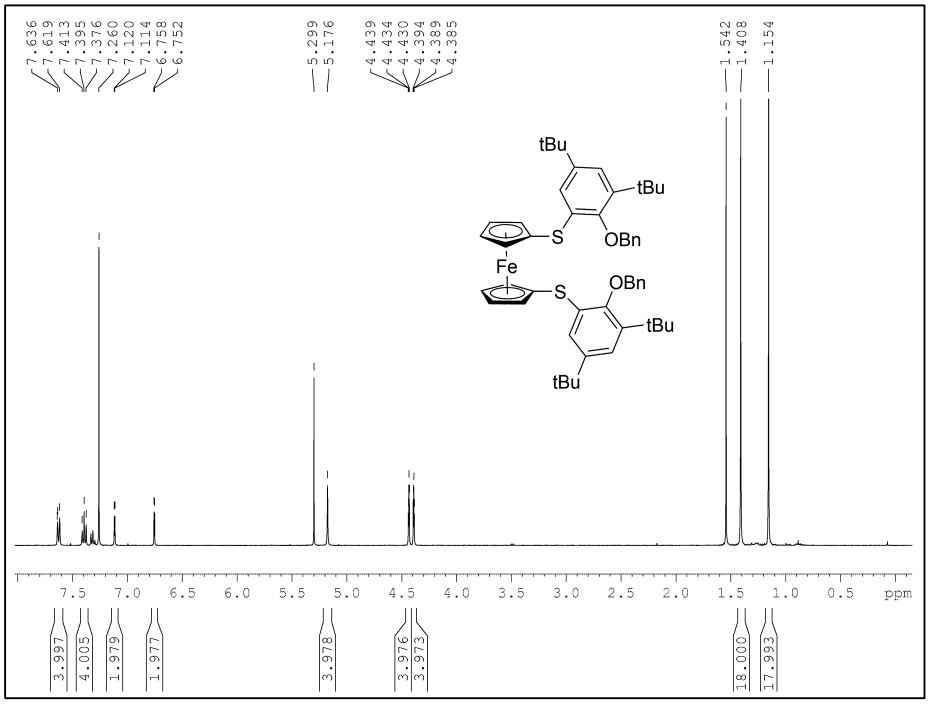

Figure S3. ^{1}H NMR spectrum (300 MHz, $CDCl_3$) of O-benzyl-thiolfan*, δ (ppm): 1.154(s, 18H, $C(CH_3)_3$), 1.408 (s, 18H, $C(CH_3)_3$), 4.385-4.394 (t, 4H, Cp*H*), 4.430-4.439 (t, 4H, Cp*H*), 5.176 (s, 4H, OCH_2), 6.752-6.758 (d, 2H, Ph*H*), 7.114-7.120 (d, 2H, Ph*H*), 7.297-7.334 (t, 2H, Ph*H*), 7.376-7.413 (t, 4H, Ph*H*), 7.619-7.636 (d, 4H, Ph*H*).

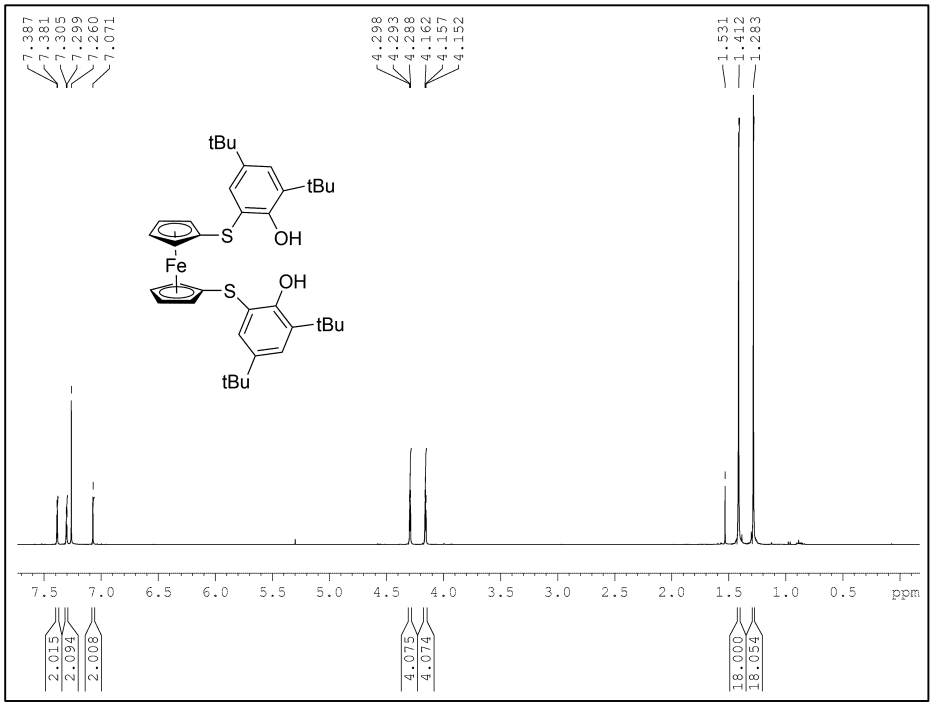

Figure S4. ^{1}H NMR spectrum (300 MHz, $CDCl_3$) of H_2(thiolfan*), δ (ppm): 1.283 (s, 18H, $C(CH_3)_3$), 1.412 (s, 18H, $C(CH_3)_3$), 4.152-4.162 (t, 4H, Cp*H*), 4.288-4.298 (t, 4H, Cp*H*), 7.071 (s, 2H, O*H*), 7.299-7.305 (d, 2H, Ph*H*), 7.381-7.387 (d, 2H, Ph*H*).

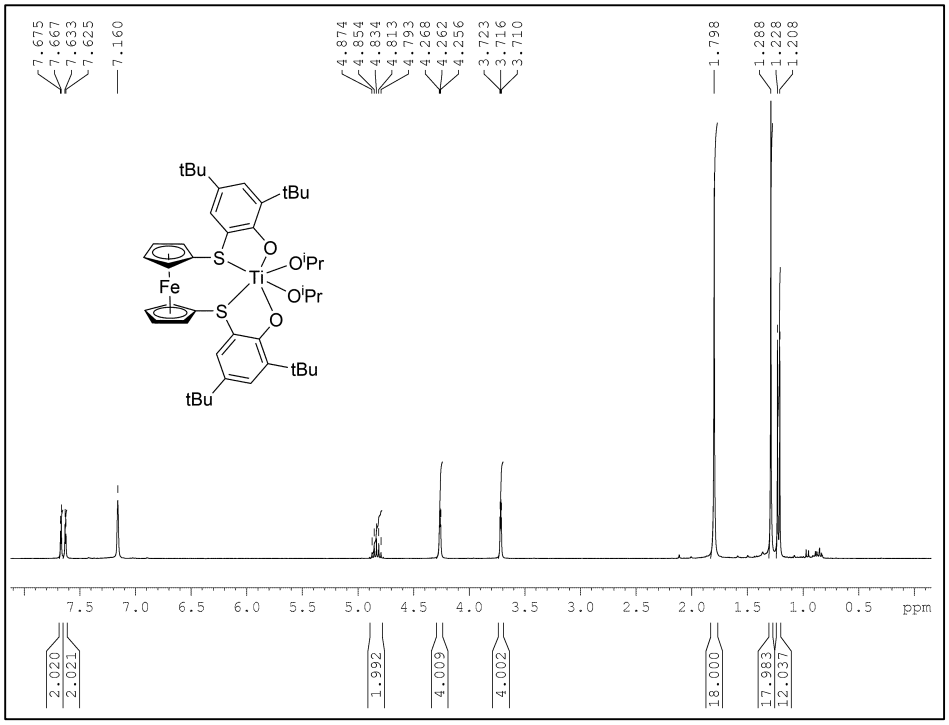

Figure S5. ^{1}H NMR spectrum (300 MHz, C_6D_6) of (thiolfan*)Ti(O^iPr)$_2$, δ (ppm): 1.21-1.23 (d, 12H, (CH_3)$_2$CH)), 1.29 (s, 18H, C(CH_3)$_3$), 1.80 (s, 18H, C(CH_3)$_3$), 3.71-3.72 (t, 4H, Cp*H*), 4.26-4.27 (t, 4H, Cp*H*), 4.79-4.87 (m, 2H, (CH_3)$_2$C*H*)), 7.62-7.63 (d, 2H, Ph*H*), 7.67-7.67 (d, 2H, Ph*H*).

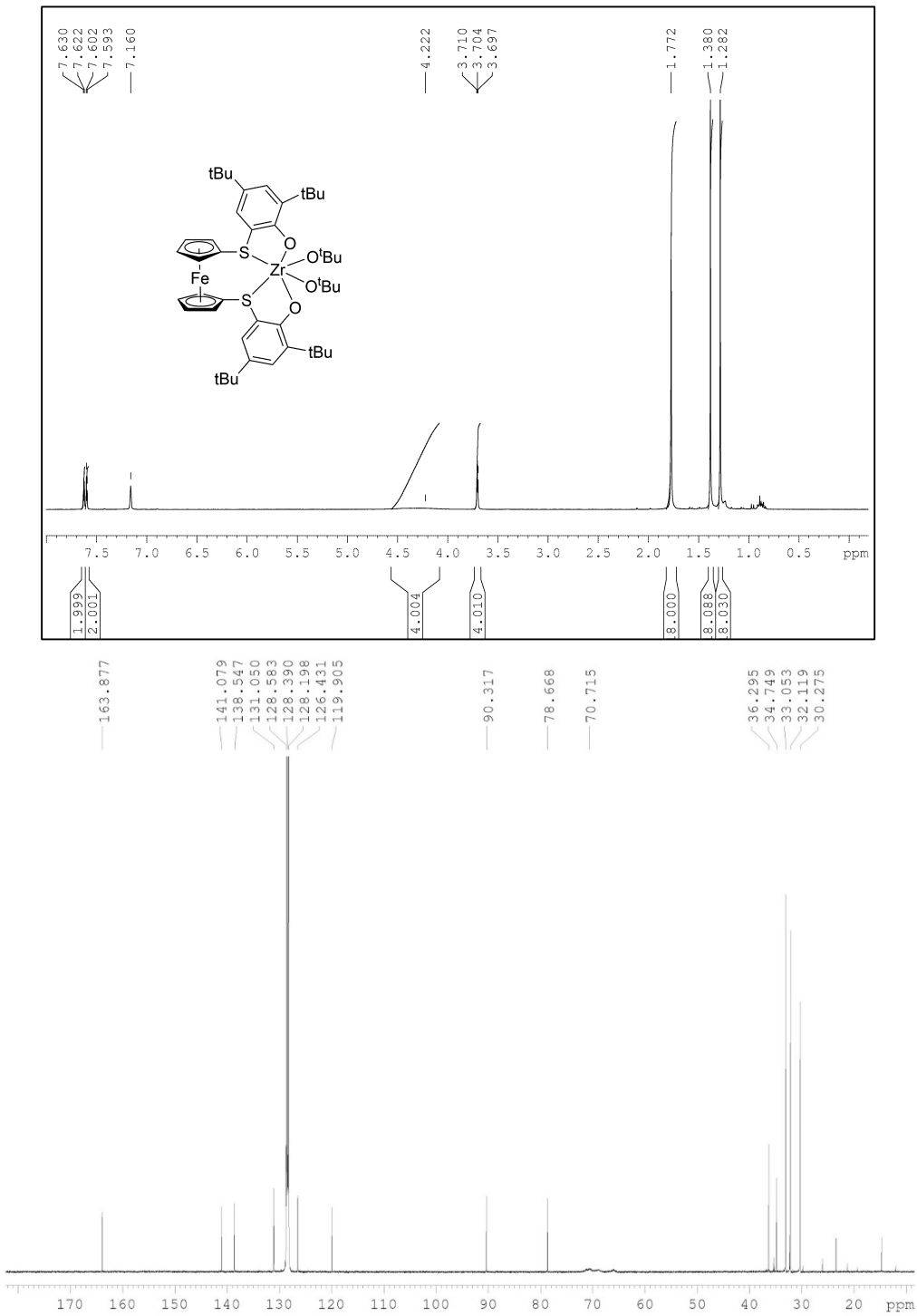

Figure S6. Top: ^{1}H NMR (300 MHz, C_6D_6) spectrum of (thiolfan*)Zr(O^{t}Bu)$_2$, δ (ppm): 1.28 (s, 18H, C(C*H*$_3$)$_3$), 1.38 (s, 18H, C(C*H*$_3$)$_3$), 1.77 (s, 18H, C(C*H*$_3$)$_3$), 3.70-3.71 (t, 4H, Cp*H*), 4.22 (s, 4H, Cp*H*), 7.59-7.60 (d, 2H, Ph*H*), 7.62-7.63 (d, 2H, Ph*H*). Bottom: ^{13}C NMR (125 MHz, 25 ºC, C_6D_6) spectrum of (thiolfan*)Zr(O^{t}Bu)$_2$, δ (ppm): 30.3 (CH(CH$_3$)$_2$), 32.1 (C(CH$_3$)$_3$), 33.1 (C(CH$_3$)$_3$), 34.7 (C(CH$_3$)$_3$), 36.3 (C(CH$_3$)$_3$), 70.7 (OCH(CH$_3$)$_2$), 78.7 (Cp-C), 90.3 (Cp-C), 119.9 (aromatic), 126.4 (aromatic), 131.0 (aromatic), 138.5 (aromatic), 141.1 (aromatic), 163.9 (aromatic).

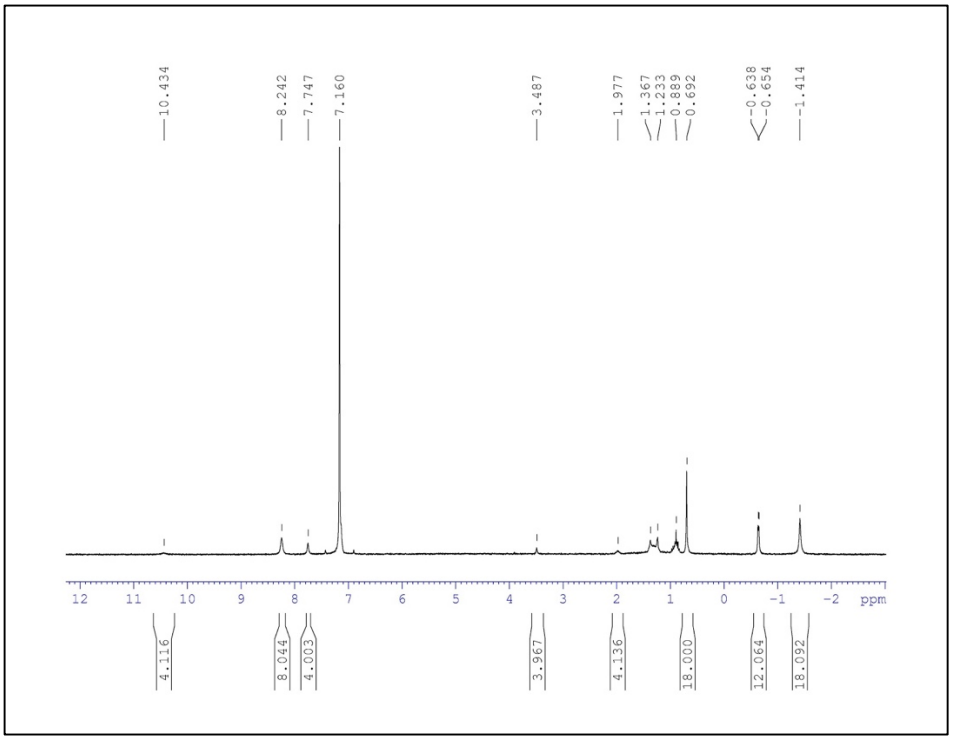

Figure S7. ^{1}H NMR spectrum (300 MHz, C_6D_6) of [(thiolfan*)Ti(O^{i}Pr)$_2$][BAr^{F}], δ (ppm): -1.41 (s, 18H, C(C*H*$_3$)$_3$), -0.65 to -0.64 (d, 12H, (C*H*$_3$)$_2$CH)), 0.69 (s, 18H, C(C*H*$_3$)$_3$), 1.98 (s, 4H, Cp*H*), 3.49 (s, 4H, Cp*H*), 7.75 (s, 4H, B(F$_6$C$_8$H$_2$*H*)$_4$), 8.24 (s, 8H, B(F$_6$C$_8$*H*$_2$H)$_4$), 10.43 (s, 4H, Ph*H*).

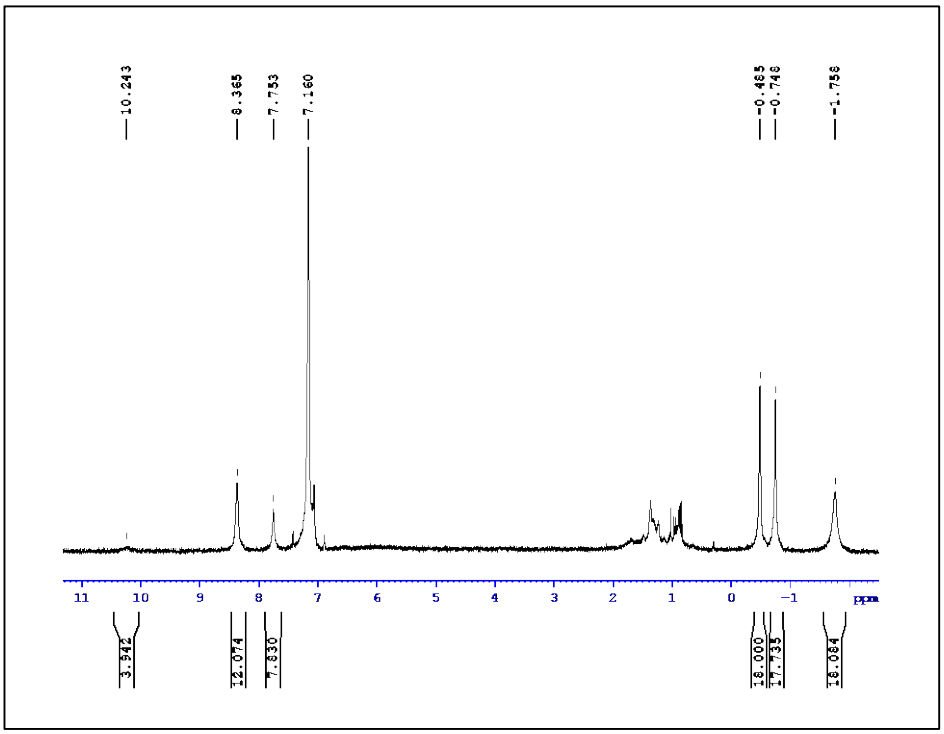

Figure S8. ^{1}H NMR spectrum (300 MHz, C_6D_6) of [(thiolfan*)Zr(O^{t}Bu)$_2$][BAr^{F}], δ (ppm): -1.28 (s, 18H, C(C*H*$_3$)$_3$), -0.75 (s, 18H, C(C*H*$_3$)$_3$), -0.49 (s, 18H, C(C*H*$_3$)$_3$), 7.75 (s, 4H, B(F$_6$C$_8$H$_2$*H*)$_4$), 8.37 (s, 8H, B(F$_6$C$_8$*H*$_2$H)$_4$), 10.24 (s, 4H, Ph*H*), 0.5-1.5 (residual hexanes).

Oxidation and reduction reactions

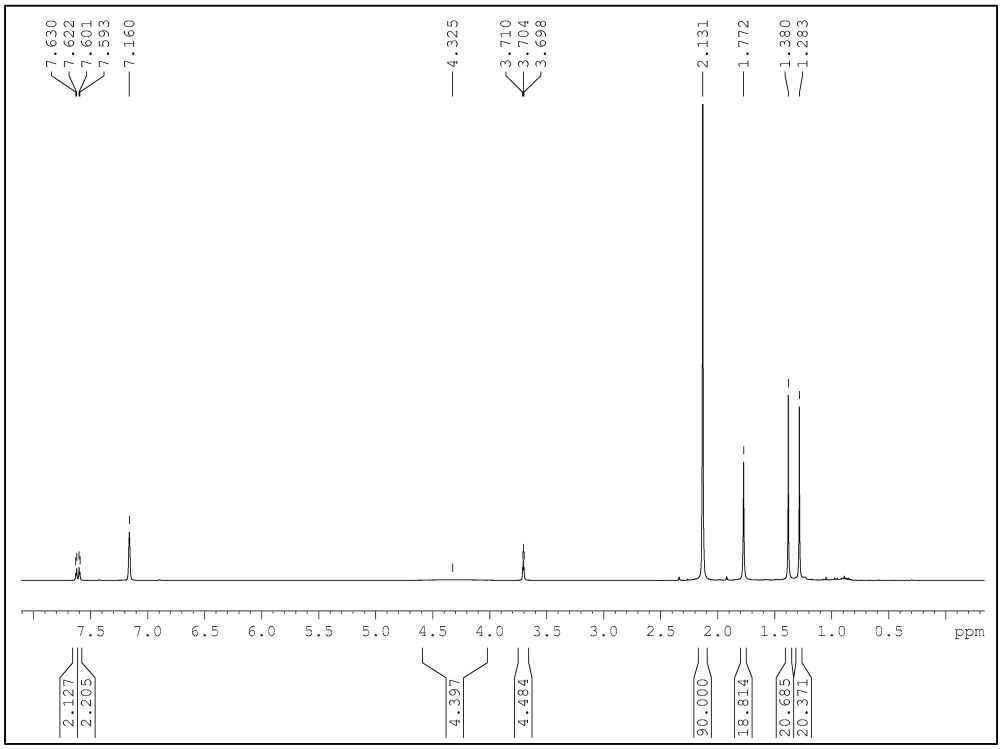

Figure S9. ^{1}H NMR spectrum (300 MHz, C_6D_6) of (thiolfan*)Zr(O^tBu)$_2$ before the addition of ^{Ac}FcBAr^F.

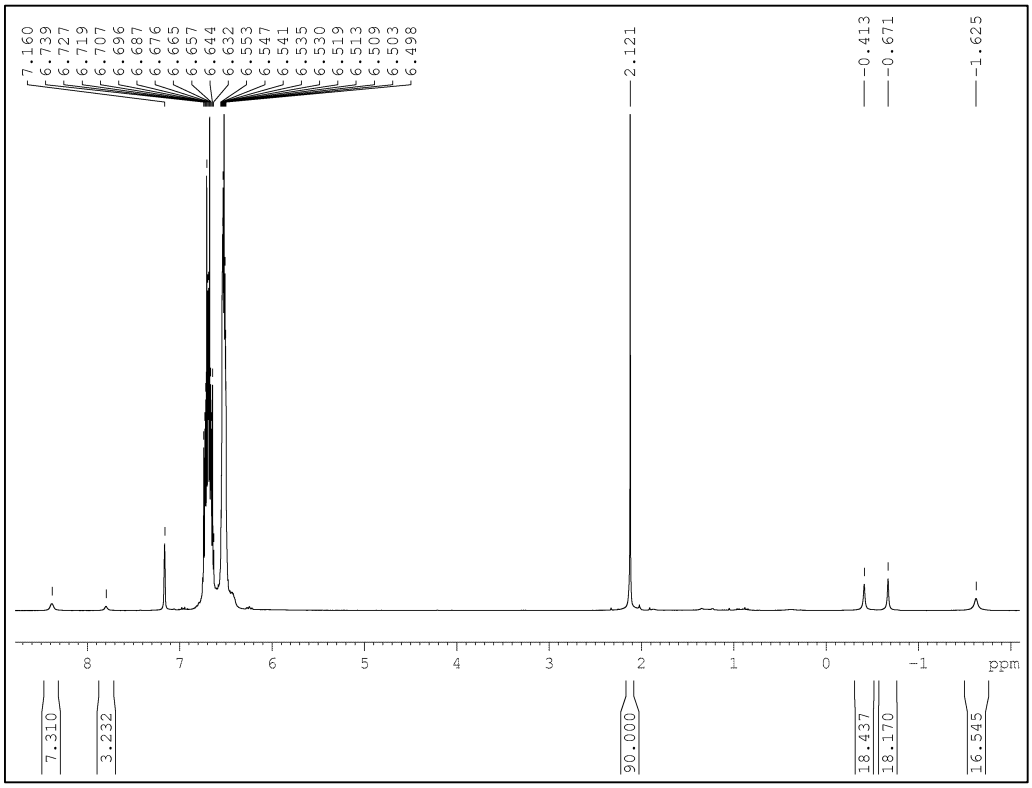

Figure S10. ^{1}H NMR spectrum (300 MHz, C_6D_6) of (thiolfan*)Zr(O^tBu)$_2$ after the addition of ^{Ac}FcBAr^F.

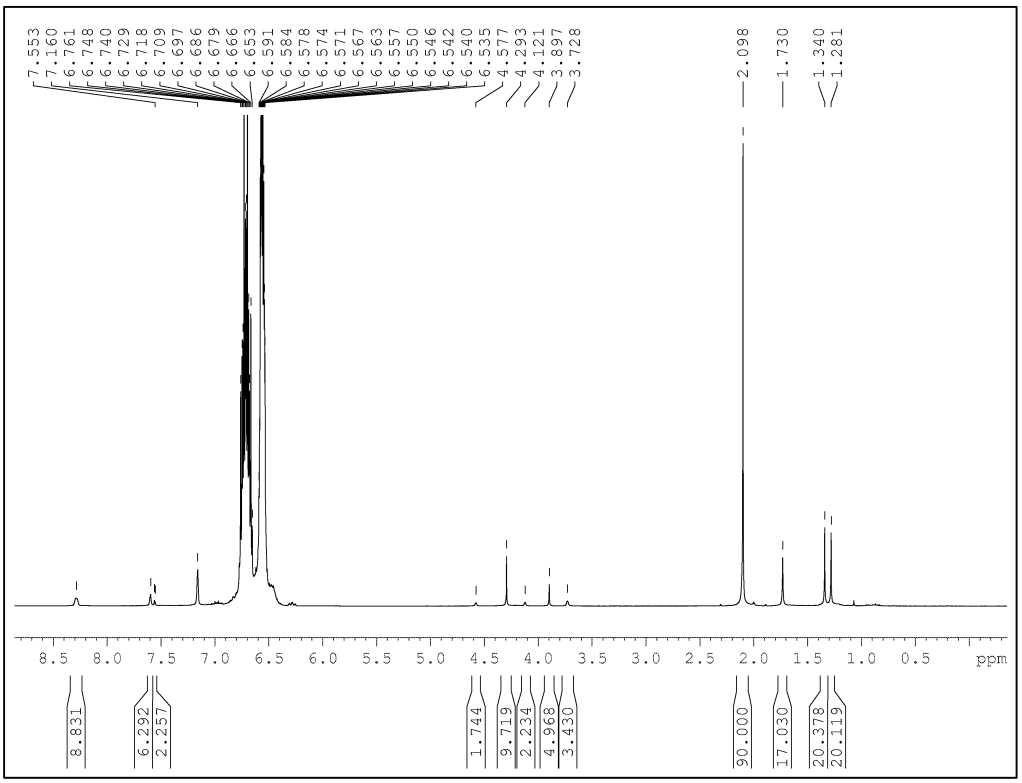

Figure S11. ^{1}H NMR spectrum (300 MHz, C_6D_6) of [(thiolfan*)Zr(O^tBu)$_2$][BAr^F] after the addition of $CoCp_2$.

Stability studies of (thiolfan*)Zr(O^{t}Bu)$_2$

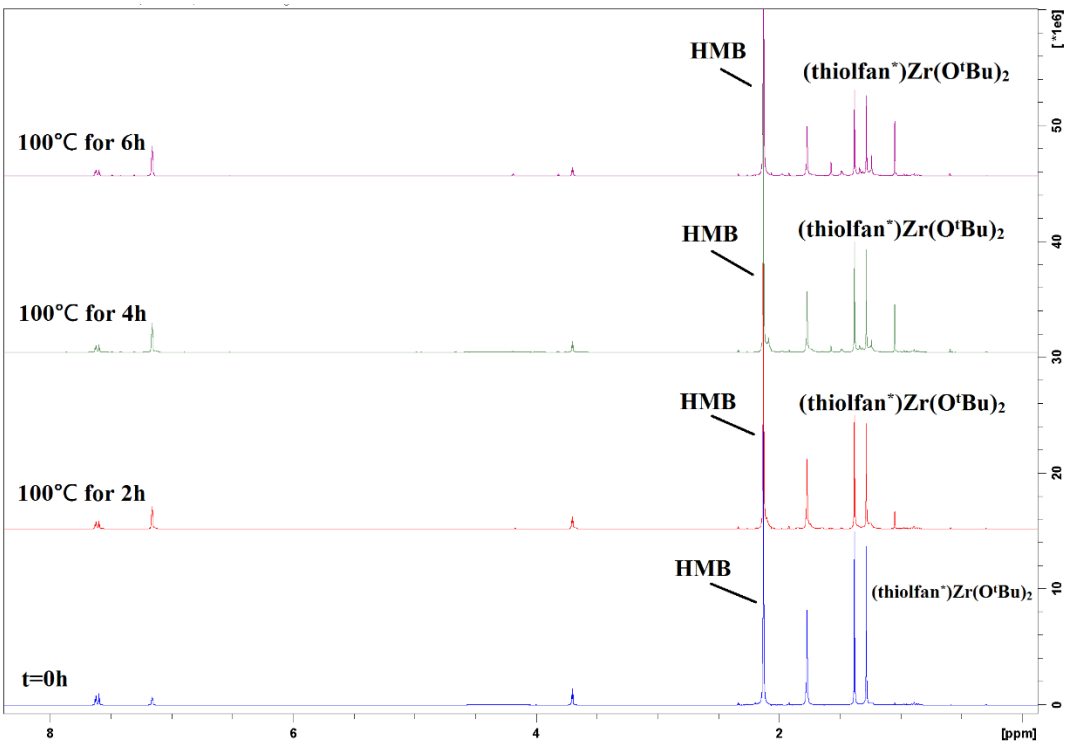

Figure S12. Stacked spectra from the decomposition study of (thiolfan*)Zr(O^{t}Bu)$_2$ at 100 °C in the presence of 5 equiv HMB (hexamethylbenzene) as an internal standard.

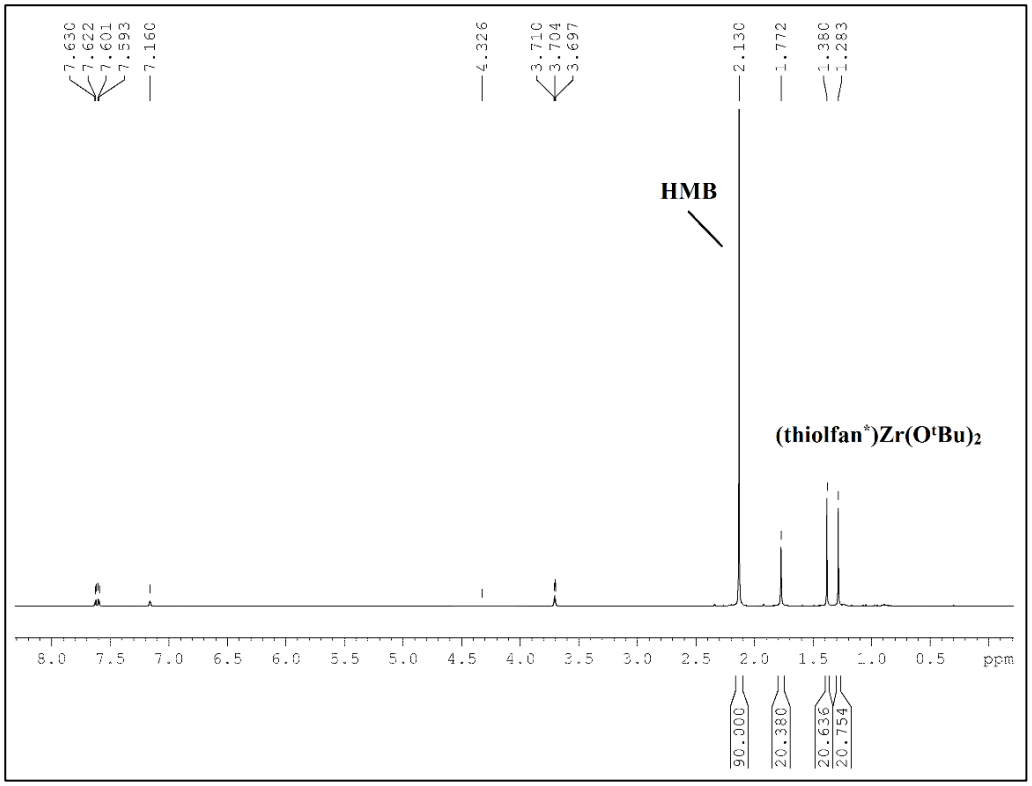

Figure S13. Decomposition study of (thiolfan*)Zr(O^{t}Bu)$_2$ at 100 °C in the presence of 5 equiv HMB (hexamethylbenzene) as an internal standard, t = 0 h.

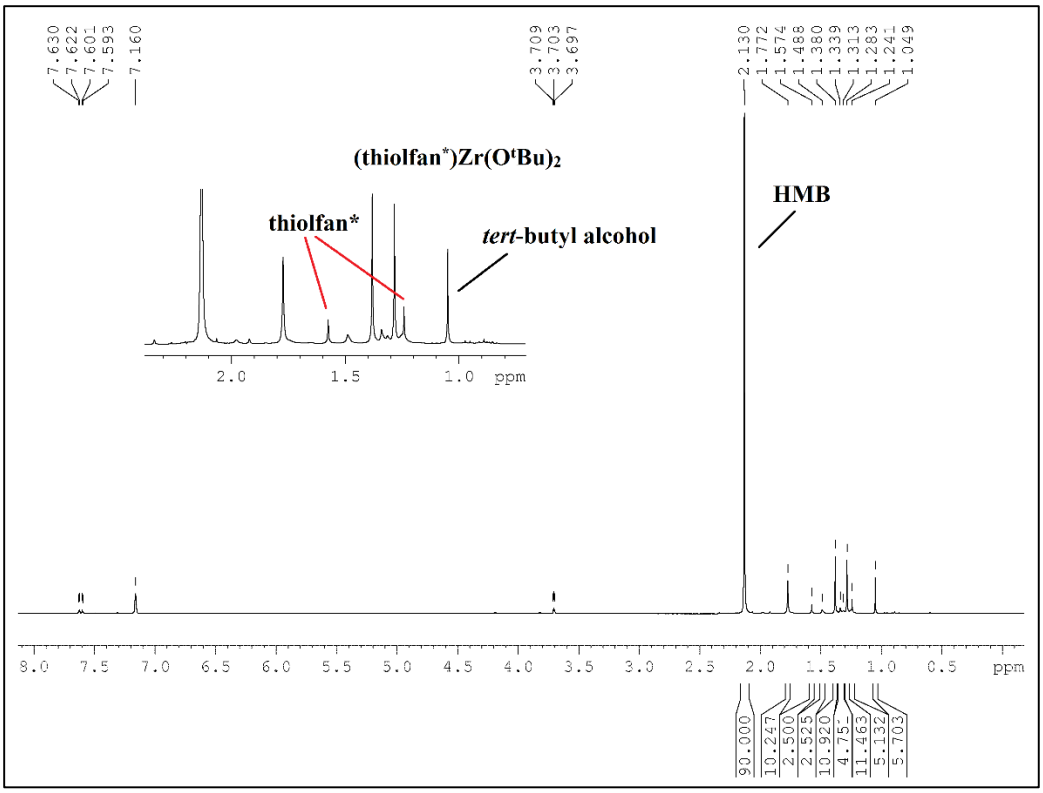

Figure S14. Decomposition study of (thiolfan*)Zr(O^{t}Bu)$_2$ at 100 °C in the presence of 5 equiv HMB (hexamethylbenzene) as an internal standard, t = 6 h; decomposition: 47%.

Time / h	Catalyst / %
1	85.9
2	73.0
3	66.4
4	60.0
5	55.5
6	53.3

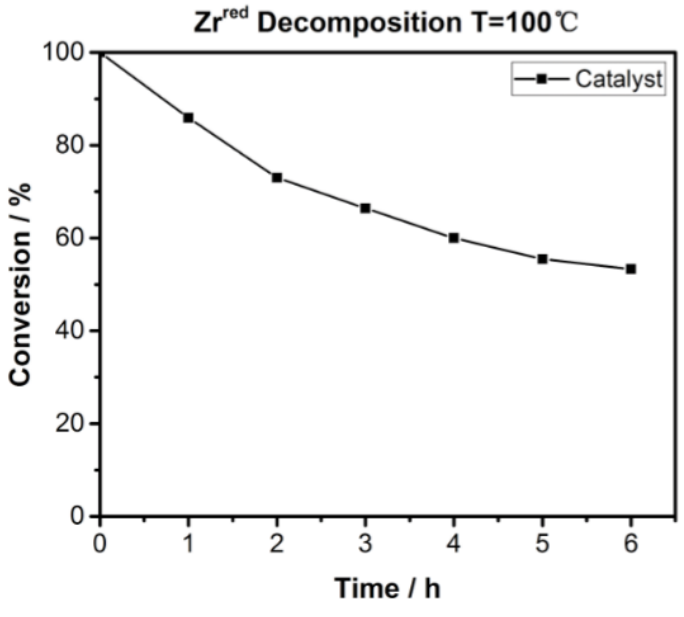

Figure S15. Decomposition study of (thiolfan*)Zr(O^{t}Bu)$_2$ at 100 °C in the presence of 5 equiv HMB (hexamethylbenzene) as an internal standard.

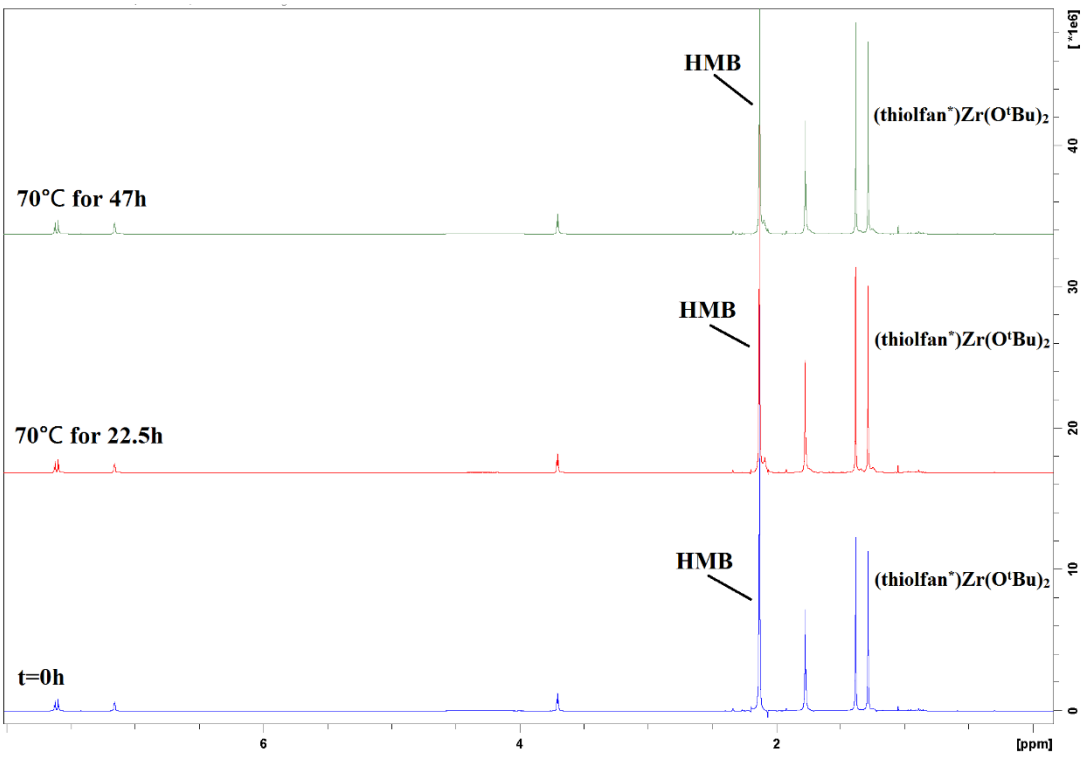

Figure S16. Stacked spectra for the decomposition study of (thiolfan*)Zr(O^tBu)$_2$ at 70 °C in the presence of 5 equiv HMB (hexamethylbenzene) as an internal standard.

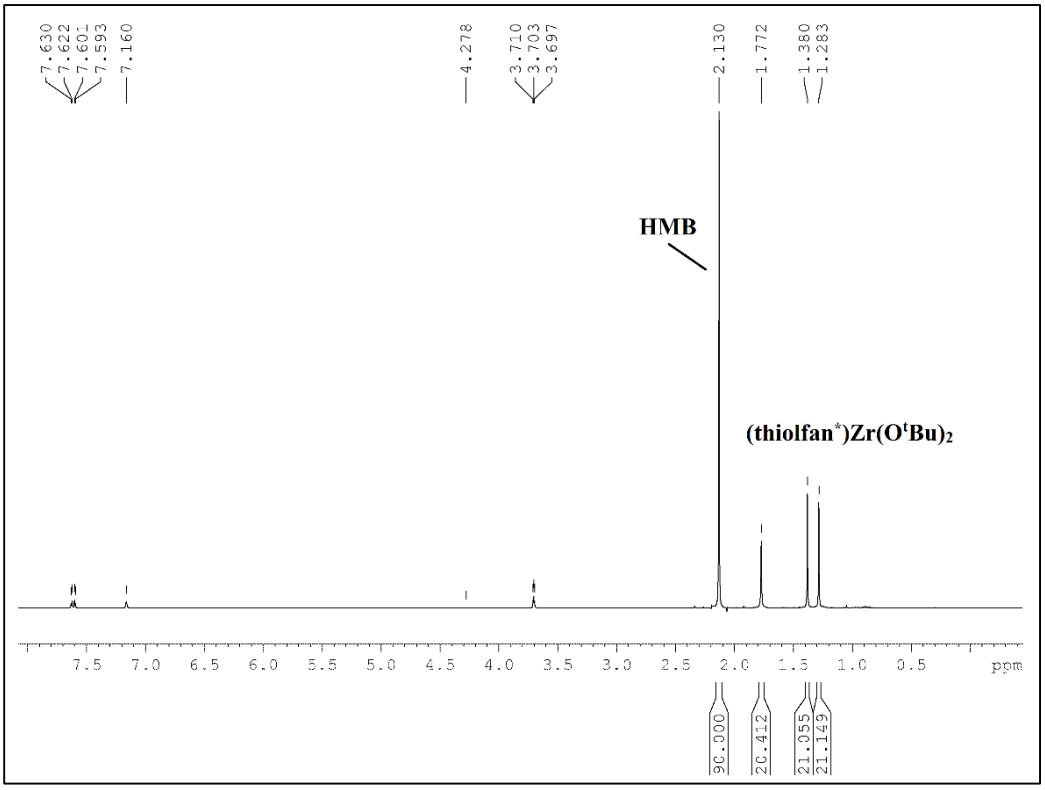

Figure S17. Decomposition study of (thiolfan*)Zr(O^tBu)$_2$ at 70 °C in the presence of 5 equiv HMB (hexamethylbenzene) as an internal standard, t = 0 h.

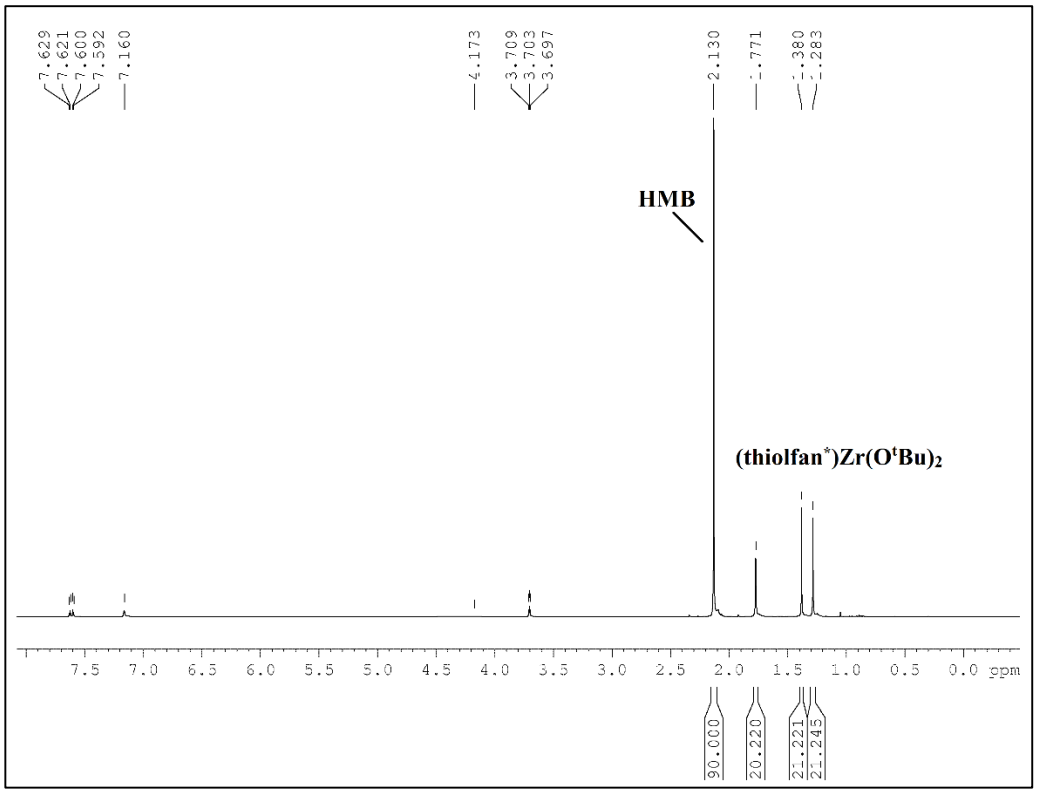

Figure S18. Decomposition study of (thiolfan*)Zr(O^tBu)$_2$ at 70 °C in the presence of 5 equiv HMB (hexamethylbenzene) as an internal standard, t = 47 h.

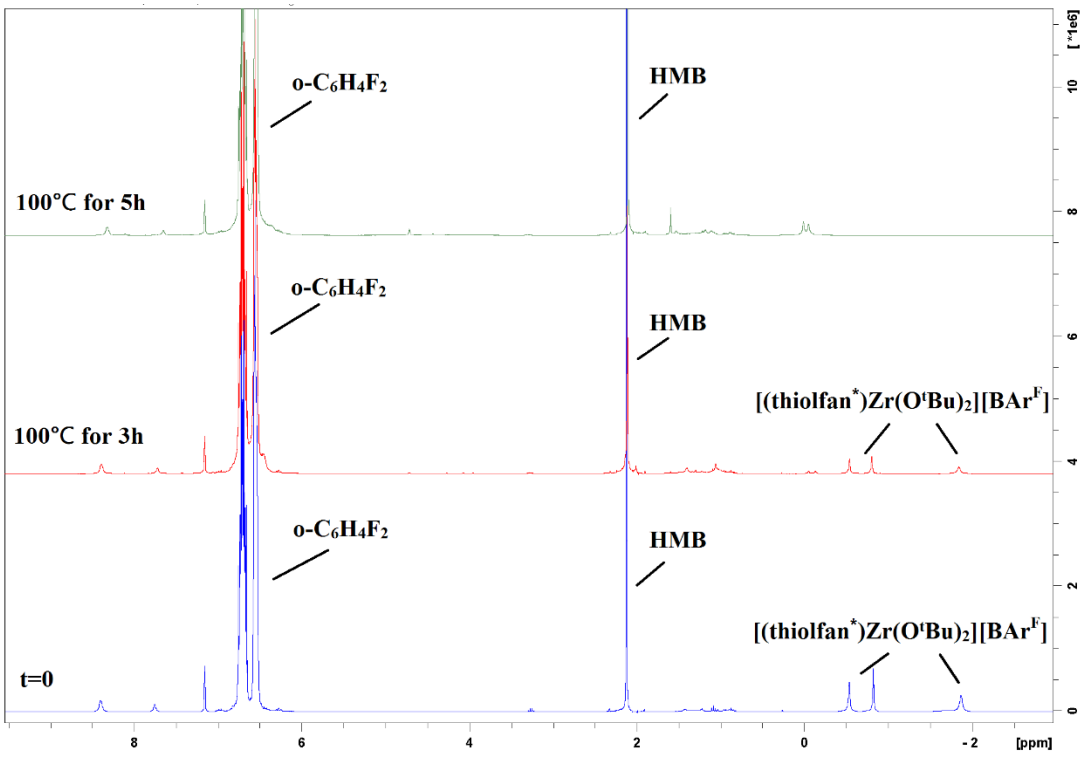

Figure S19. Stacked spectra for the decomposition study of [(thiolfan*)Zr(O^tBu)$_2$][BAr^F] at 100 °C in the presence of 5 equiv HMB (hexamethylbenzene) as an internal standard.

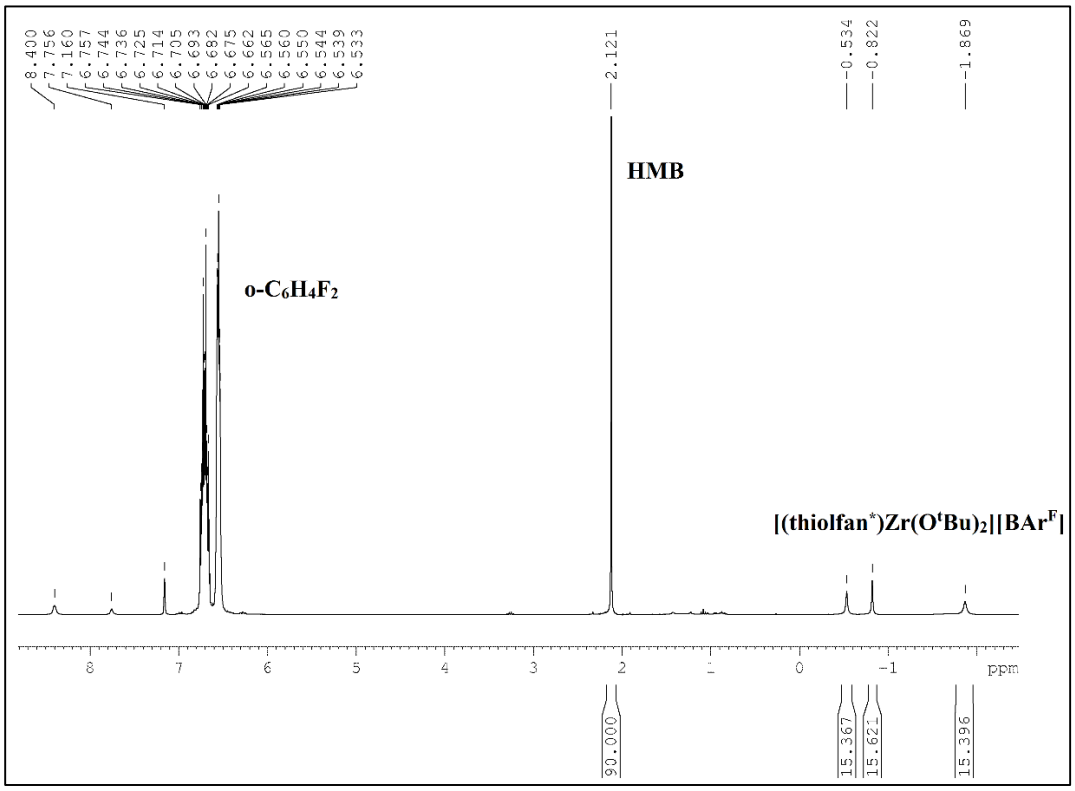

Figure S20. Decomposition study of [(thiolfan*)Zr(O^{t}Bu)$_2$][BAr^F] at 100 °C in the presence of 5 equiv HMB (hexamethylbenzene) as an internal standard, t = 0 h.

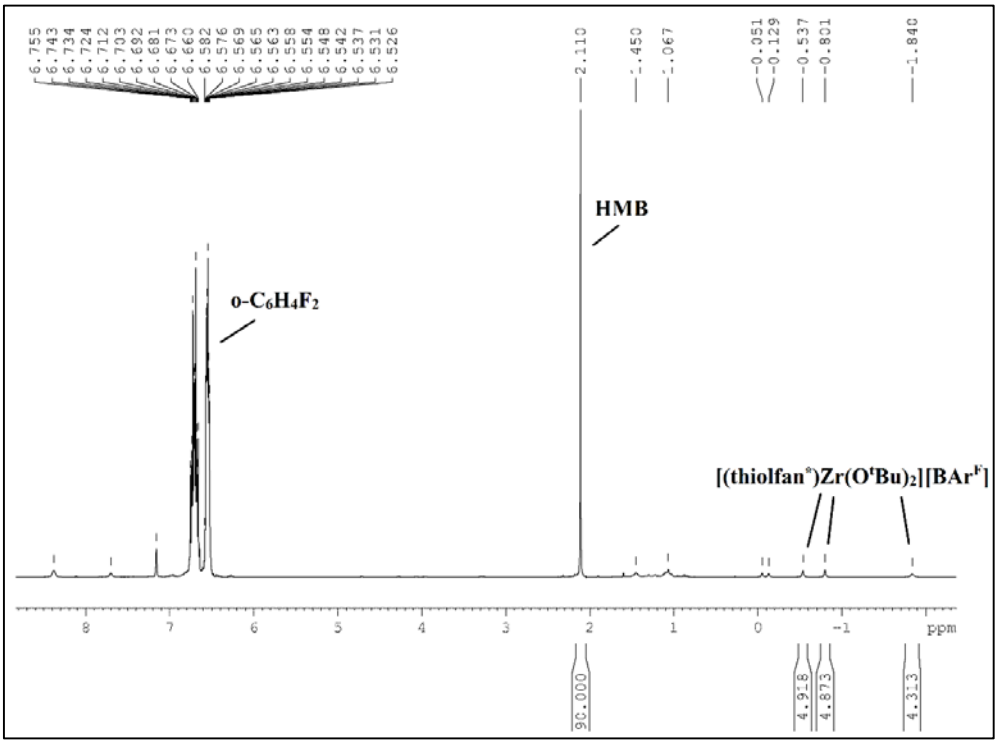

Figure S21. Decomposition study of [(thiolfan*)Zr(O^{t}Bu)$_2$][BAr^F] at 100 °C in the presence of 5 equiv HMB (hexamethylbenzene) as an internal standard, t = 4 h; decomposition: 68%.

Time / h	Catalyst / %
1	79.1
2	65.7
3	52.3
4	32.5
5	0

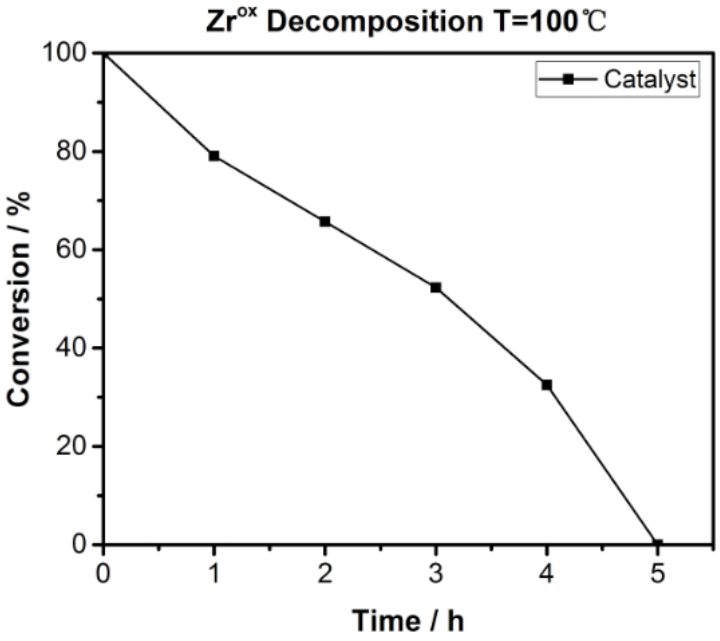

Figure S22. Decomposition study of [(thiolfan*)Zr(O^{t}Bu)$_2$][BAr^F] at 100 °C in the presence of 5 equiv HMB (hexamethylbenzene) as an internal standard.

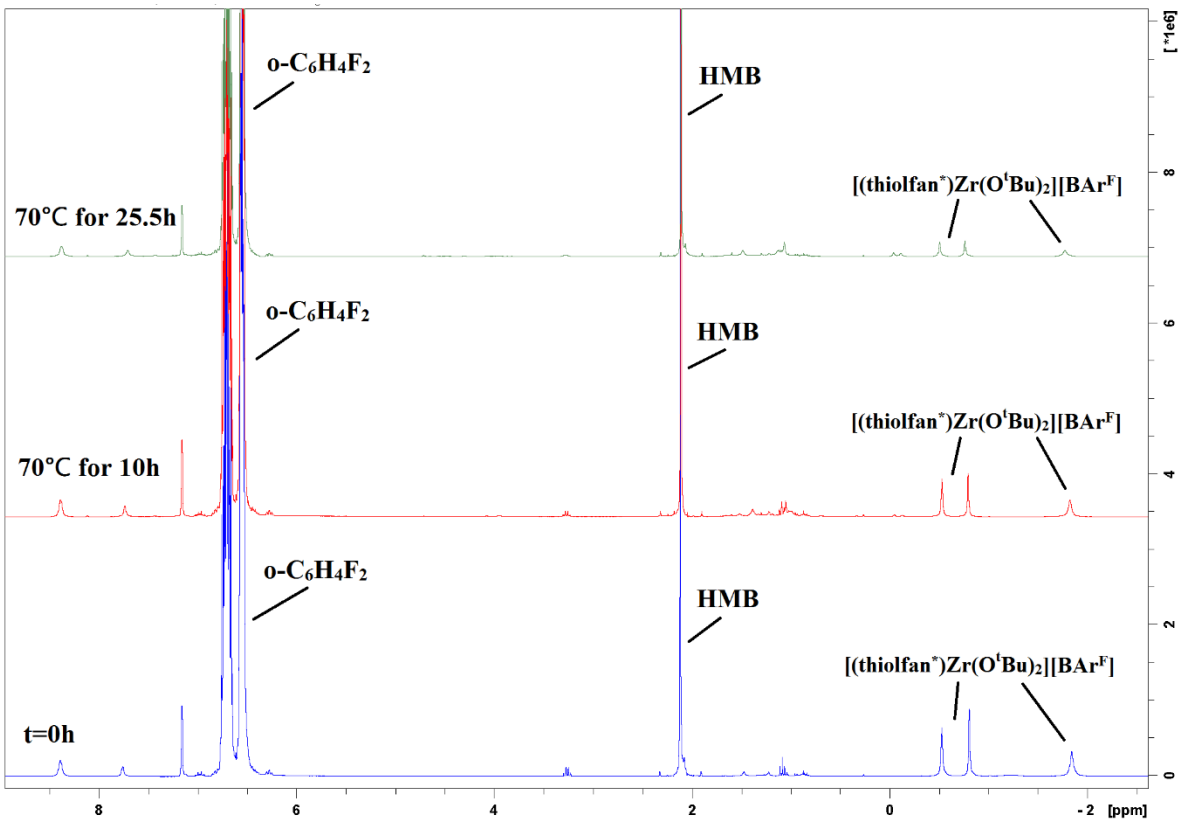

Figure S23. Stacked spectra for the decomposition study of [(thiolfan*)Zr(O^{t}Bu)$_2$][BAr^F] at 70 °C in the presence of 5 equiv HMB (hexamethylbenzene) as an internal standard.

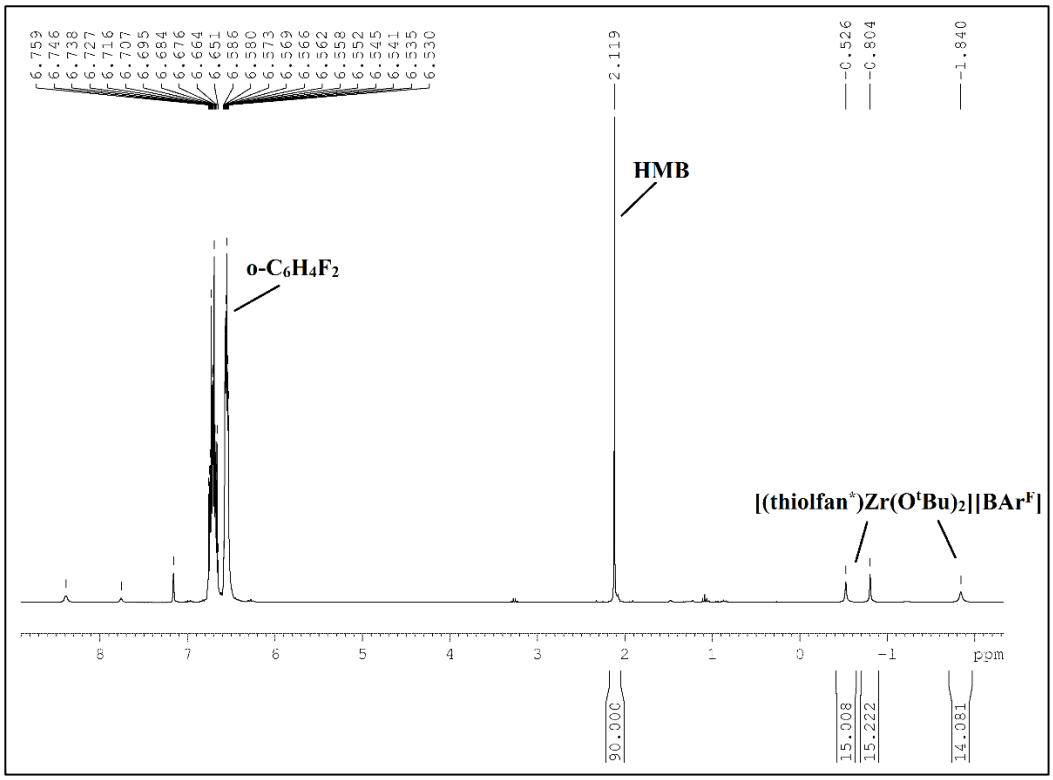

Figure S24. Decomposition study of [(thiolfan*)Zr(O^{t}Bu)$_2$][BAr^F] at 70 °C in the presence of 5 equiv HMB (hexamethylbenzene) as an internal standard, t = 0 h.

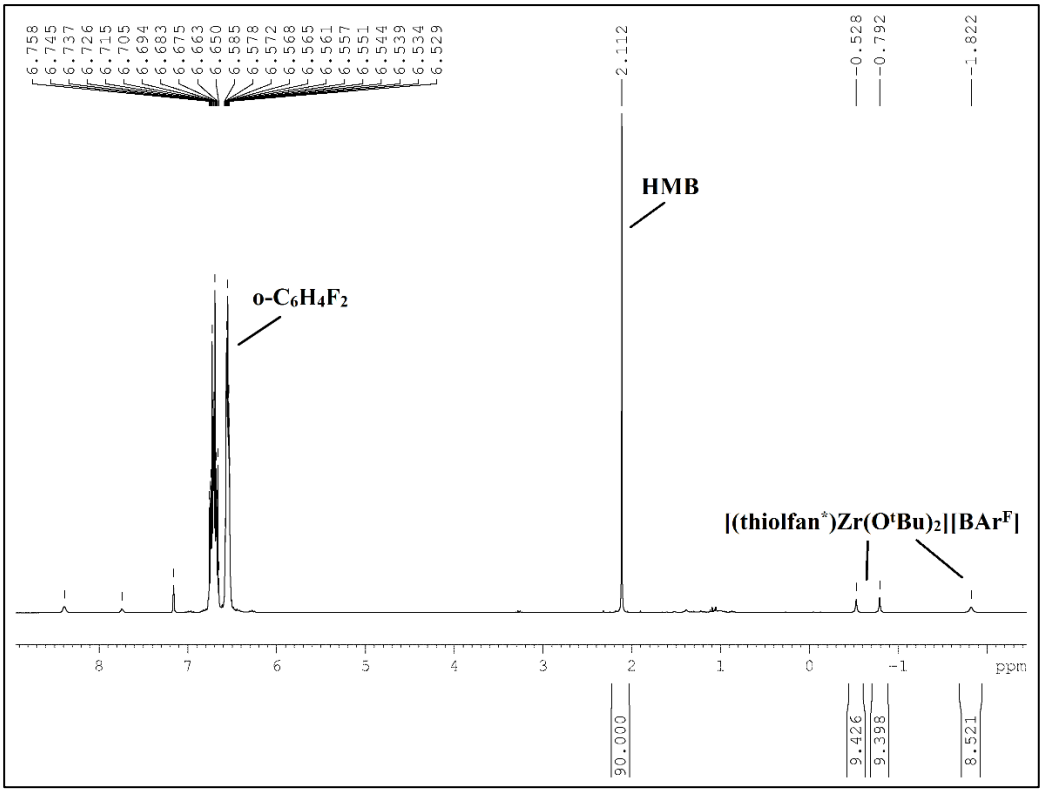

Figure S25. Decomposition study of [(thiolfan*)Zr(O^{t}Bu)$_2$][BAr^F] at 70 °C in the presence of 5 equiv HMB (hexamethylbenzene) as an internal standard, t = 10 h; decomposition: 38%.

Time / h	Catalyst / %
2	89.0
4	77.9
6	71.7
8	66.9
10	62.1
25.5	41.4

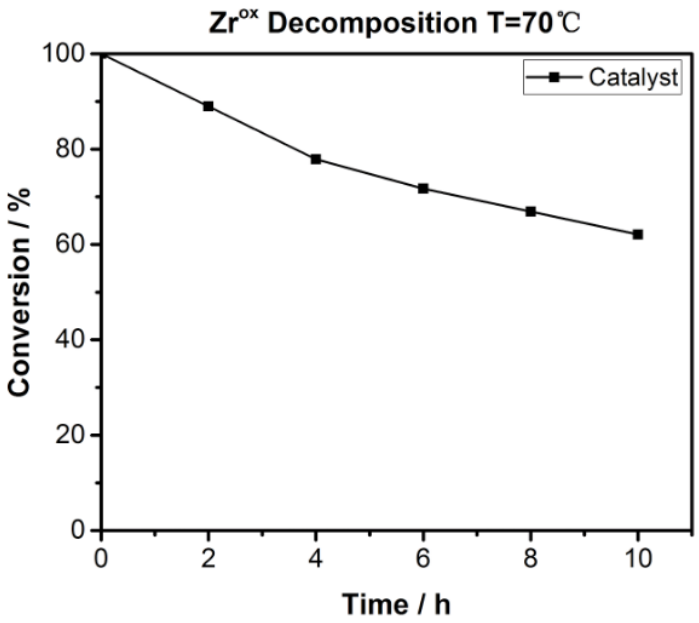

Figure S26. Decomposition study of [(thiolfan*)Zr(O^{t}Bu)$_2$][BAr^F] at 70 °C in the presence of 5 equiv HMB (hexamethylbenzene) as an internal standard.

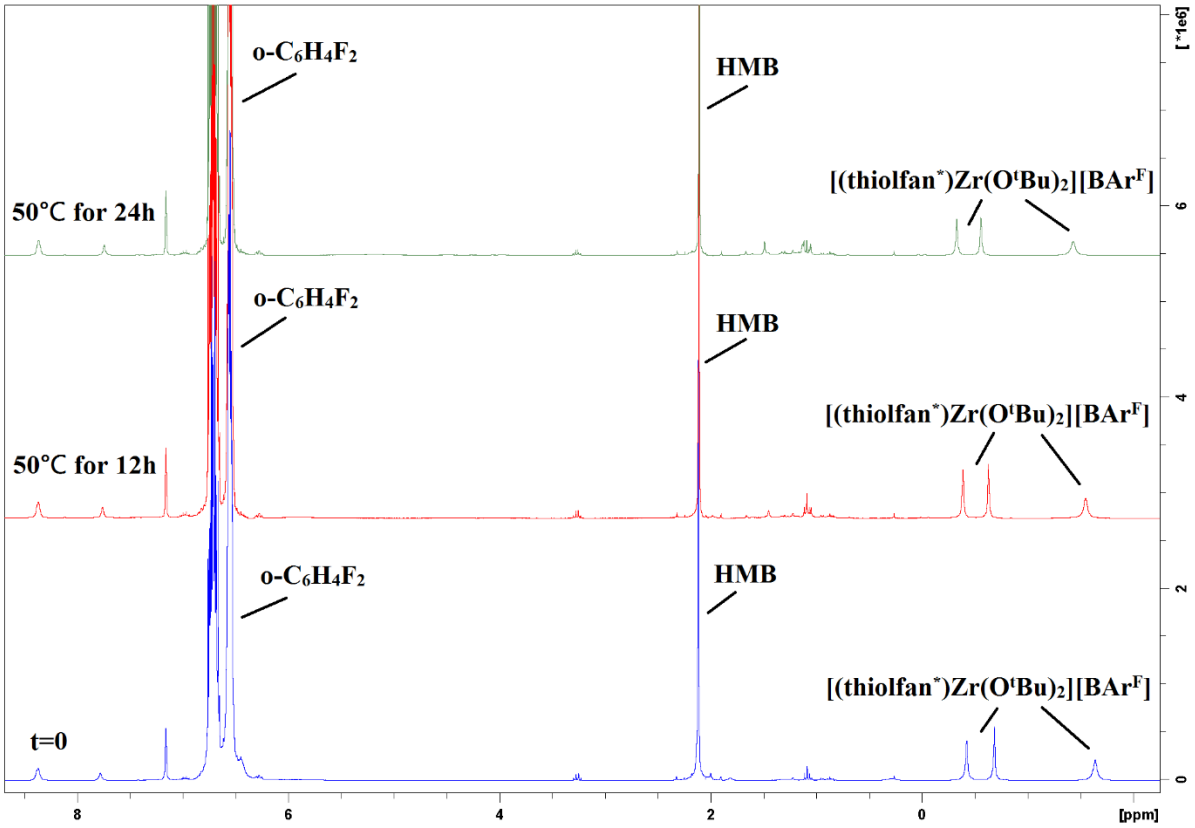

Figure S27. Stacked spectra for the decomposition study of [(thiolfan*)Zr(O^{t}Bu)$_2$][BAr^F] at 50 °C in the presence of 5 equiv HMB (hexamethylbenzene) as an internal standard.

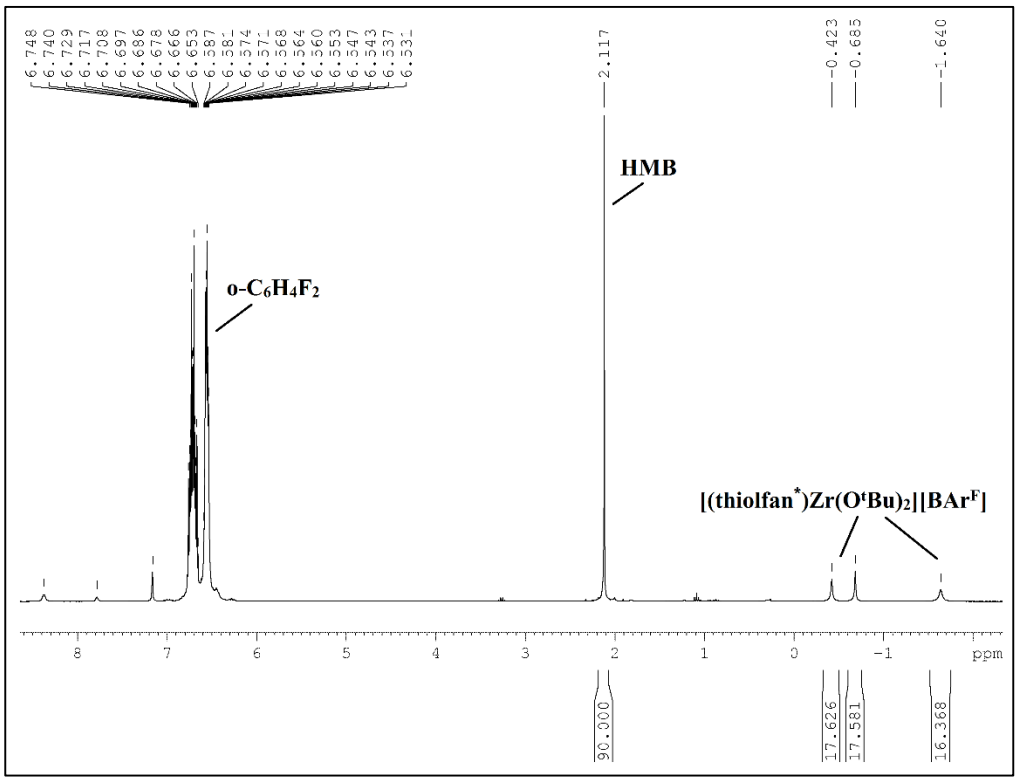

Figure S28. Decomposition study of [(thiolfan*)Zr(O^{t}Bu)$_2$][BAr^F] at 50 °C in the presence of 5 equiv HMB (hexamethylbenzene) as an internal standard, t = 0 h.

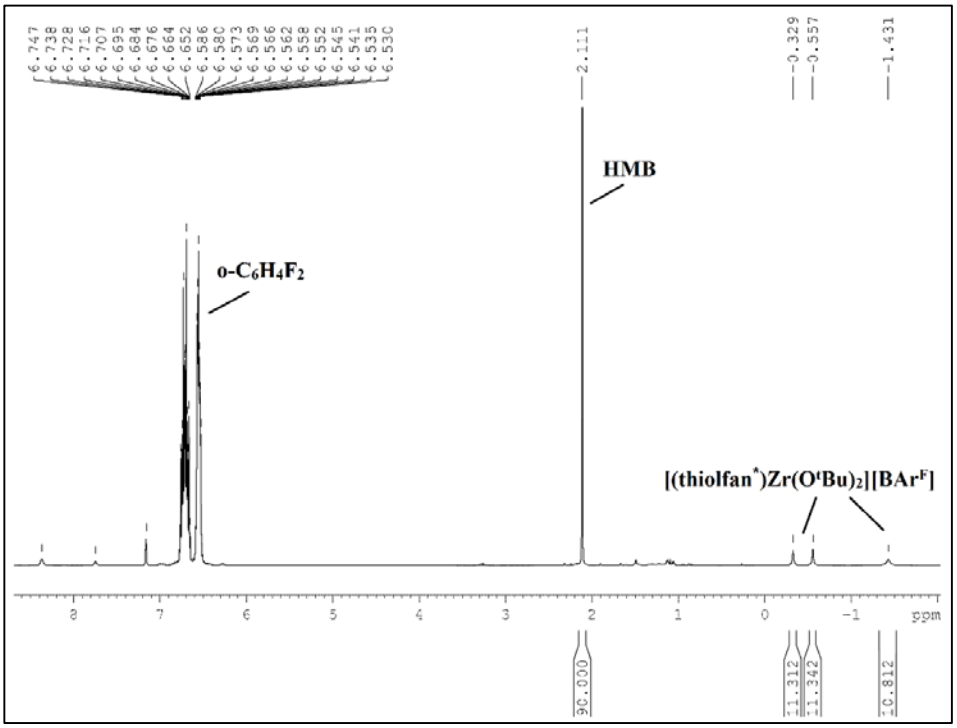

Figure S29. Decomposition study of [(thiolfan*)Zr(O^{t}Bu)$_2$][BAr^F] at 50 °C in the presence of 5 equiv HMB (hexamethylbenzene) as an internal standard, t = 24 h; decomposition: 36%.

Time / h	Catalyst / %	Time / h	Catalyst / %
2	94.3	14	75.6
4	90.9	16	72.2
6	87.5	18	69.9
8	84.6	20	66.5
10	81.8	22	65.3
12	78.4	24	64.2

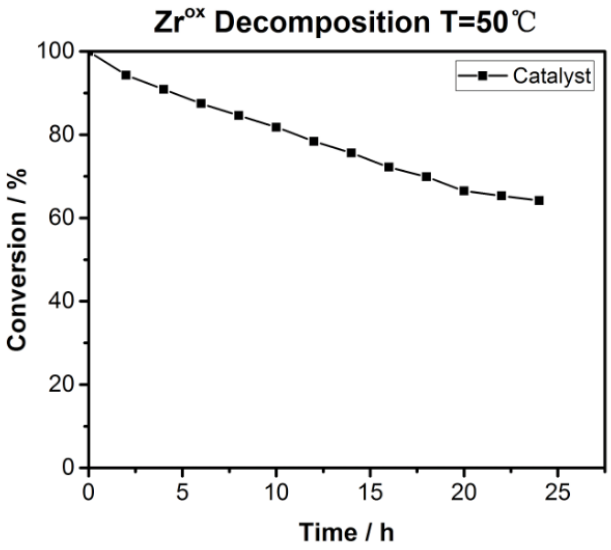

Figure S30. Decomposition study of [(thiolfan*)Zr(O^{t}Bu)$_2$][BAr^F] at 50 °C in the presence of 5 equiv HMB (hexamethylbenzene) as an internal standard.

Decomposition reactions in the presence of monomer

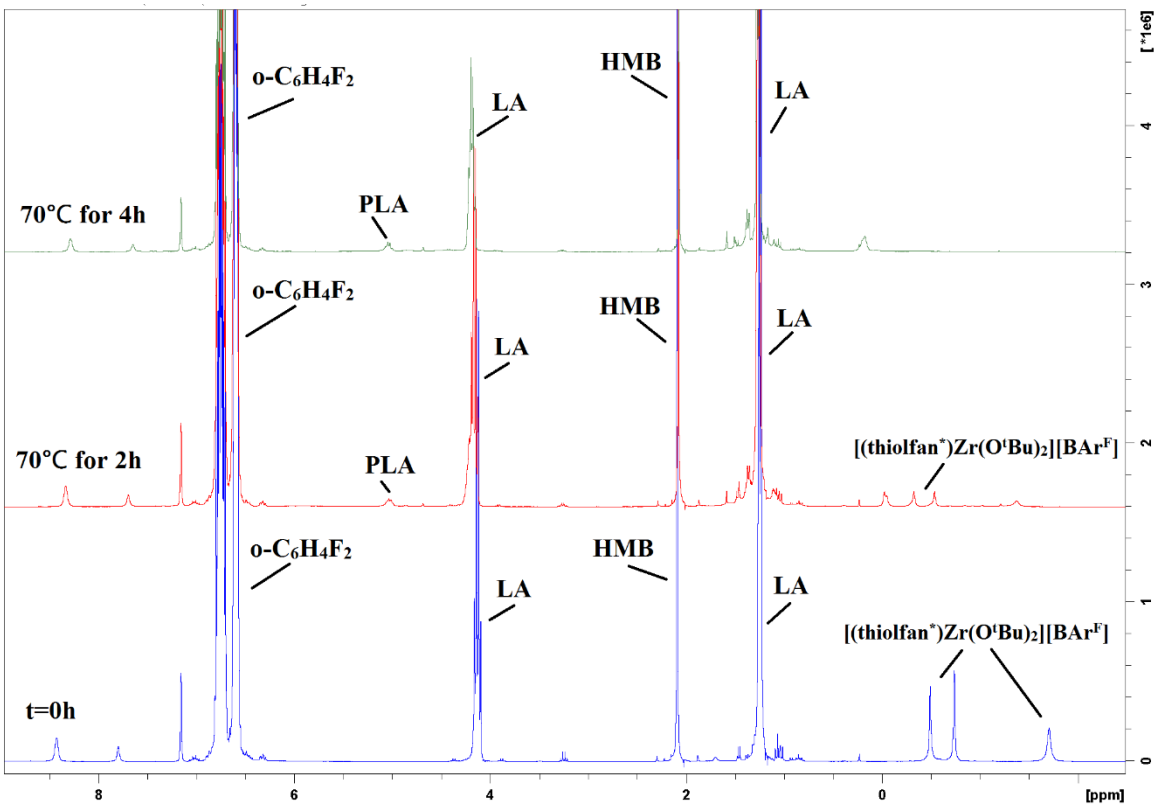

Figure S31. Stacked spectra for the decomposition study of [(thiolfan*)Zr(O^{t}Bu)$_2$][BAr^F] at 70 °C in the presence of 100 equiv L-lactide and 5 equiv HMB (hexamethylbenzene) as an internal standard.

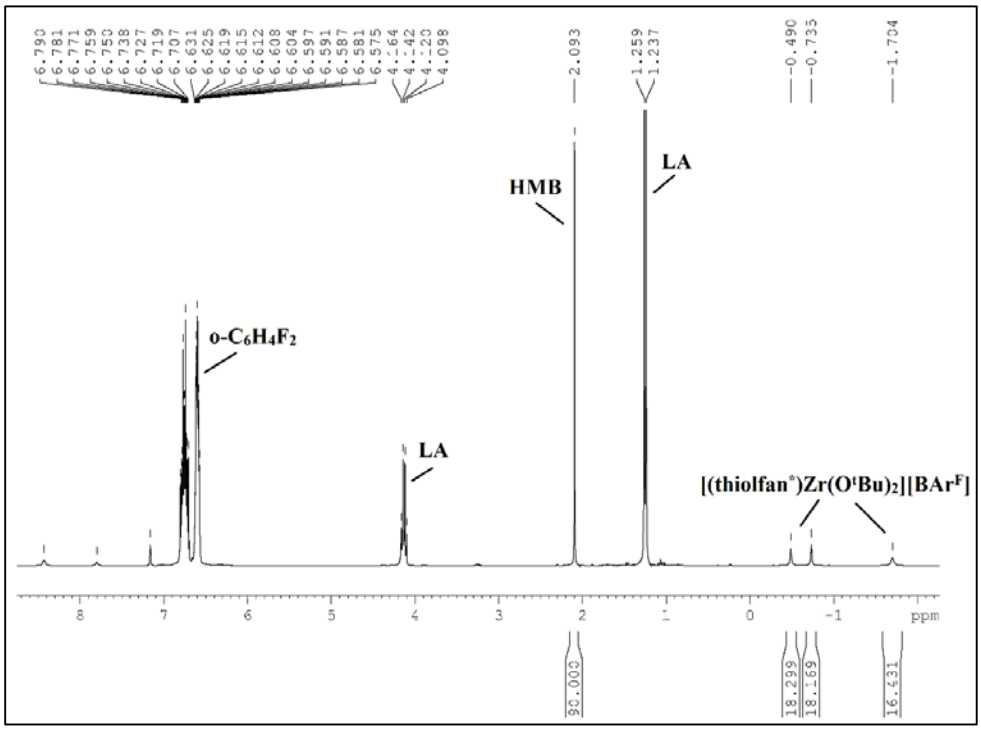

Figure S32. Decomposition study of [(thiolfan*)Zr(O^{t}Bu)$_2$][BAr^F] at 70 °C in the presence of 100 equiv L-lactide and 5 equiv HMB (hexamethylbenzene) as an internal standard, t = 0 h.

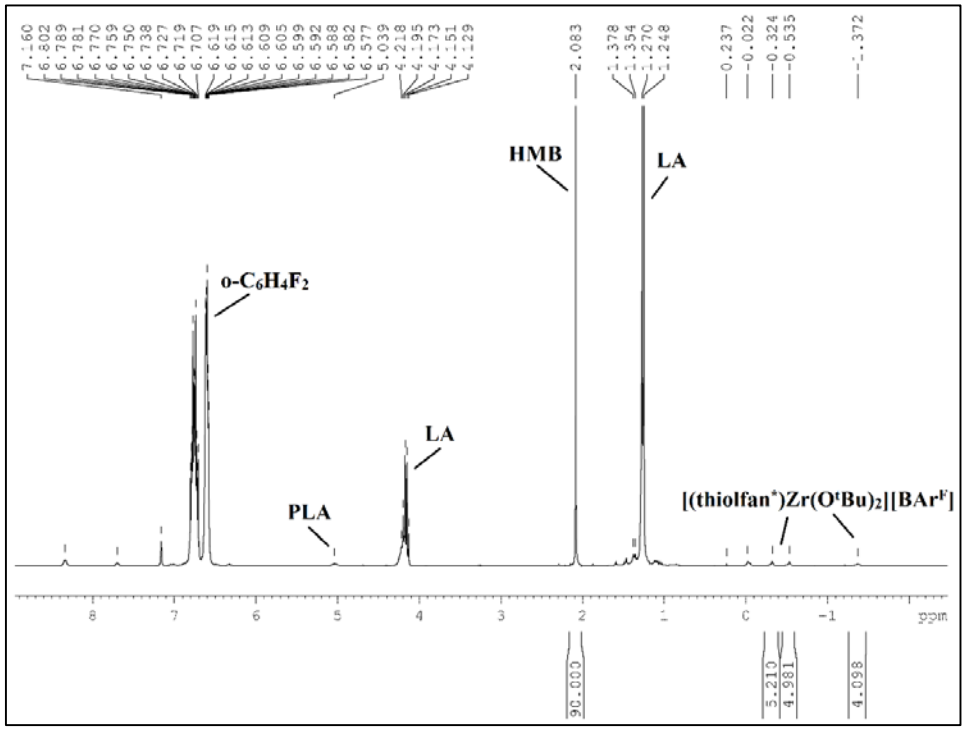

Figure S33. Decomposition study of [(thiolfan*)Zr(O^{t}Bu)$_2$][BAr^F] at 70 °C in the presence of 100 equiv L-lactide and 5 equiv HMB (hexamethylbenzene) as an internal standard, t = 2 h; decomposition: 72%.

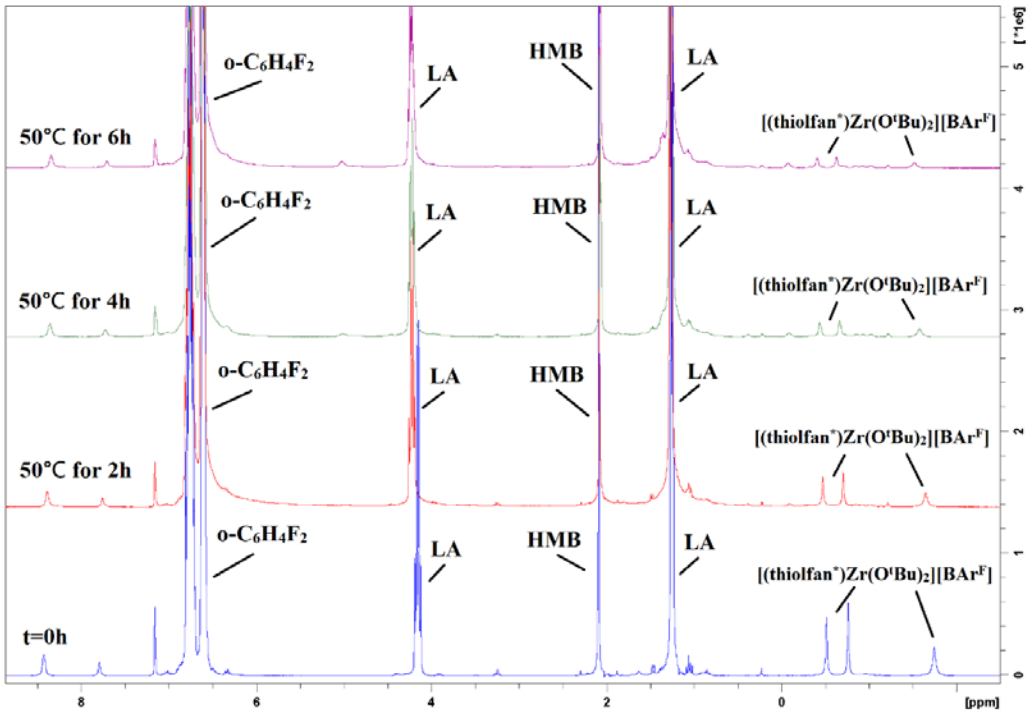

Figure S34. Stacked spectra for the decomposition study of [(thiolfan*)Zr(O^{t}Bu)$_2$][BAr^F] at 50 °C in the presence of 100 equiv L-lactide and 5 equiv HMB (hexamethylbenzene) as an internal standard.

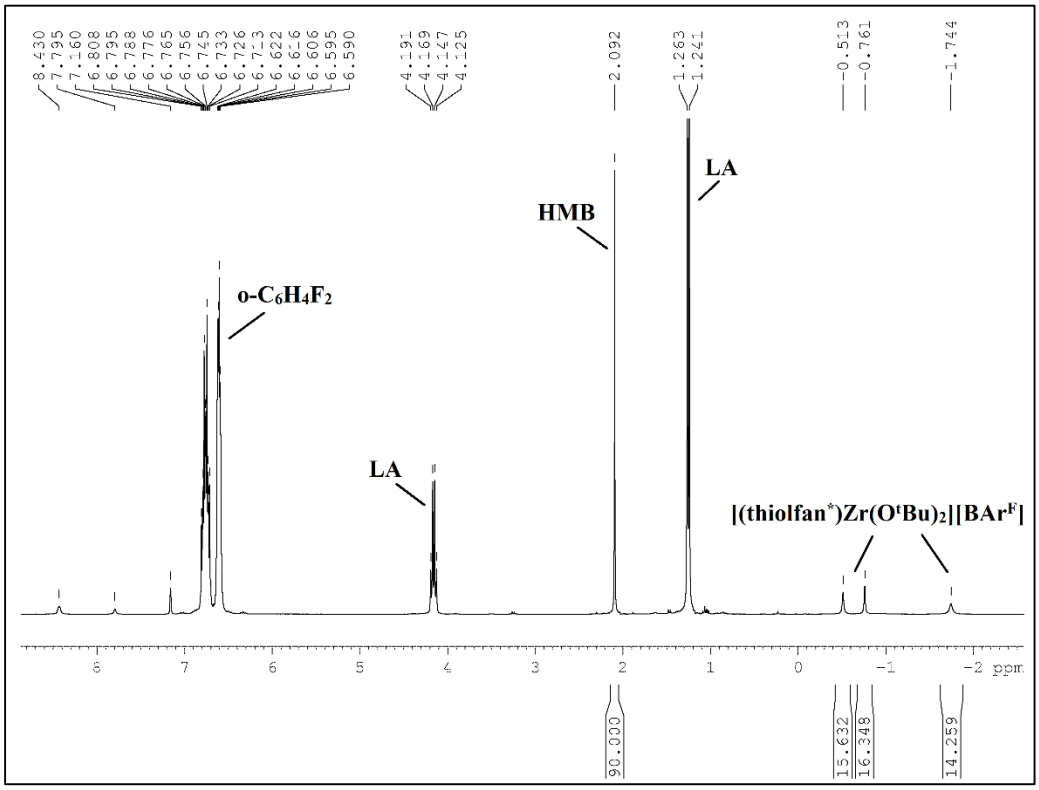

Figure S35. Decomposition study of [(thiolfan*)Zr(O^{t}Bu)$_2$][BAr^F] at 50 °C in the presence of 100 equiv L-lactide and 5 equiv HMB (hexamethylbenzene) as an internal standard, t = 0 h.

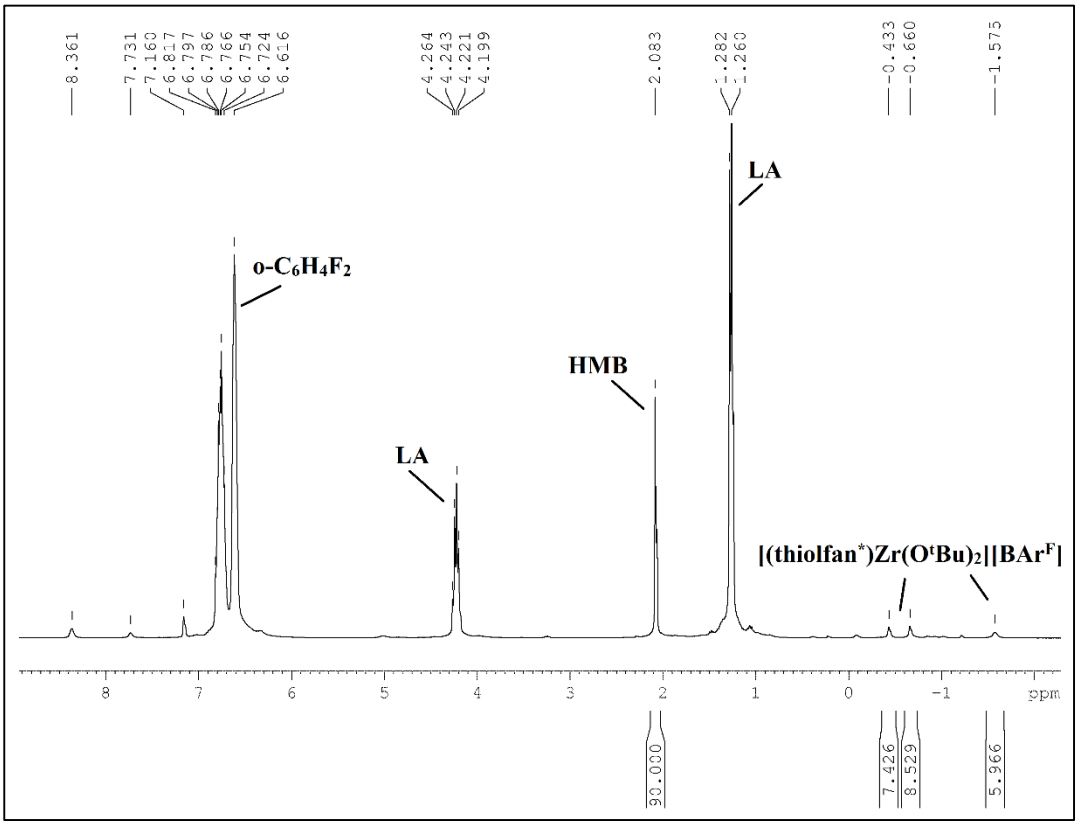

Figure S36. Decomposition study of [(thiolfan*)Zr(O^{t}Bu)$_2$][BAr^F] at 70 °C in the presence of 100 equiv L-lactide and 5 equiv HMB (hexamethylbenzene) as an internal standard, t = 4 h; decomposition: 53%.

Polymerization studies

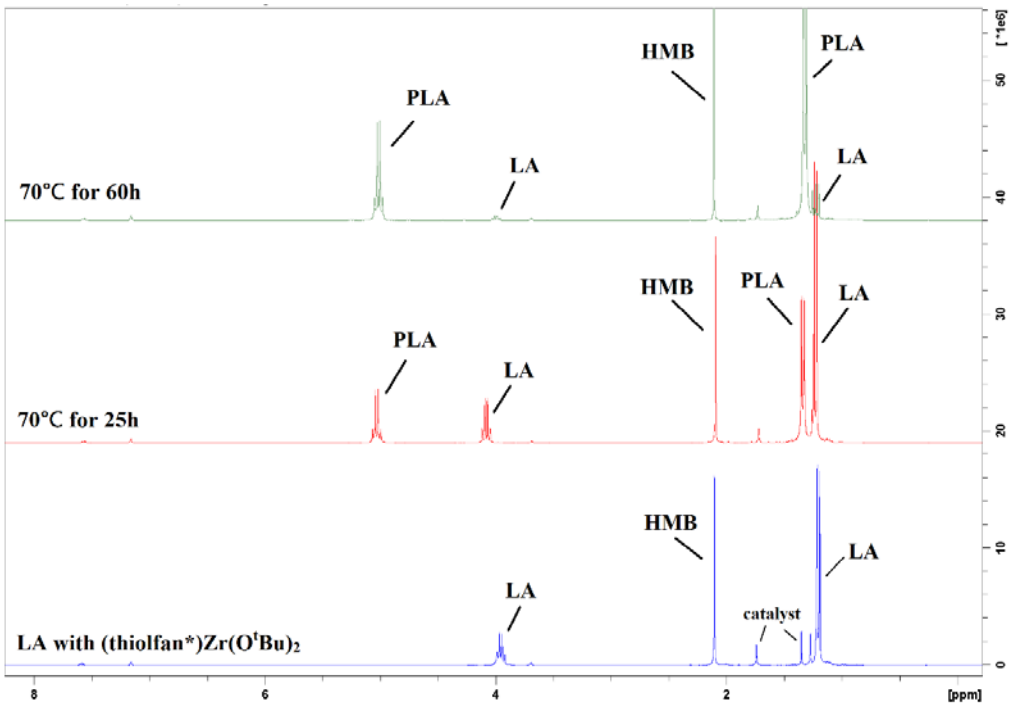

Figure S37. Stacked spectra for the reaction of [(thiolfan*)Zr(O^{t}Bu)$_2$][BAr^F] with 100 equiv L-lactide at 70 °C; HMB (hexamethylbenzene) as an internal standard.

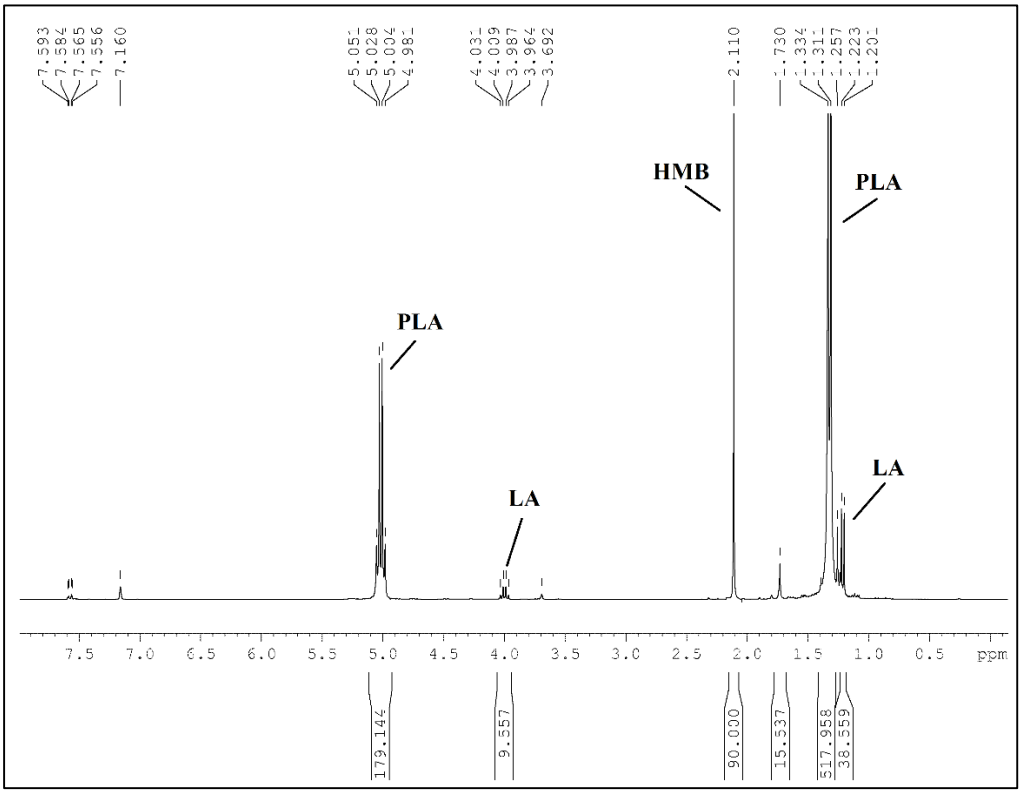

Figure S38. Reaction of (thiolfan*)Zr(O^{t}Bu)$_2$ with 100 equiv L-lactide at 70 °C; HMB (hexamethylbenzene) as an internal standard; t = 60 h, conversion: 94%.

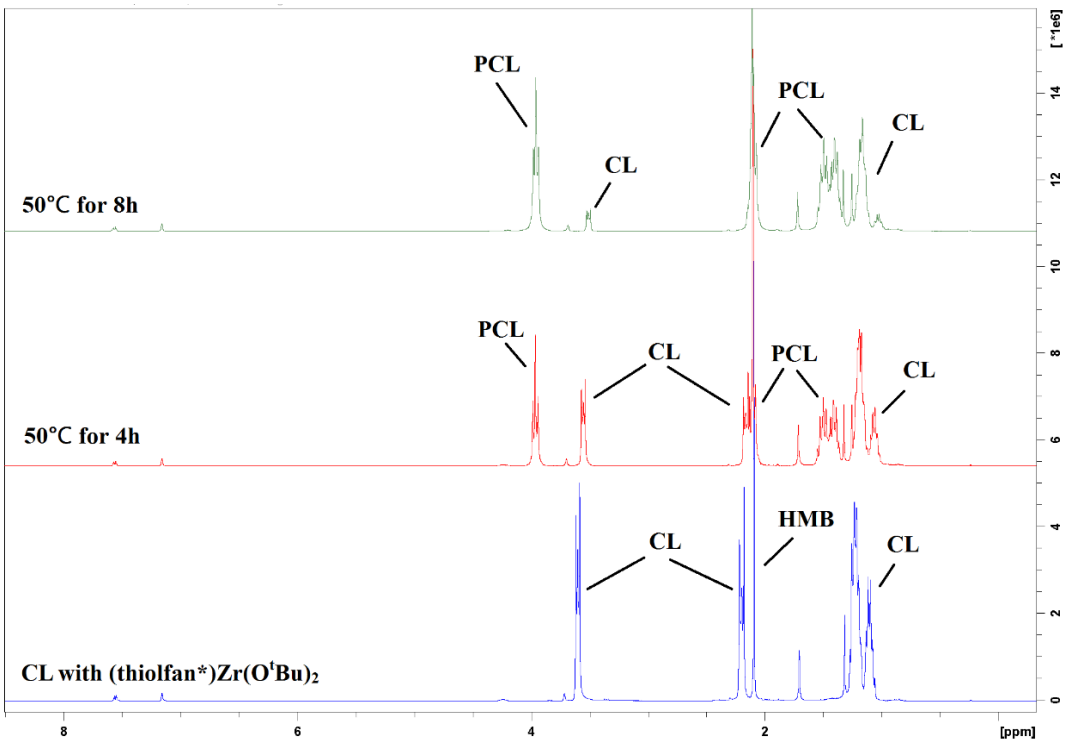

Figure S39. Stacked spectra for the reaction of (thiolfan*)Zr(O^{t}Bu)$_2$ with 100 equiv CL at 50 °C; HMB (hexamethylbenzene) as an internal standard.

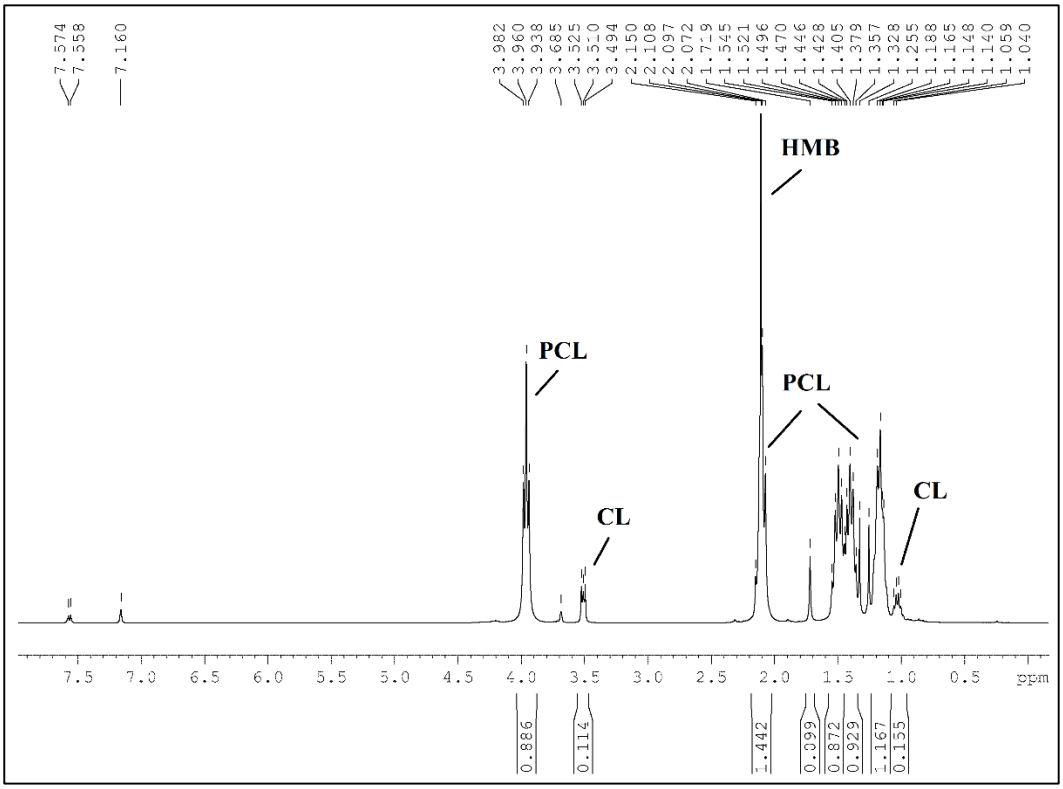

Figure S40. Reaction of (thiolfan*)Zr(O^{t}Bu)$_2$ with 100 equiv CL at 50 °C; HMB (hexamethylbenzene) as an internal standard; t = 8 h, conversion: 88%.

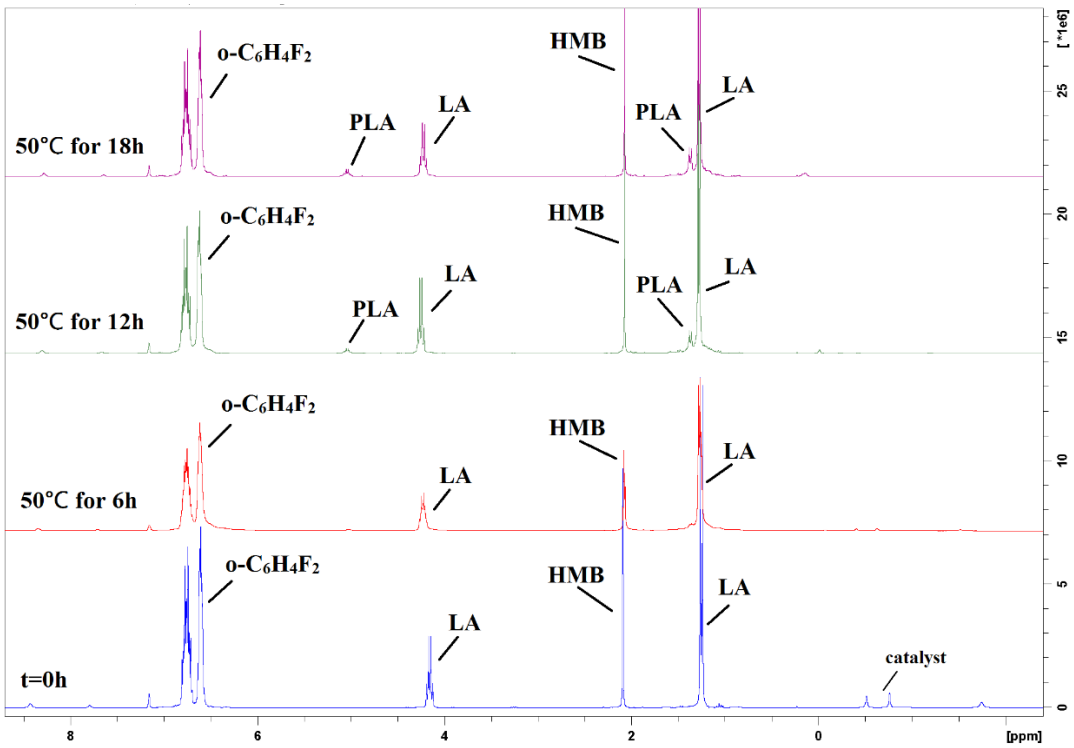

Figure S41. Stacked spectra for the reaction of [(thiolfan*)Zr(O^{t}Bu)$_2$][BAr^F] with 100 equiv L-lactide at 50 °C; HMB (hexamethylbenzene) as an internal standard; t final = 18 h; conversion < 15%.

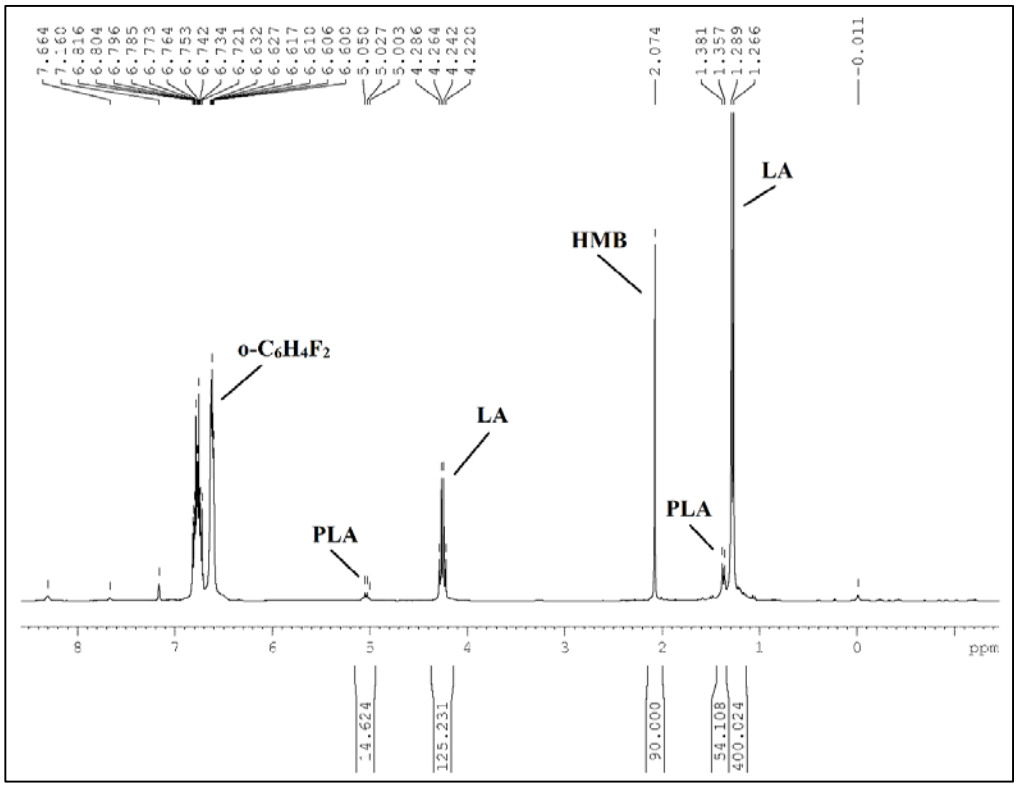

Figure S42. Polymerization of 100 equivalents of L-lactide with [(thiolfan*)Zr(O^{t}Bu)$_2$][BAr^F] at 50 °C for 12 h; conversion: 10%; HMB = hexamethylbenzene.

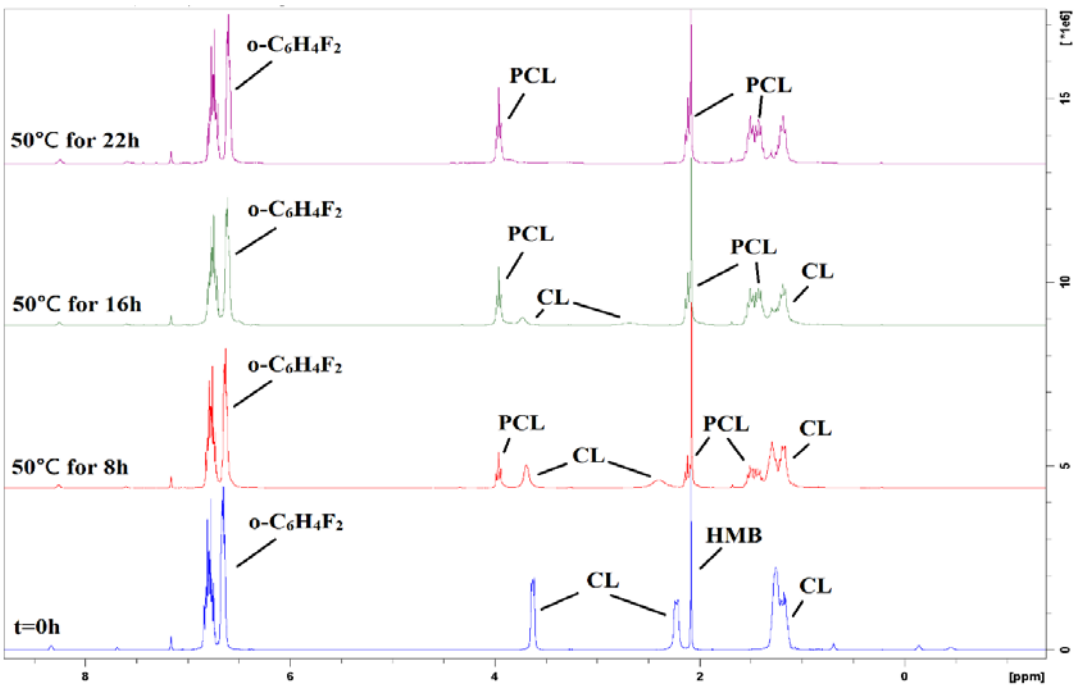

Figure S43. Stacked spectra for the polymerization of 100 equivalents of ε-caprolactone with [(thiolfan*)Zr(O^{t}Bu)$_2$][BAr^F] at 50 °C; HMB = hexamethylbenzene.

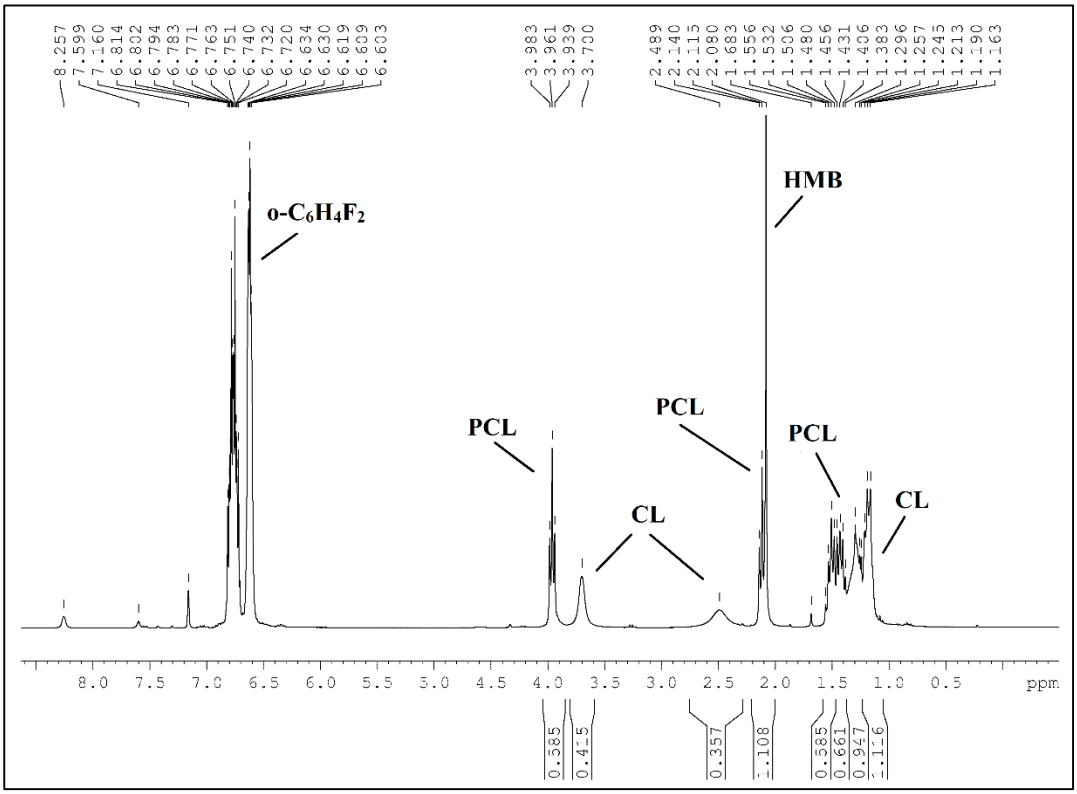

Figure S44. Polymerization of 100 equivalents of ε-caprolactone with [(thiolfan*)Zr(O^{t}Bu)$_2$][BAr^F] at 50 °C for 12 h; conversion: 58%; HMB = hexamethylbenzene.

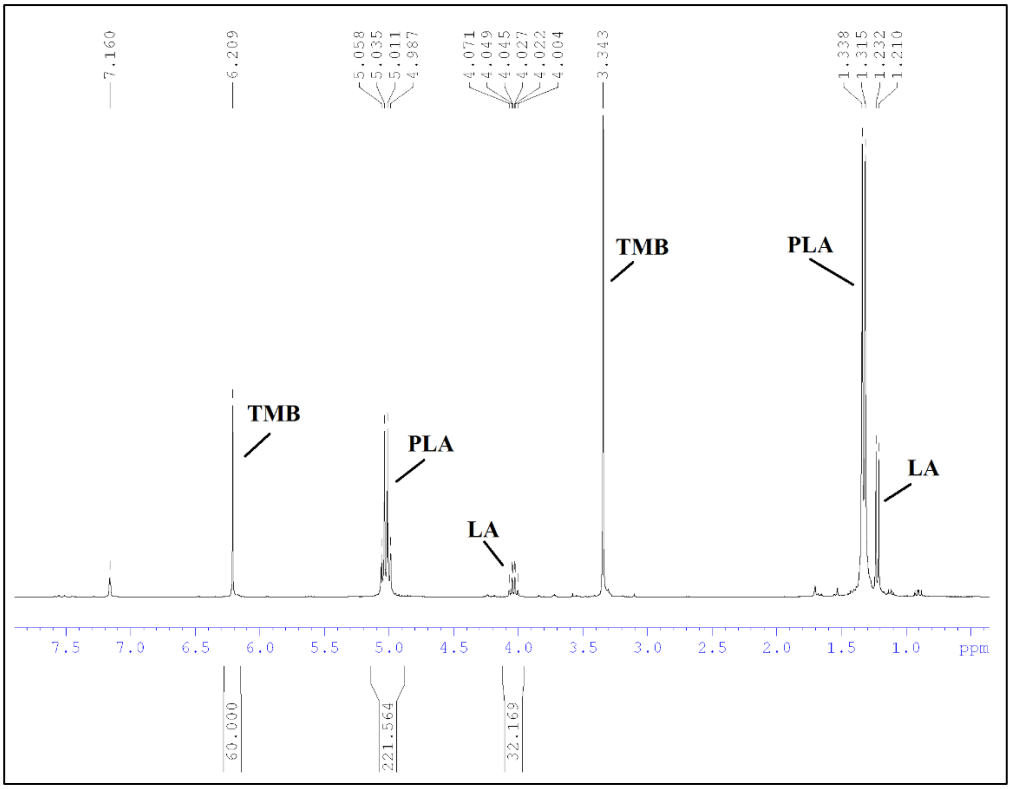

Figure S45. Polymerization of 100 equivalents of L-lactide with (thiolfan*)Ti(O^iPr)$_2$ at 100 °C; TMB = trimethoxybenzene (Table 1, Entry 1).

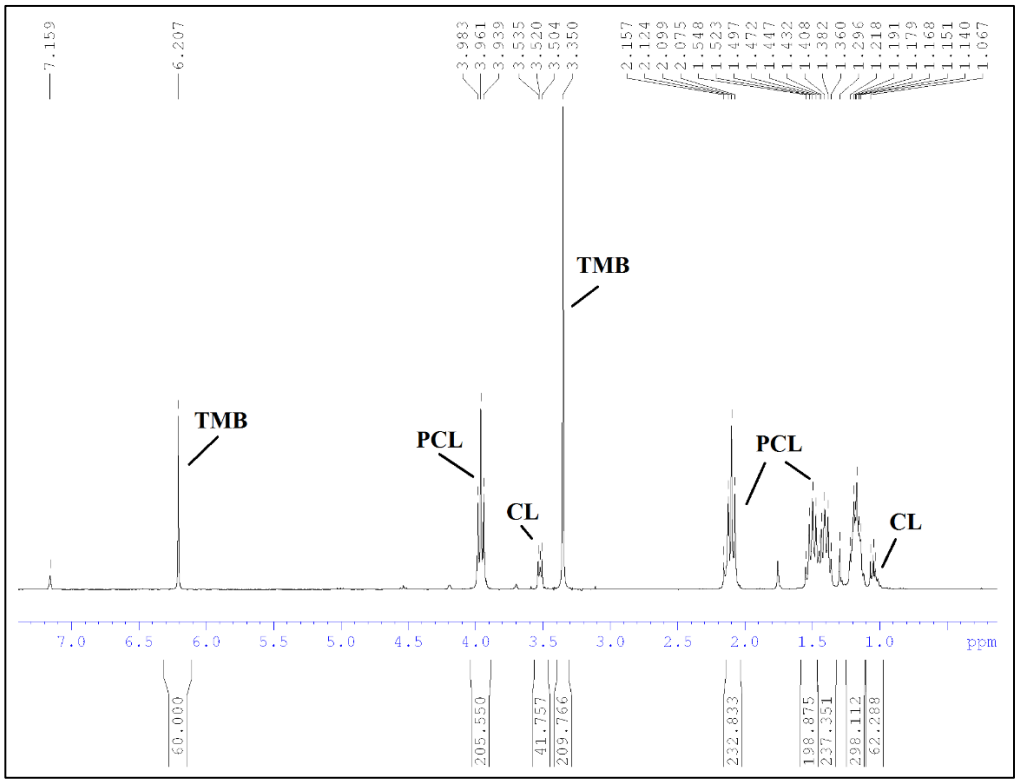

Figure S46. Polymerization of 100 equivalents of ε-caprolactone with [(thiolfan*)Ti(O^iPr)$_2$] [BAr^F] at 100 °C; TMB = trimethoxybenzene (Table 1, Entry 3).

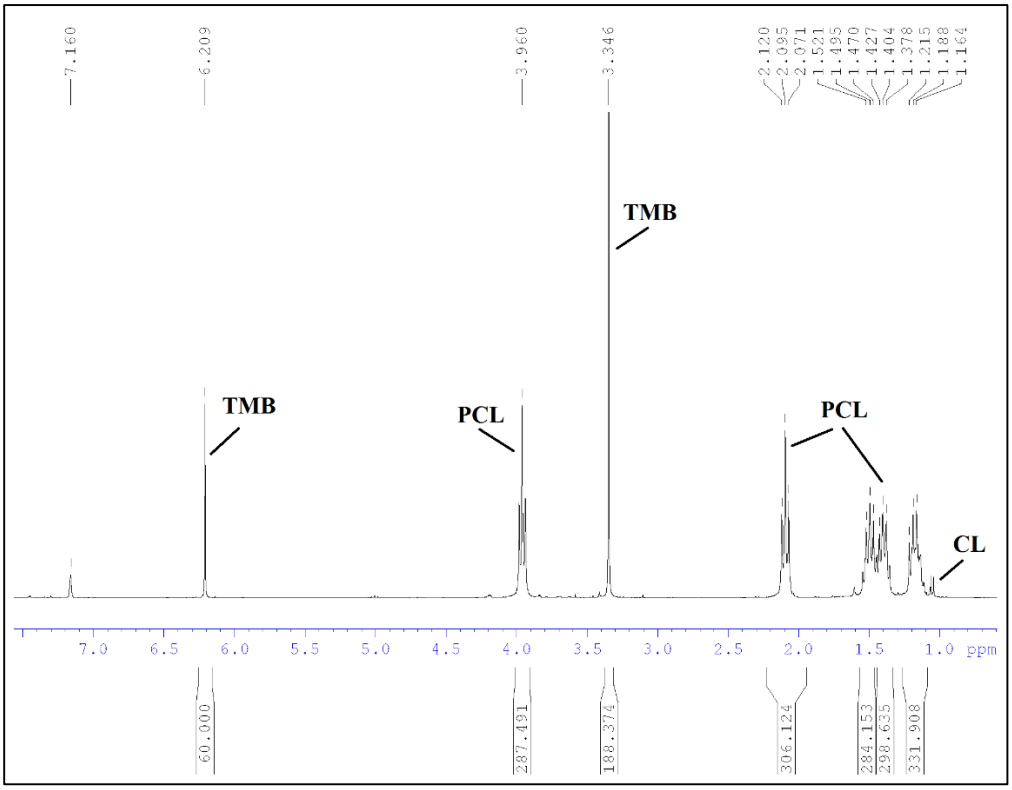

Figure S47. Polymerization of 100 equivalents of ε-caprolactone with [(thiolfan*)Ti(O^iPr)$_2$][BAr^F] at 100 °C; TMB = trimethoxybenzene (Table 1, Entry 4).

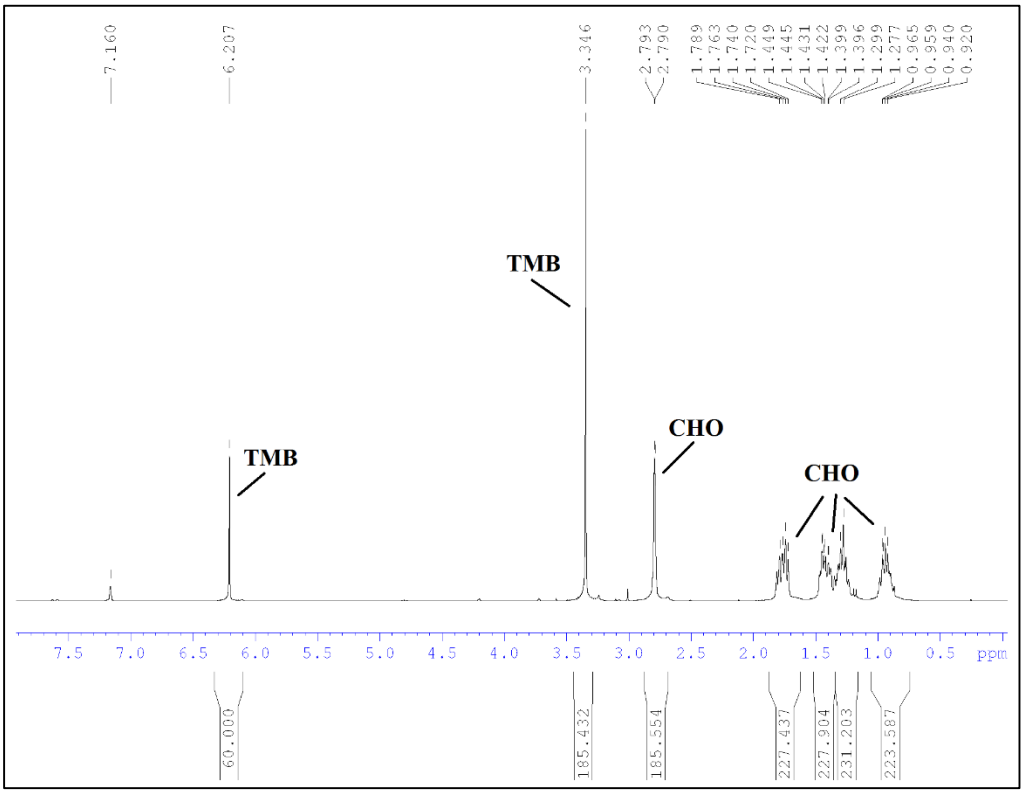

Figure S48. Polymerization of 100 equivalents of cyclohexene oxide with (thiolfan*)Ti(O^iPr)$_2$ at 100 °C; TMB = trimethoxybenzene (Table 2, Entry 1).

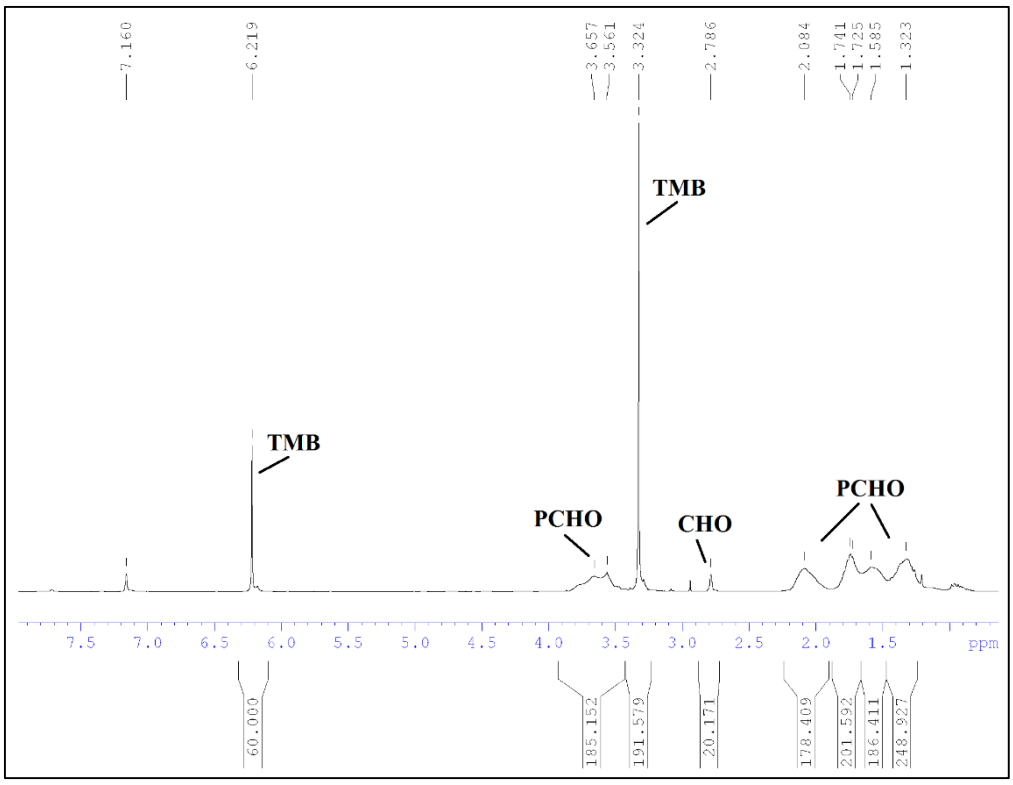

Figure S49. Polymerization of 100 equivalents of cyclohexene oxide [(thiolfan*)Ti(O^iPr)$_2$][BAr^F] at 25 °C; TMB = trimethoxybenzene (Table 2, Entry 2).

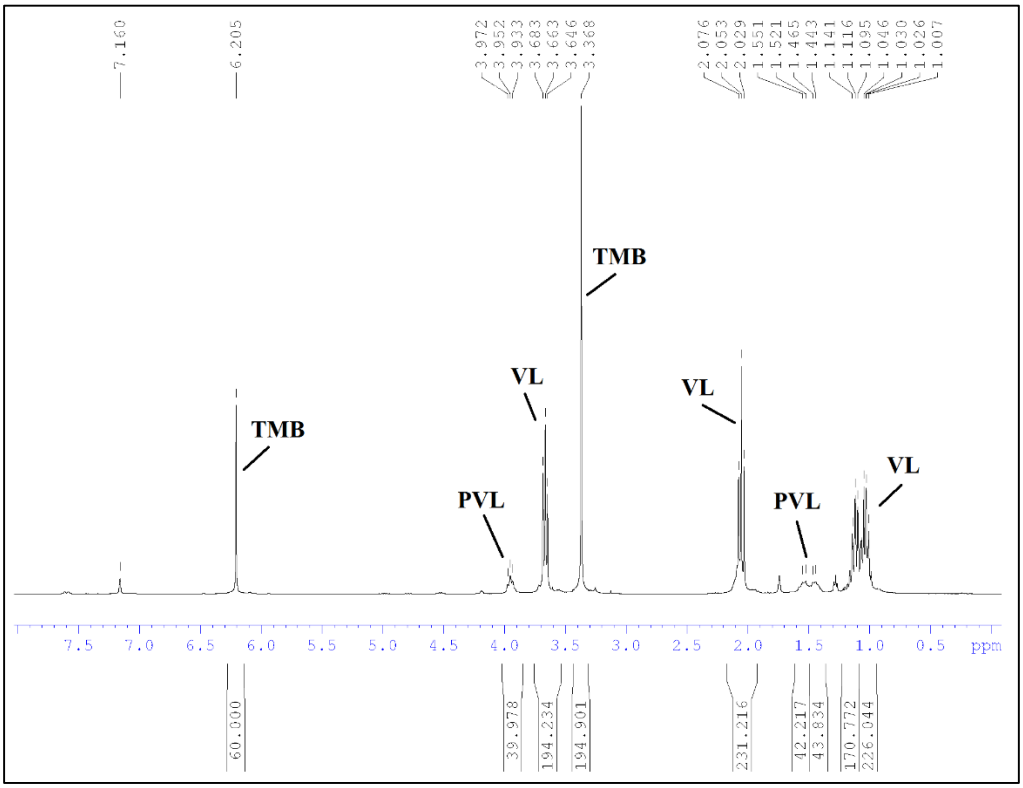

Figure S50. Polymerization of 100 equivalents of δ-valerolactone with (thiolfan*)Ti(O^iPr)$_2$ at 100 °C; TMB = trimethoxybenzene (Table 2, Entry 3).

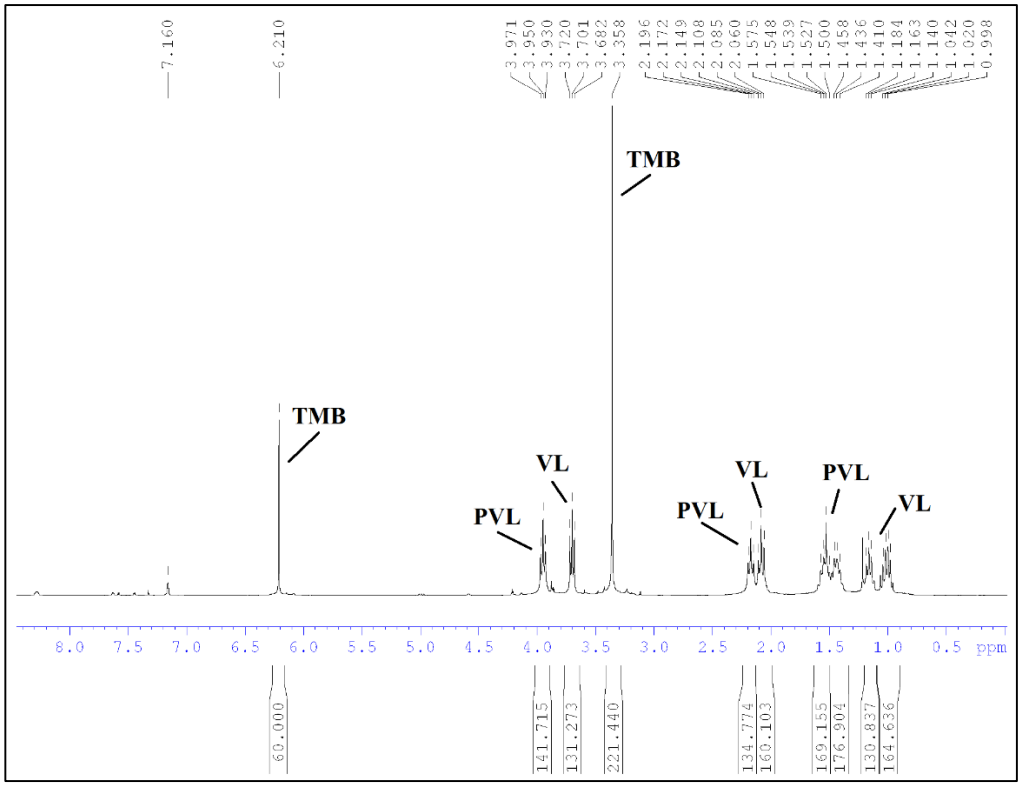

Figure S51. Polymerization of 100 equivalents of δ-valerolactone with [(thiolfan*)Ti(O^iPr)$_2$][BAr^F] at 100 °C; TMB = trimethoxybenzene (Table 2, Entry 4).

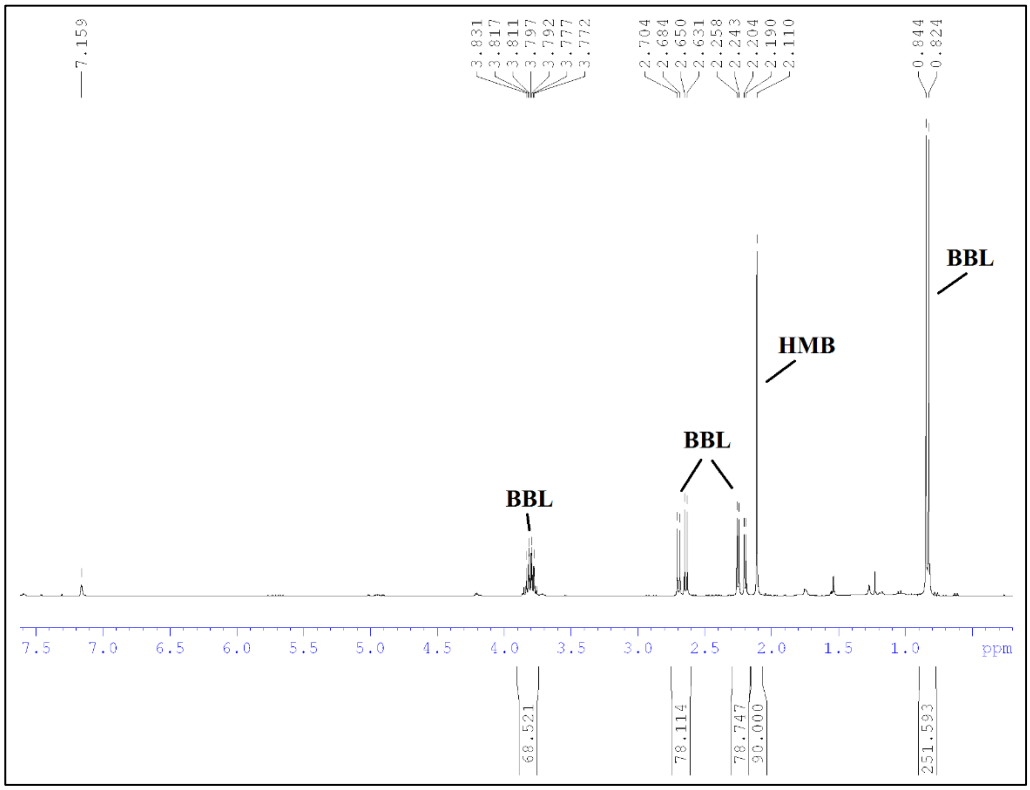

Figure S52. Polymerization of 100 equivalents of β-butyrolactone with (thiolfan*)Ti(O^iPr)$_2$ at 100 °C; HMB = hexamethylbenzene (Table 2, Entry 5).

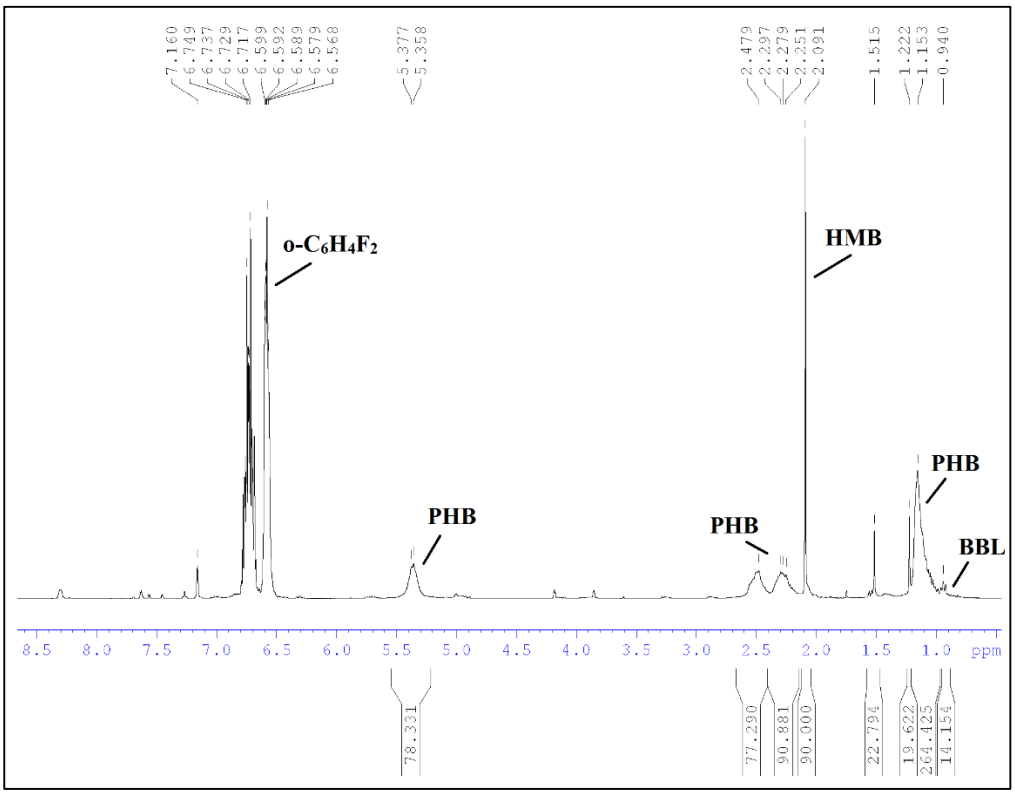

Figure S53. Polymerization of 100 equivalents of β-butyrolactone with [(thiolfan*)Ti(O^{i}Pr)$_2$][BAr^F] at 100 °C; HMB = hexamethylbenzene (Table 2, Entry 6).

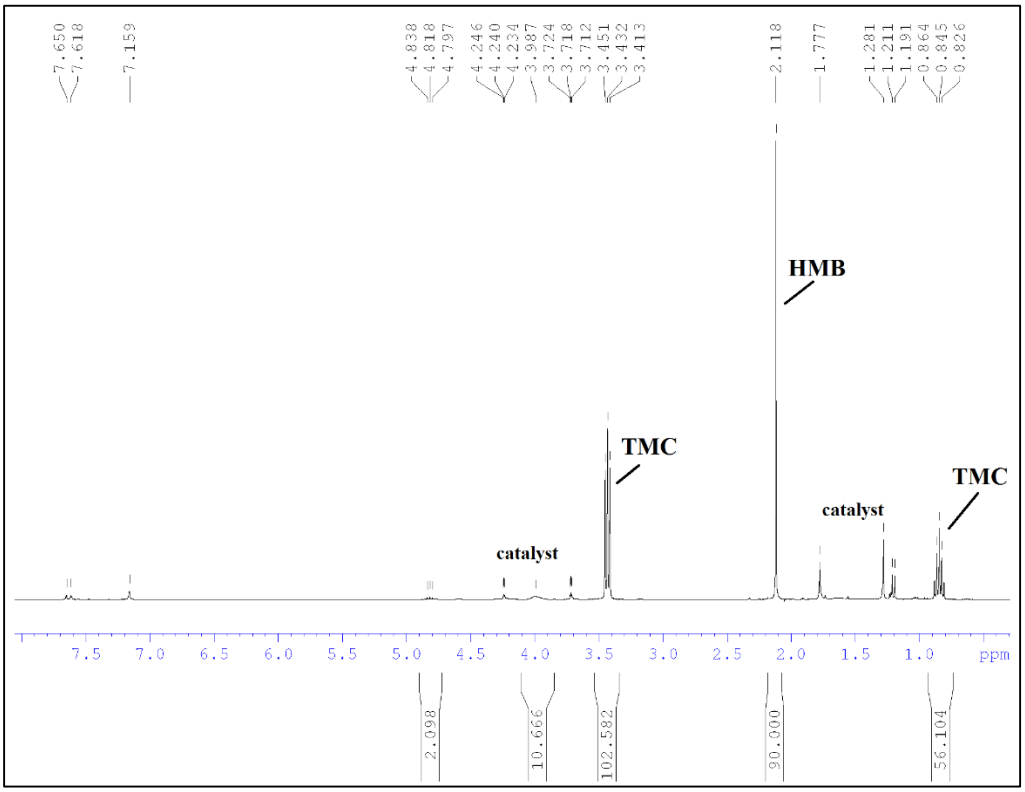

Figure S54. Polymerization of 30 equivalents of trimethylene carbonate with [(thiolfan*)Ti(O^{i}Pr)$_2$][BAr^F] at 100 °C; HMB = hexamethylbenzene (Table 2, Entry 7).

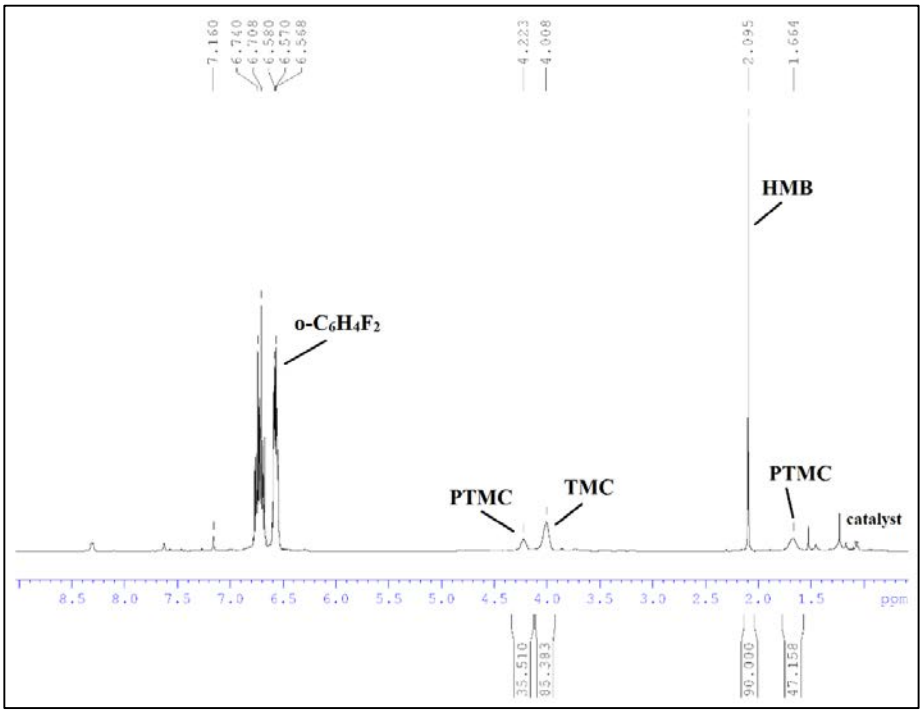

Figure S55. Polymerization of 30 equivalents of trimethylene carbonate with [(thiolfan*)Ti(O^{i}Pr)$_2$][BAr^{F}] at 70 °C; HMB = hexamethylbenzene (Table 2, Entry 8).

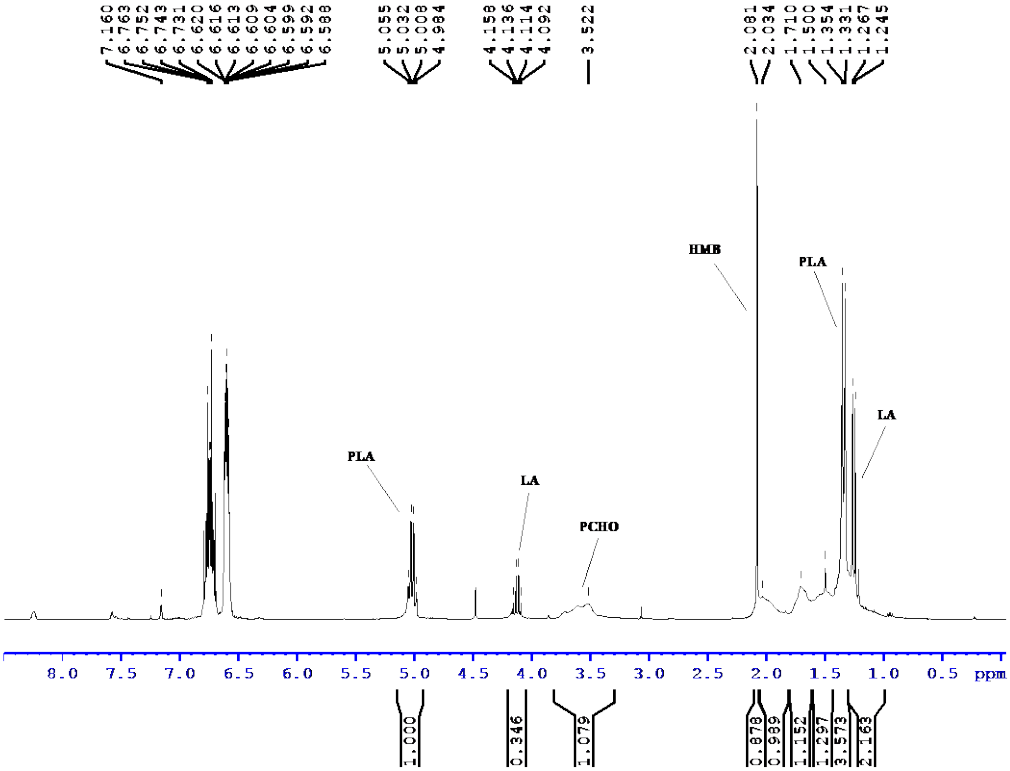

Figure S56. PLA-PCHO: Polymerization of 100 equivalents of L-lactide in the presence of 100 equivalents of cyclohexene oxide with [(thiolfan*)Ti(O^{i}Pr)$_2$][BAr^{F}] in a one-pot ox-red process (Table 3, Entry 2).

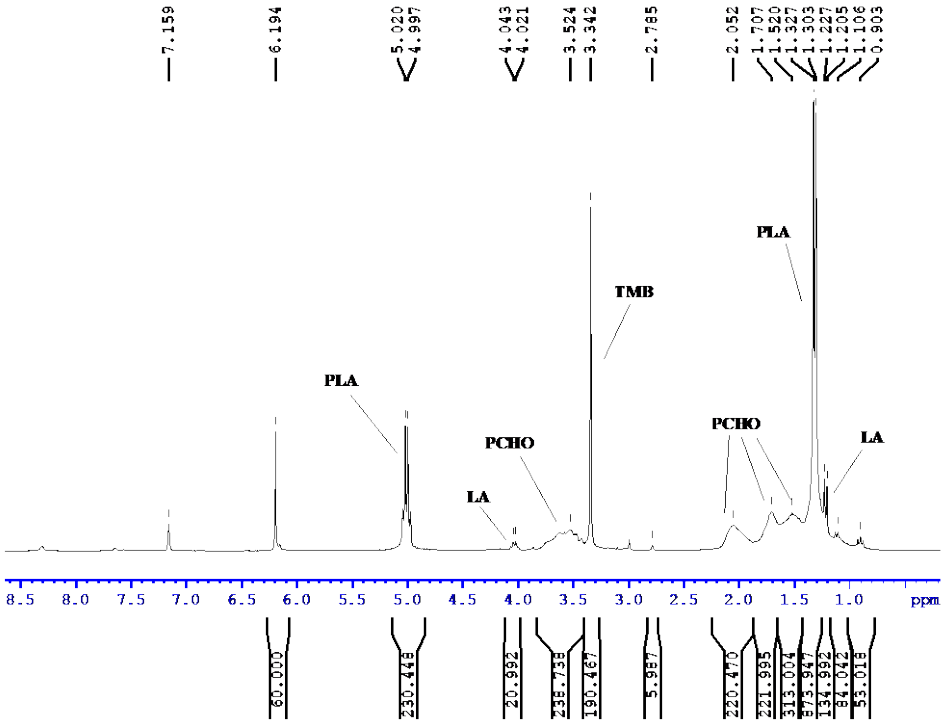

Figure S57. PCHO-PLA: Polymerization of 100 equivalents of L-lactide in the presence of 100 equivalents of cyclohexene oxide with [(thiolfan*)Ti(O^{i}Pr)$_2$] in a one-pot red-ox process; TMB = 1,3,5-trimethoxybenzene (Table 3, Entry 3).

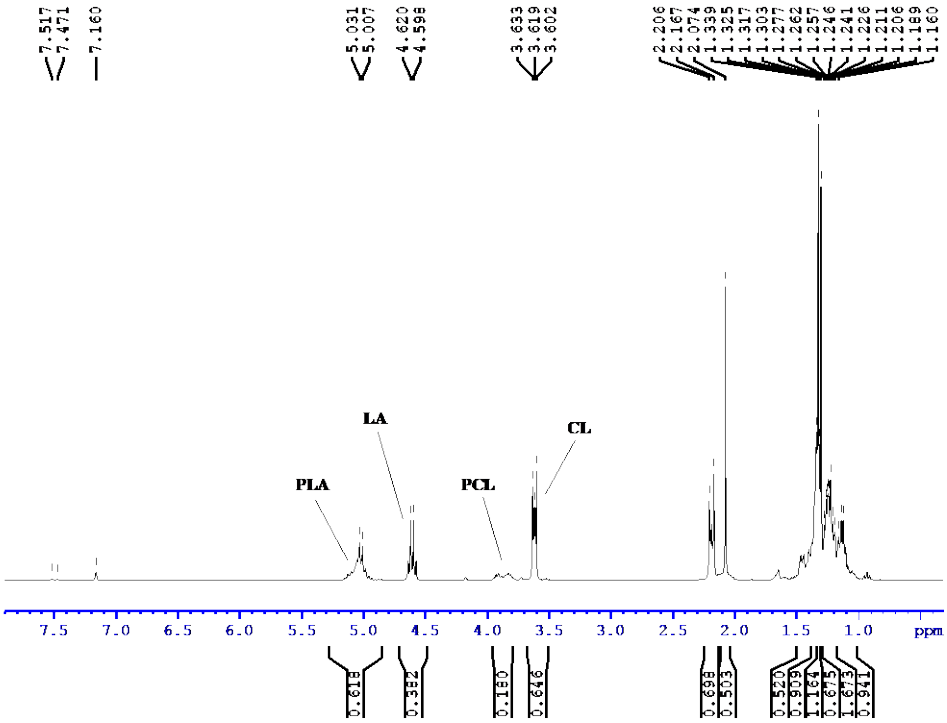

Figure S58. PLA-PCL-PLA. Polymerization of 100 equivalents of L-lactide in the presence of 100 equivalents of ε-caprolactone with [(thiolfan*)Ti(O^{i}Pr)$_2$] after 36 hours at 100 ºC (Table 3, Entry 4).

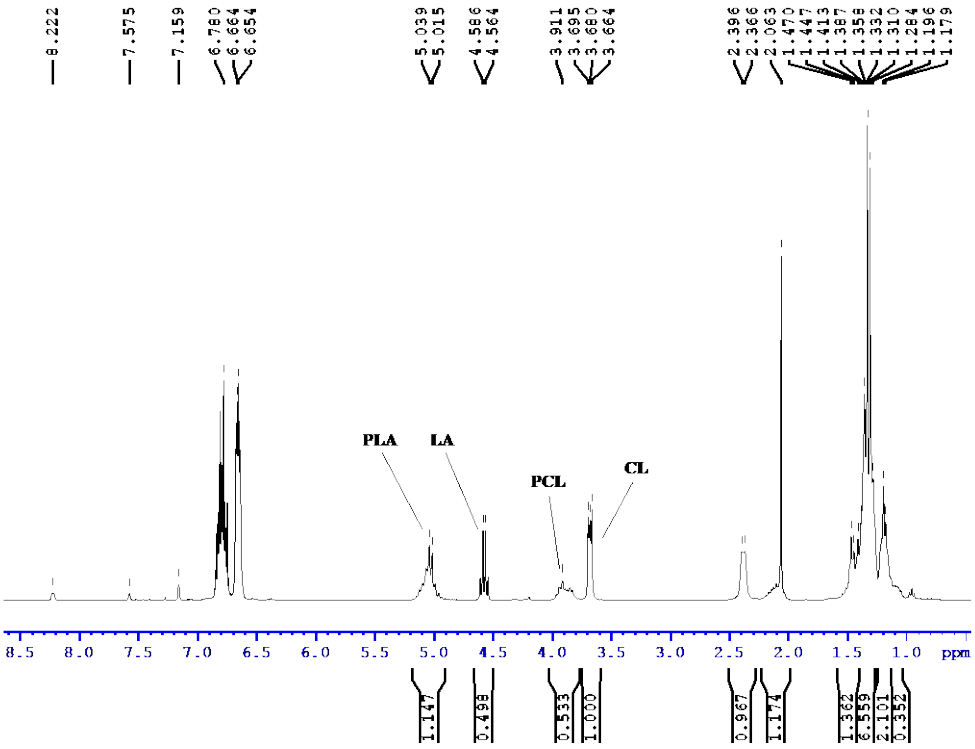

Figure S59. PLA-PCL-PLA: Polymerization of 100 equiv ε-caprolactone in the presence of 100 equiv L-lactide with [(thiolfan*)Ti(O^iPr)$_2$] after oxidation with ^{Ac}FcBAr^F for 3 h at 100 ºC (Table 3, Entry 4).

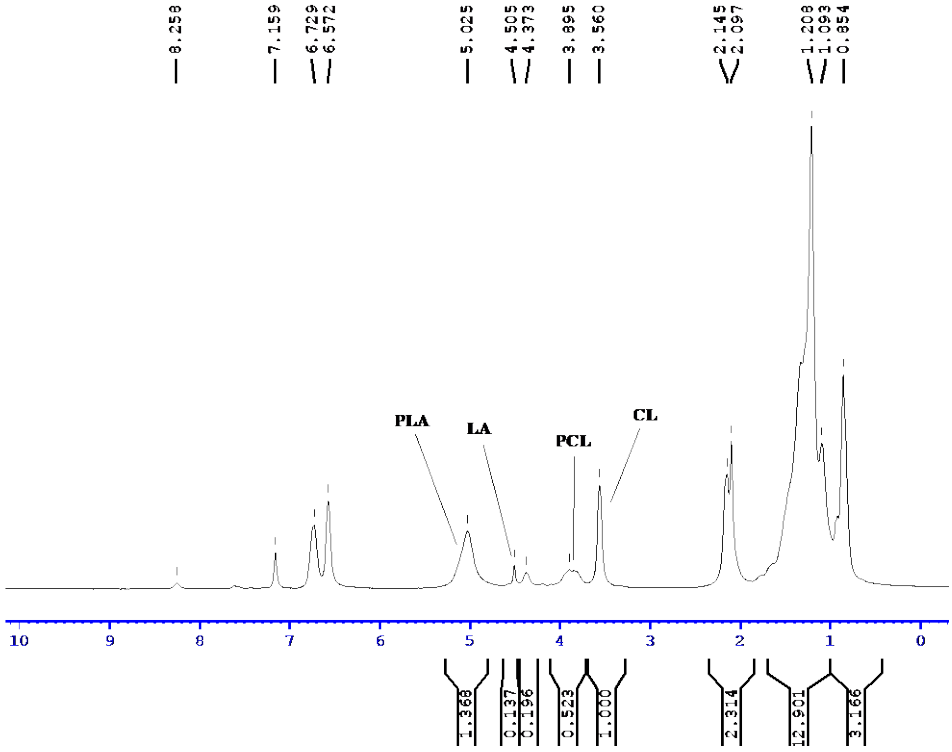

Figure S60. PLA-PCL-PLA: Polymerization of 100 equivalents of L-lactide in the presence of 100 equivalents of ε-caprolactone with [(thiolfan*)Ti(O^iPr)$_2$] after oxidation with ^{Ac}FcBAr^F for 3 hours at 100 ºC, then subsequent reduction with $CoCp_2$ at 100 ºC for 6 hours (Table 3, Entry 4).

Conversion versus molecular weight studies

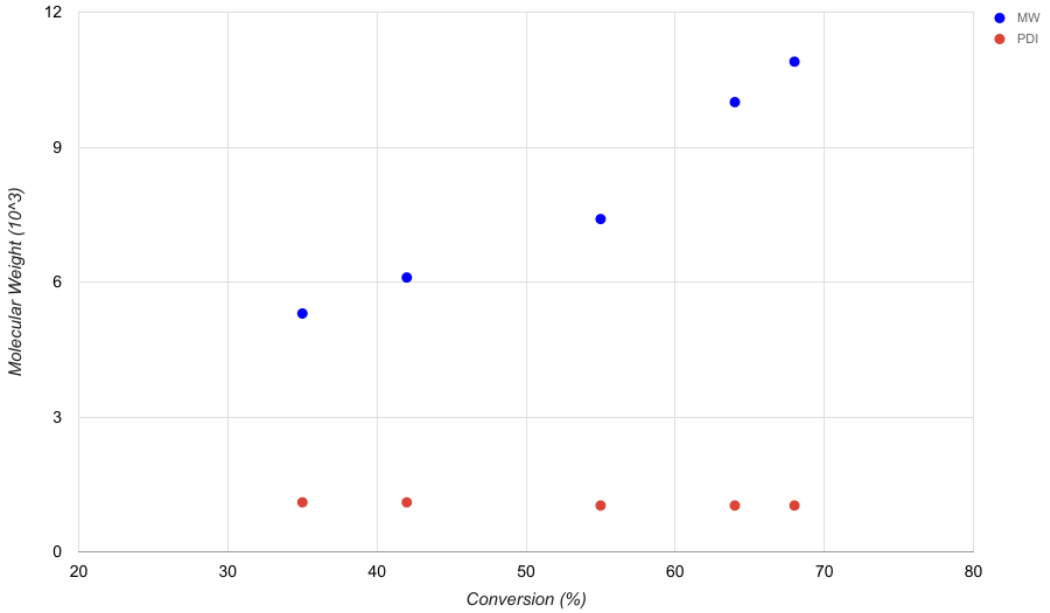

Figure S61. Conversion of L-lactide by (thiolfan*)Ti(O^iPr)$_2$ at 100 ºC.

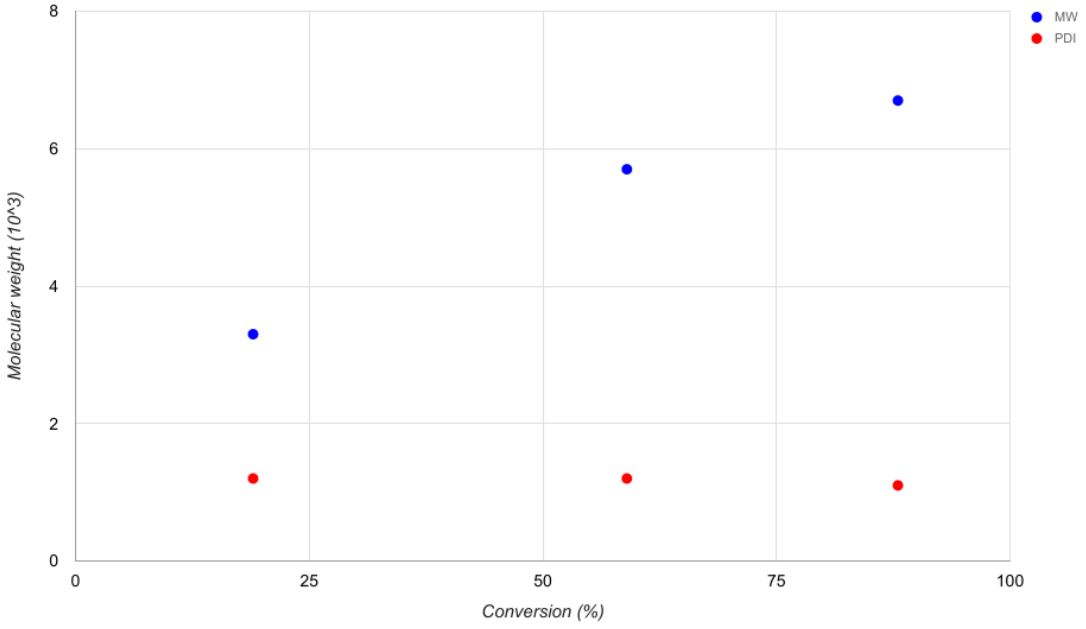

Figure S62. Conversion of ε-caprolactone by [(thiolfan*)Ti(O^iPr)$_2$][BAr^F] at 100 ºC.

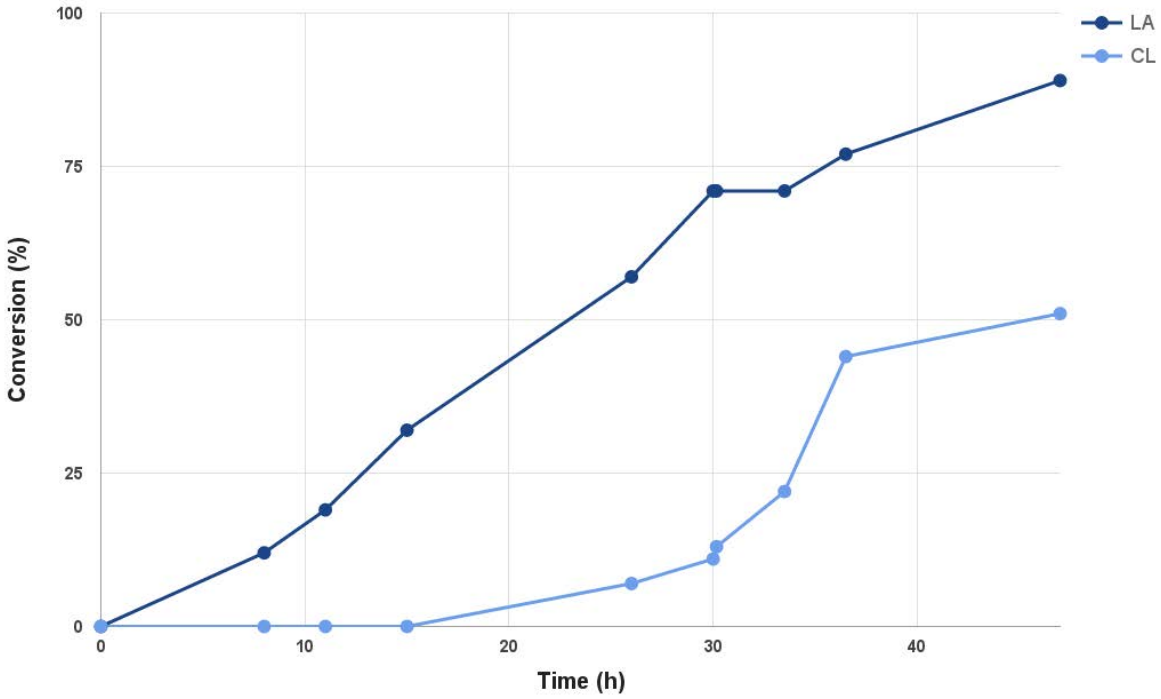

Figure S63. One-pot redox switch polymerization of LA and CL starting with (thiolfan*)Ti(O^iPr)$_2$ at 100 ºC. The oxidant (^{Ac}FcBAr^F) was added at t = 30 hours.

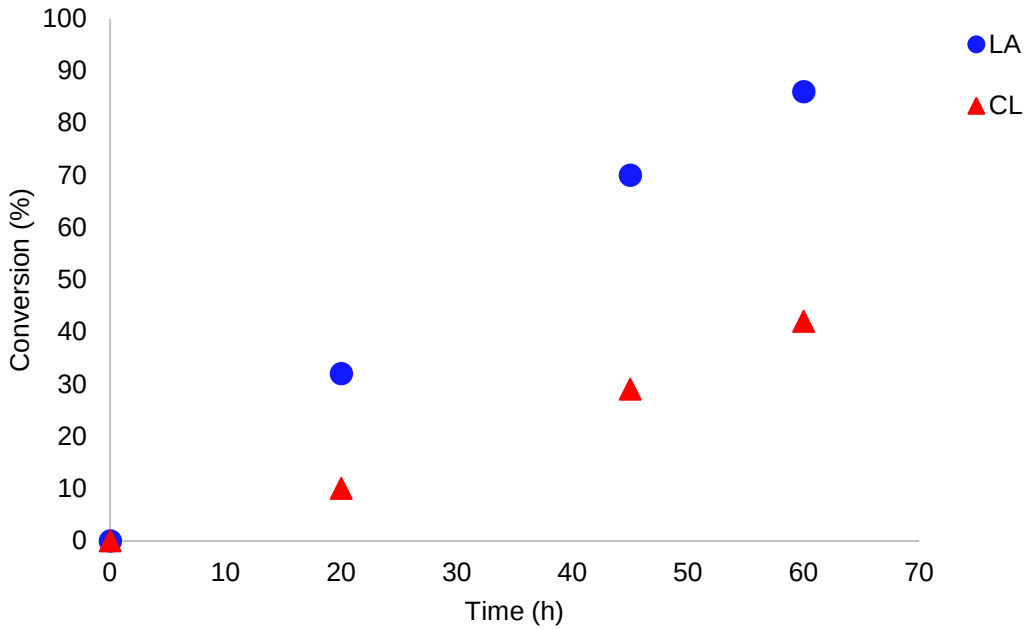

Figure S64. One-pot polymerization of LA and CL with (thiolfan*)Ti(O^iPr)$_2$ at 100 ºC.

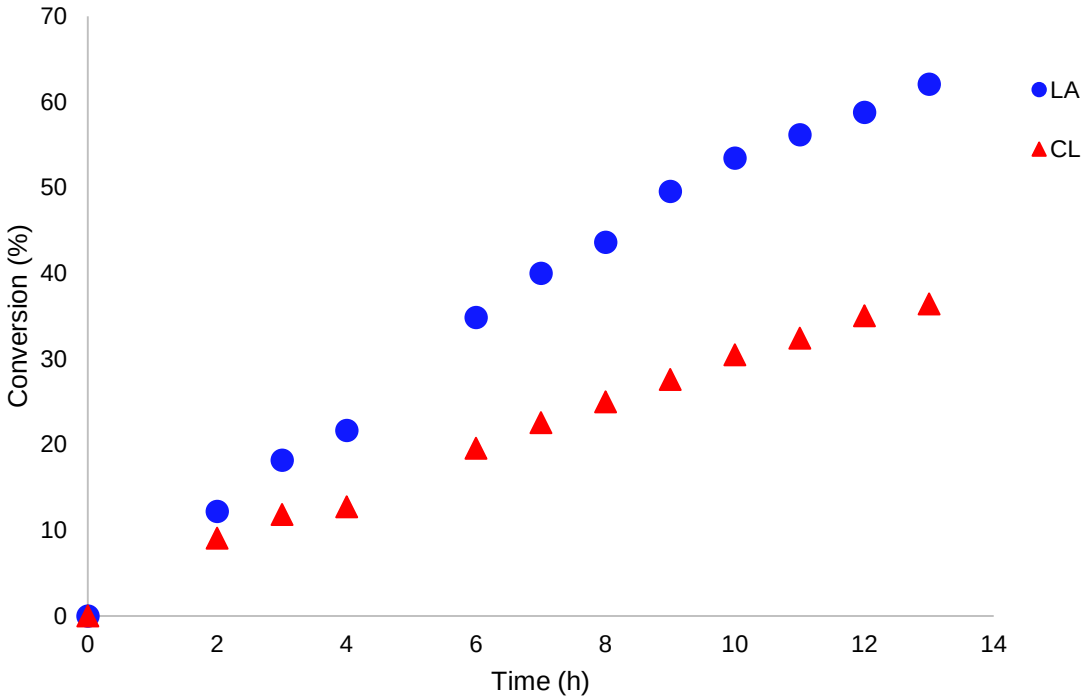

Figure S65. One-pot polymerization of LA and CL with [(thiolfan*)Ti(O^{i}Pr)$_2$][BAr^{F}] at 100 ºC.

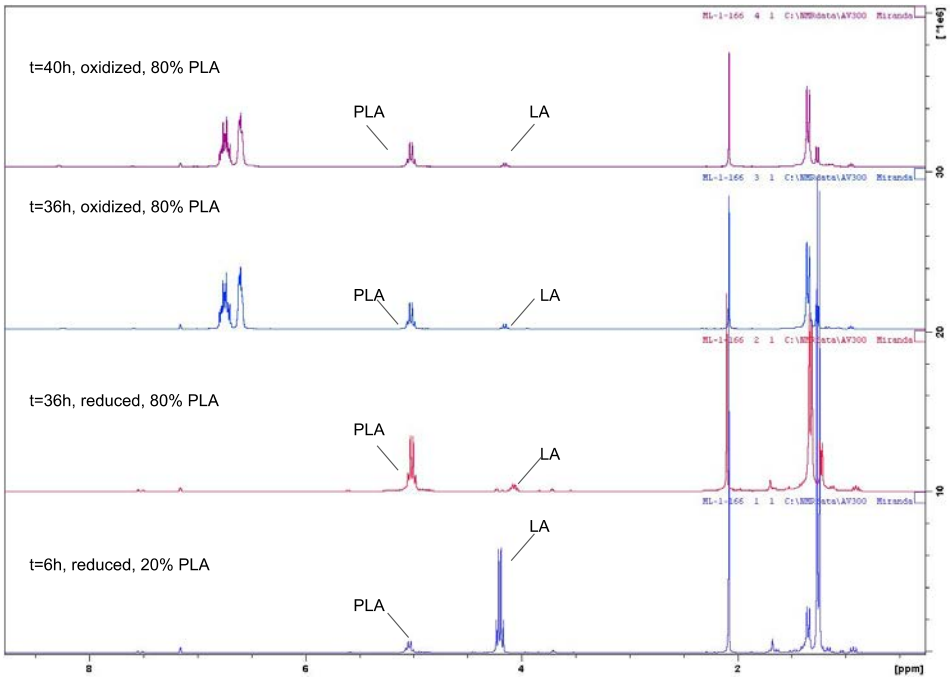

Figure S66. Redox switch of L-lactide polymerization catalyzed by (thiolfan*)Ti(O^{i}Pr)$_2$ at 100 ºC. ^{Ac}FcBAr^{F} was added at t = 36 hours.

DOSY Experiments

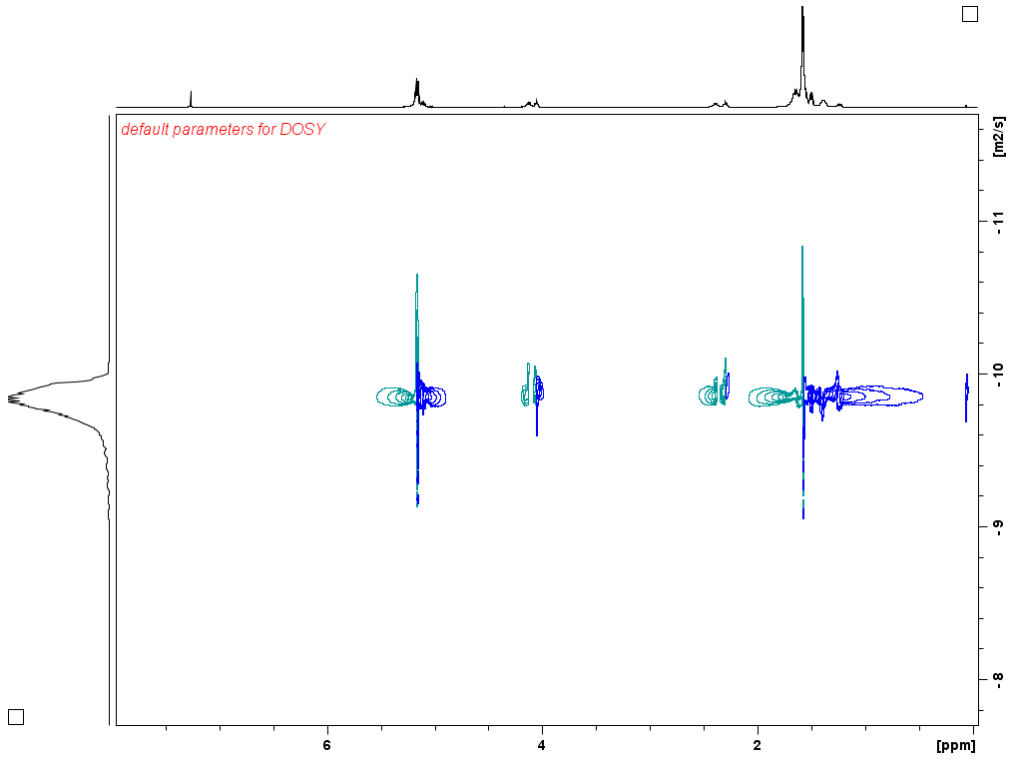

Figure S67. DOSY ^{1}H NMR (500 MHz, 25°C, C_6D_6) spectrum of a PLA-PCL diblock copolymer; D = 1.39 x 10^{-10} m^2s^{-1}

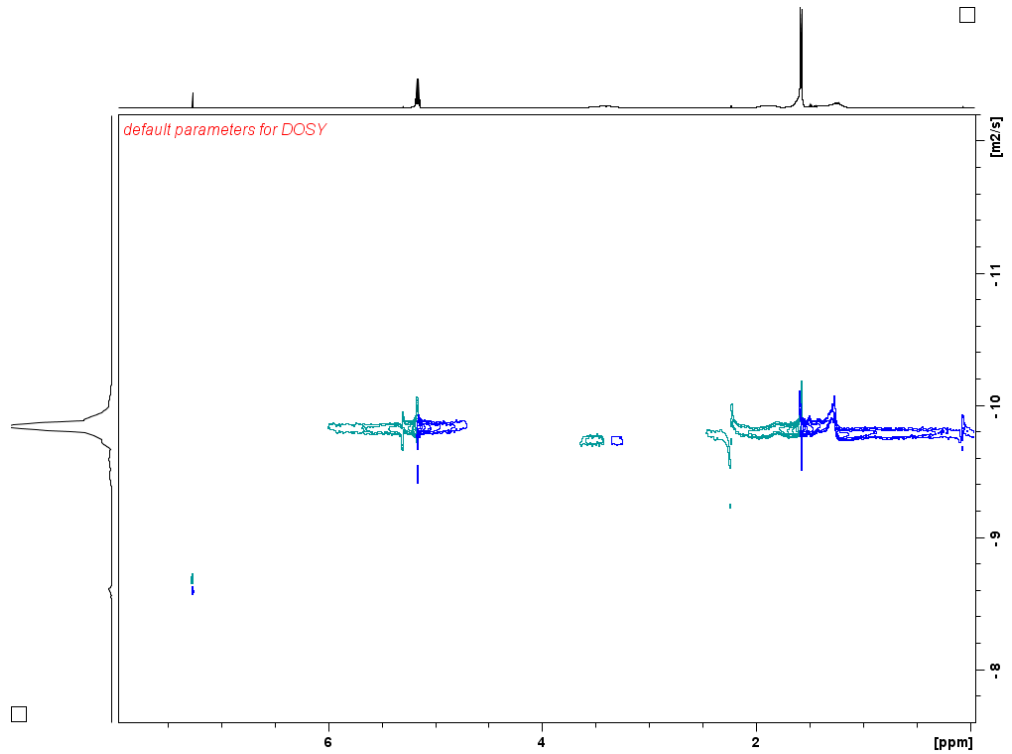

Figure S68. DOSY ^{1}H NMR (500 MHz, 25°C, C_6D_6) spectrum of a PLA-PCHO diblock copolymer; D = 1.43 x 10^{-10} m^2s^{-1}

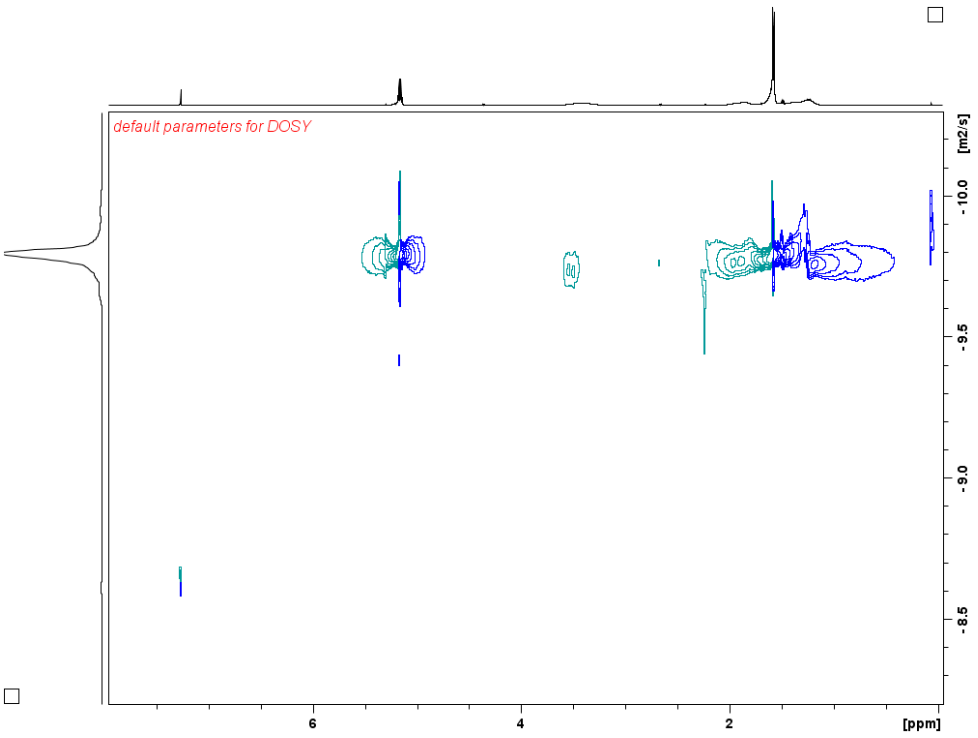

Figure S69. DOSY ^{1}H NMR (500 MHz, 25°C, C_6D_6) spectrum of a PCHO-PLA diblock copolymer; D = 1.60 x 10^{-10} m^2s^{-1}

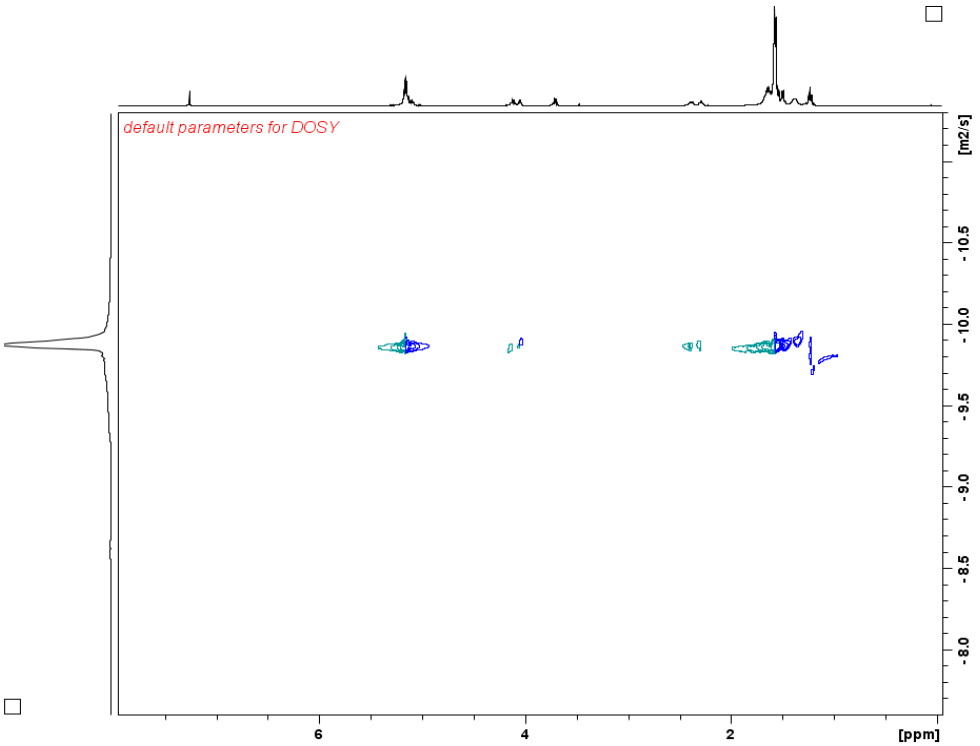

Figure S70. DOSY ^{1}H NMR (500 MHz, 25°C, C_6D_6) spectrum of a PLA-PCL-PLA triblock copolymer; D = 1.34 x 10^{-10} m^2s^{-1}

GPC Data

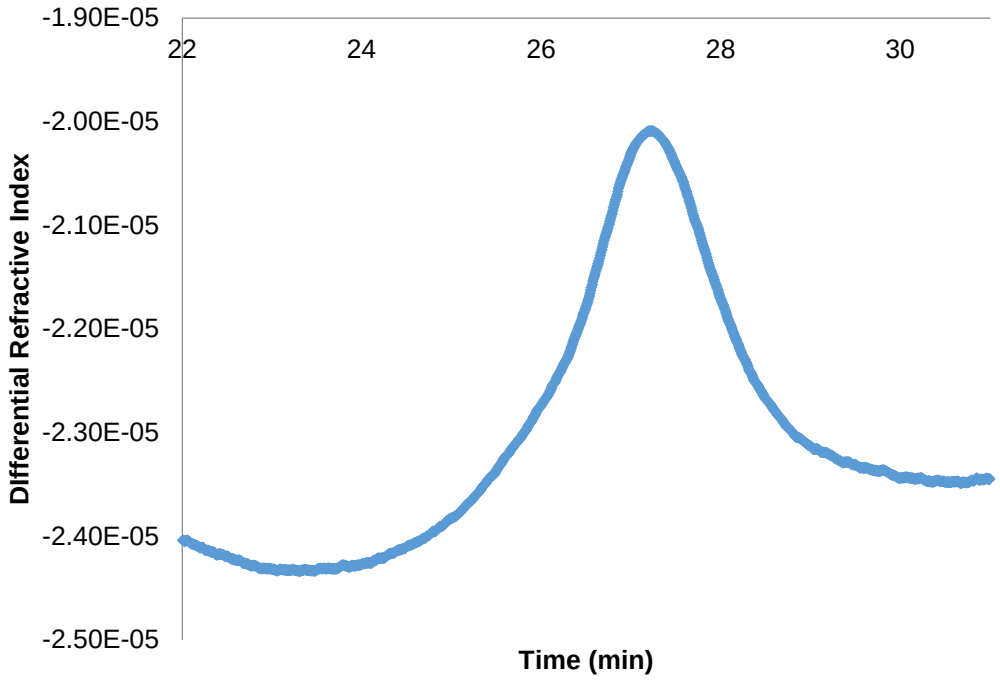

Figure S71. GPC trace from the polymerization of 100 equivalents of L-lactide at 100 ºC by (thiolfan*)Ti(O^iPr)$_2$ (Table 1, Entry 1).

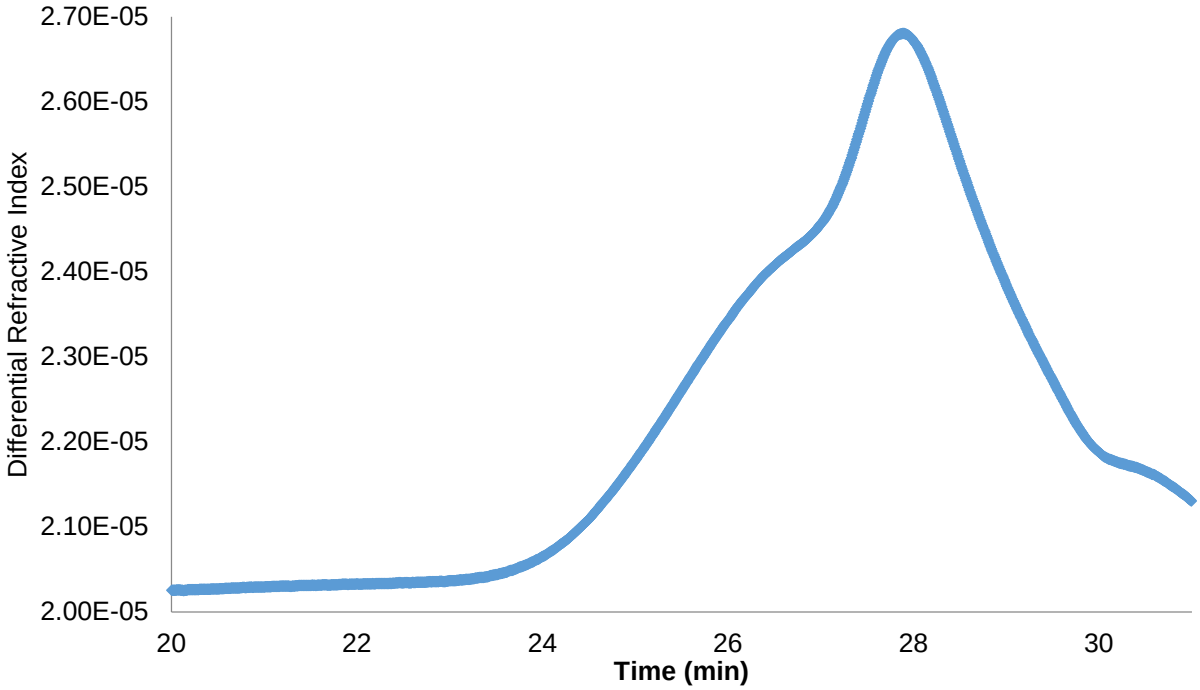

Figure S72. GPC trace from the polymerization of 100 equivalents of ε-caprolactone at 100 ºC by (thiolfan*)Ti(O^iPr)$_2$ (Table 1, Entry 3).

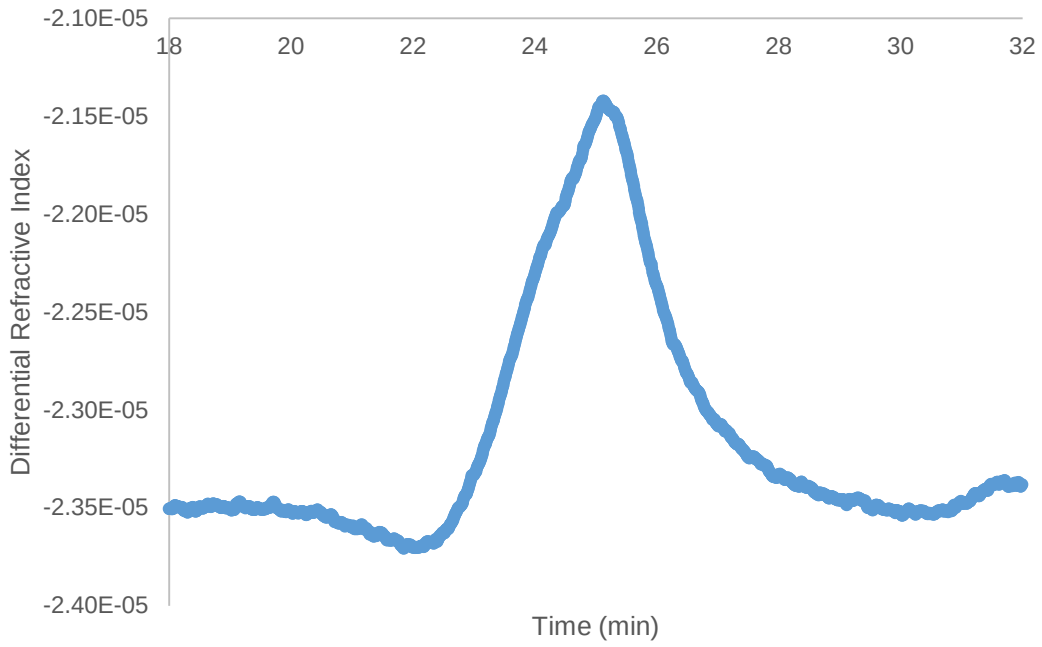

Figure S73. GPC trace from the polymerization of 100 equivalents of ε-caprolactone at 100 ºC by [(thiolfan*)Ti(O^{i}Pr)$_2$][BAr^{F}] (Table 1, Entry 4).

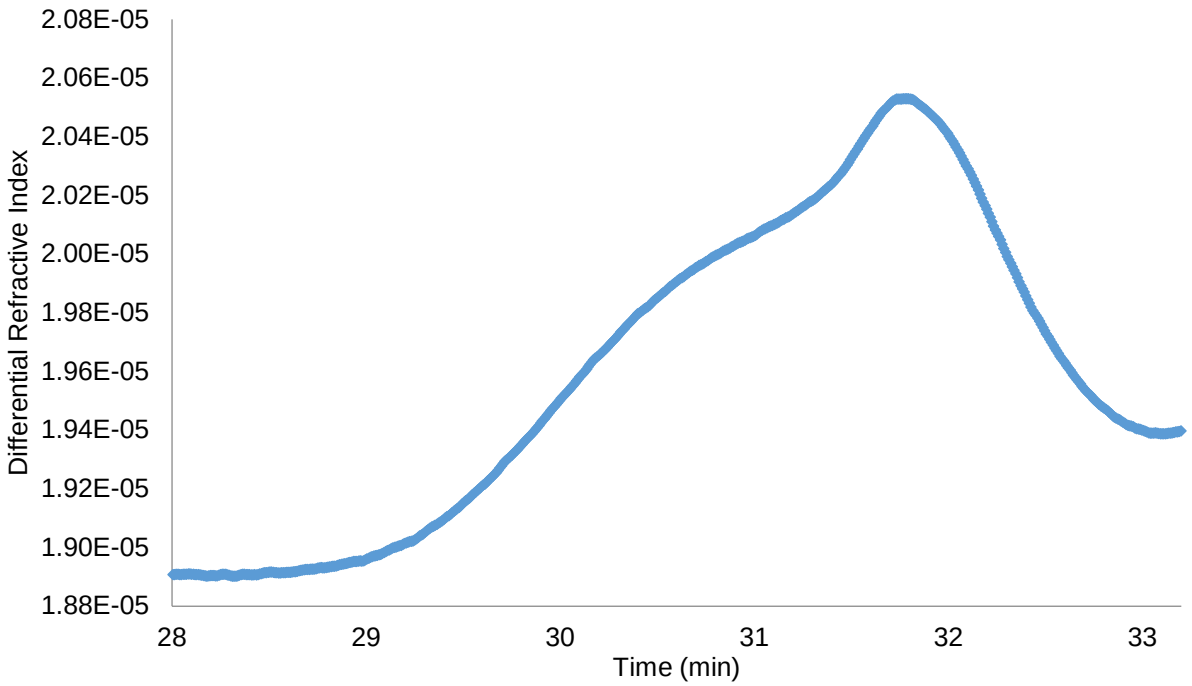

Figure S74. GPC trace from the polymerization of 100 equivalents of L-lactide at 70 ºC by (thiolfan*)Zr(O^{t}Bu)$_2$ (Table 1, Entry 5).

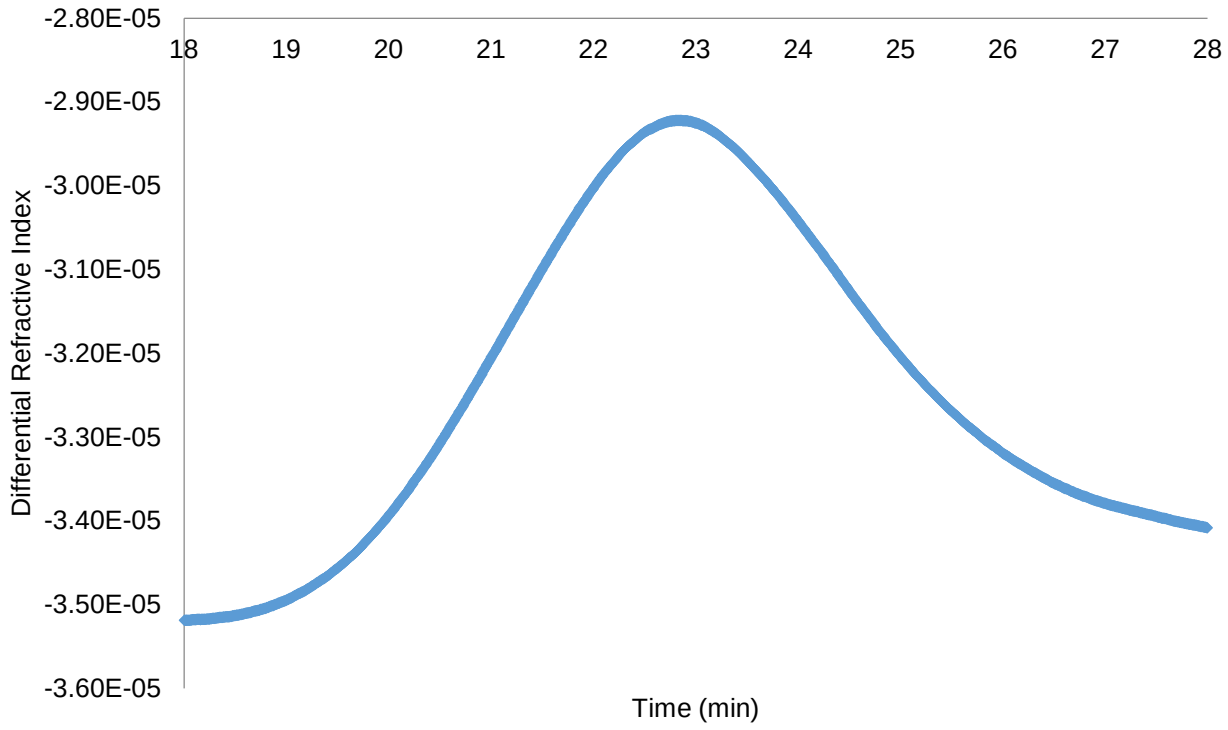

Figure S75. GPC trace from the polymerization of 100 equivalents of ε-caprolactone at 100 ºC by (thiolfan*)Zr(O^{t}Bu)$_2$ (Table 1, Entry 7).

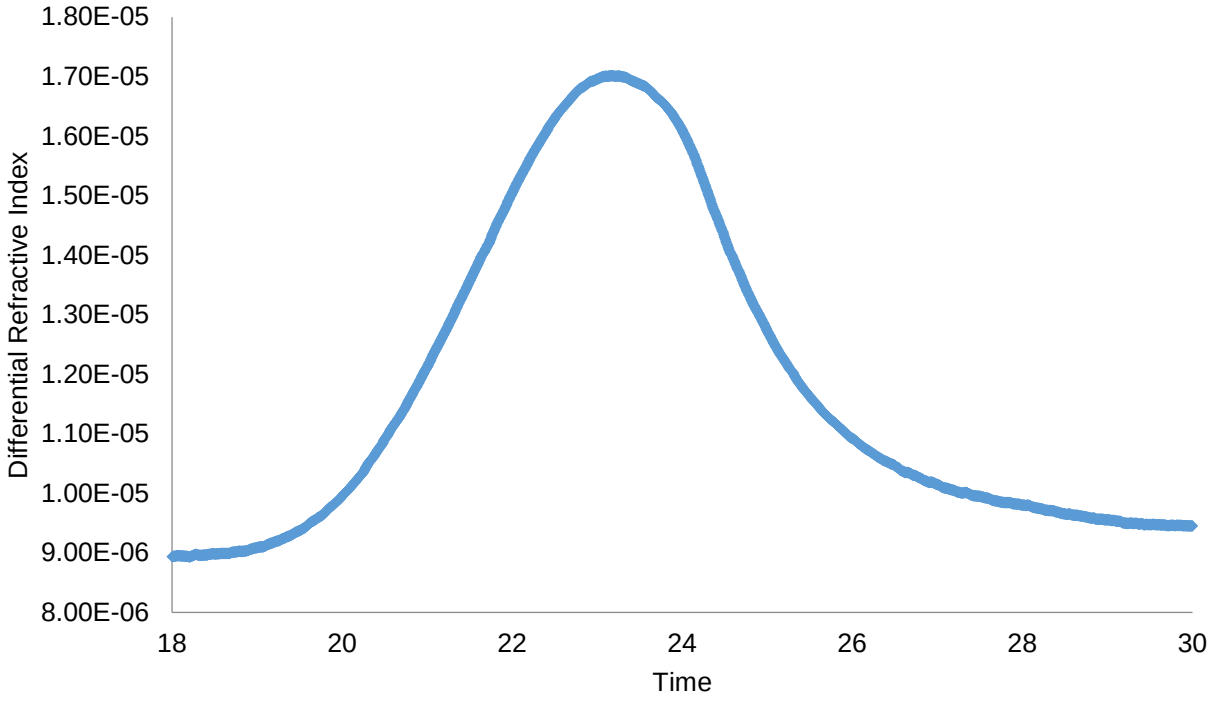

Figure S76. GPC trace from the polymerization of 100 equivalents of ε-caprolactone at 100 ºC by [(thiolfan*)Zr(O^{t}Bu)$_2$][BAr^F] (Table 1, Entry 8).

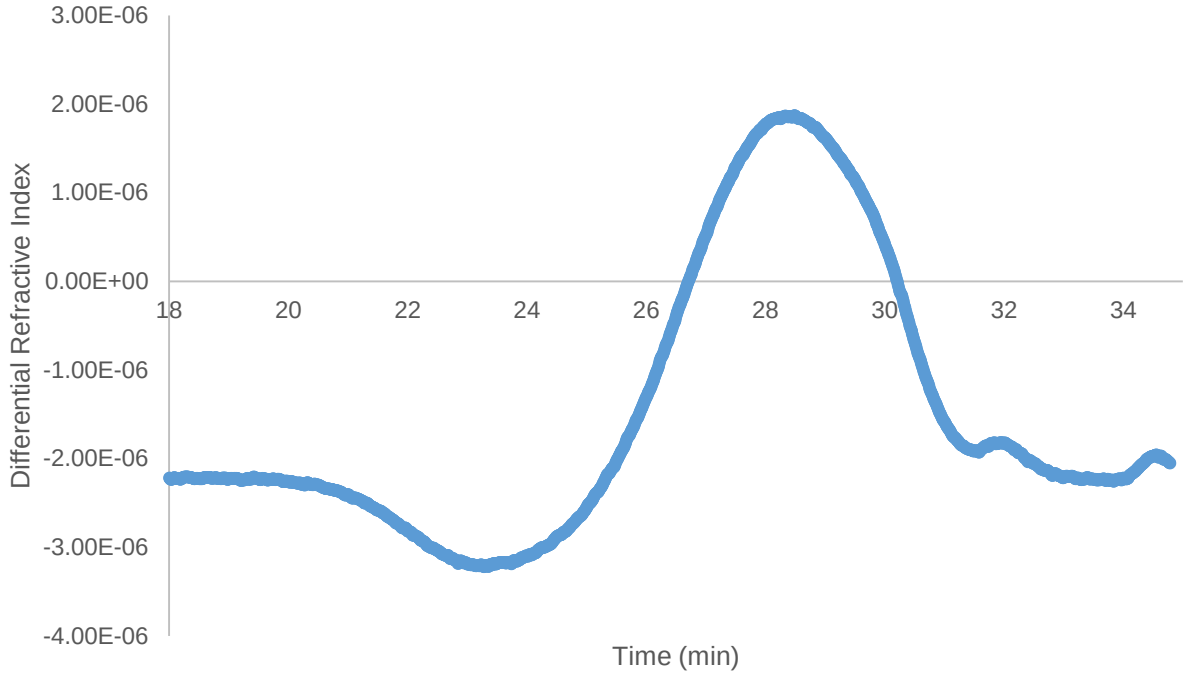

Figure S77. GPC trace from the polymerization of 100 equivalents of cyclohexene oxide at 100 ºC by [(thiolfan*)Ti(O^{i}Pr)$_2$][BAr^{F}] (Table 2, Entry 2).

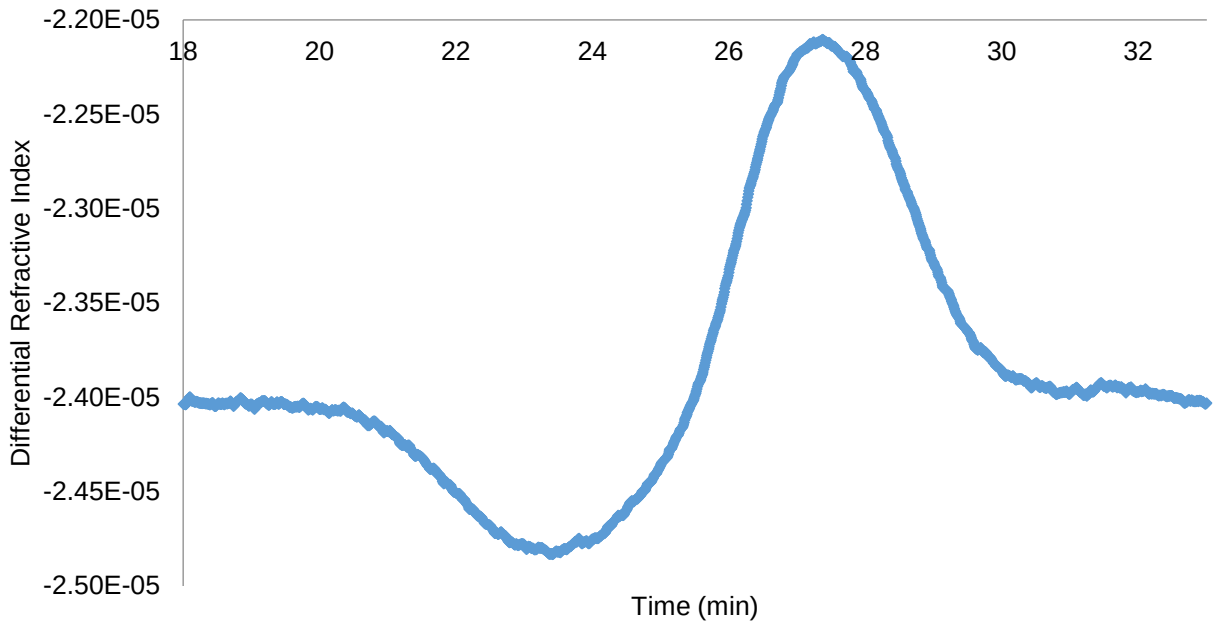

Figure S78. GPC trace from the polymerization of 100 equivalents of δ-valerolactone at 100 ºC by [(thiolfan*)Ti(O^{i}Pr)$_2$][BAr^{F}] (Table 2, Entry 4).

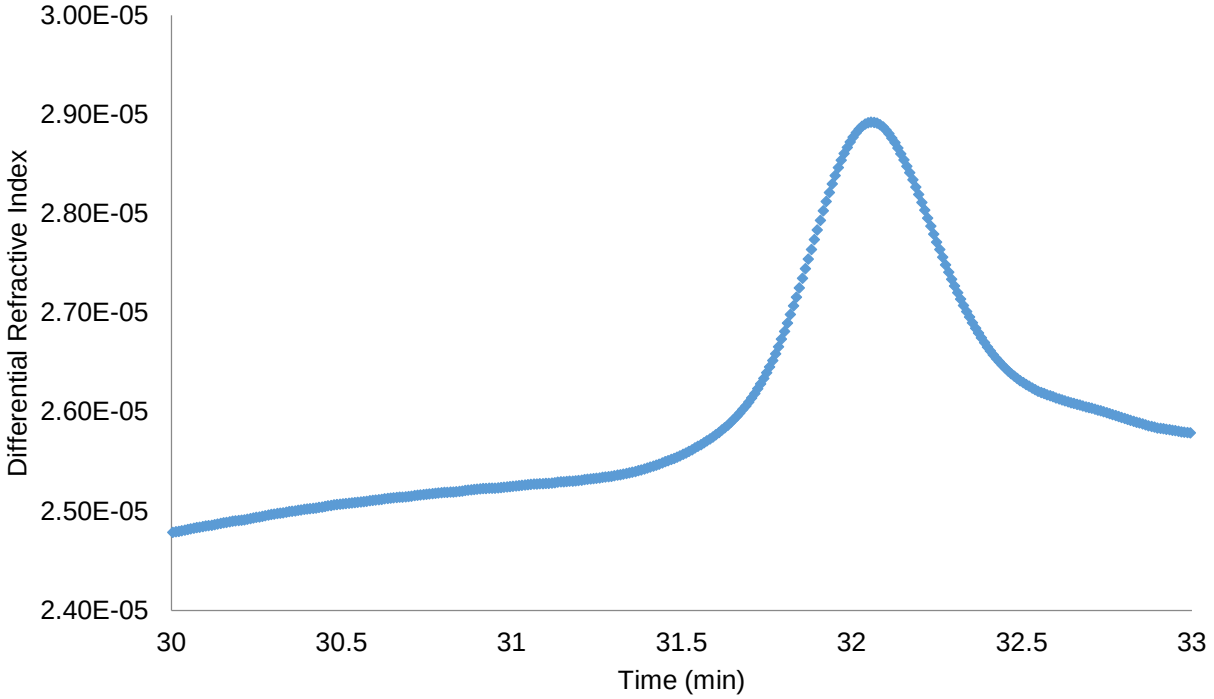

Figure S79. GPC trace from the polymerization of 100 equivalents of β-butyrolactone at 100 ºC by [(thiolfan*)Ti(O^{i}Pr)$_2$][BAr^{F}] (Table 2, Entry 6).

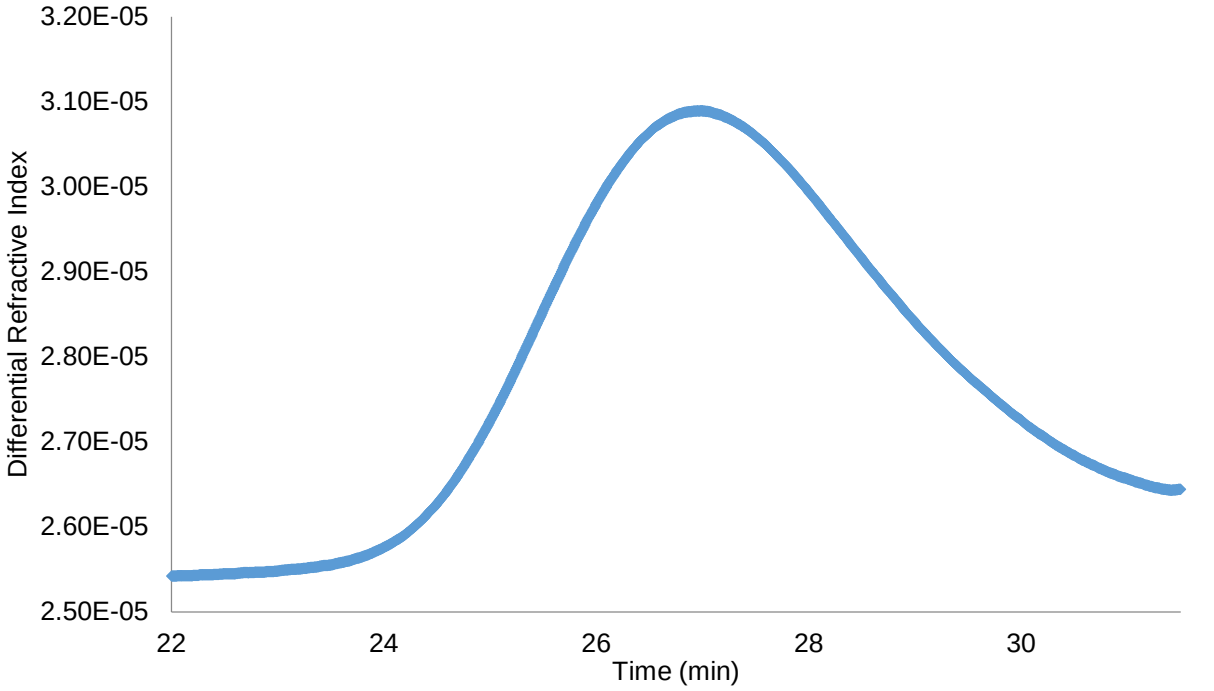

Figure S80. GPC trace from the polymerization of 100 equivalents of trimethylene carbonate at 100 ºC by [(thiolfan*)Ti(O^{i}Pr)$_2$][BAr^{F}] (Table 2, Entry 8).

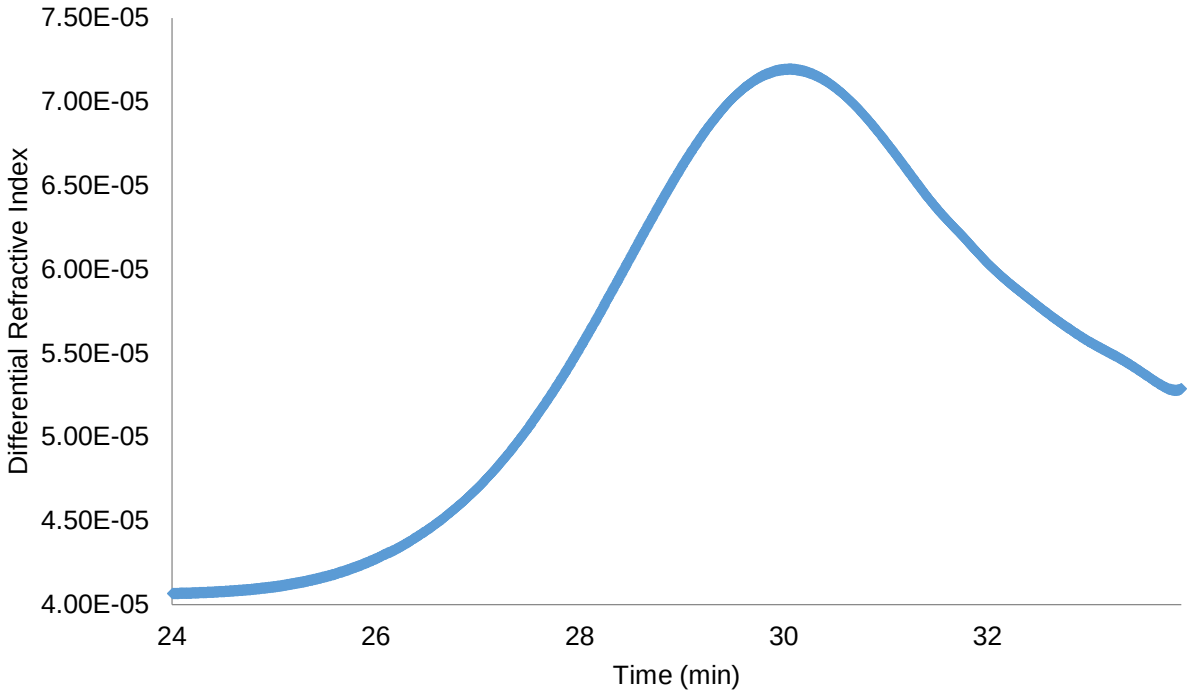

Figure S81. GPC trace from the polymerization of 100 equivalents of oxetane at 100 ºC by [(thiolfan*)Ti(O^iPr)$_2$][BAr^F] (Table 2, Entry 10).

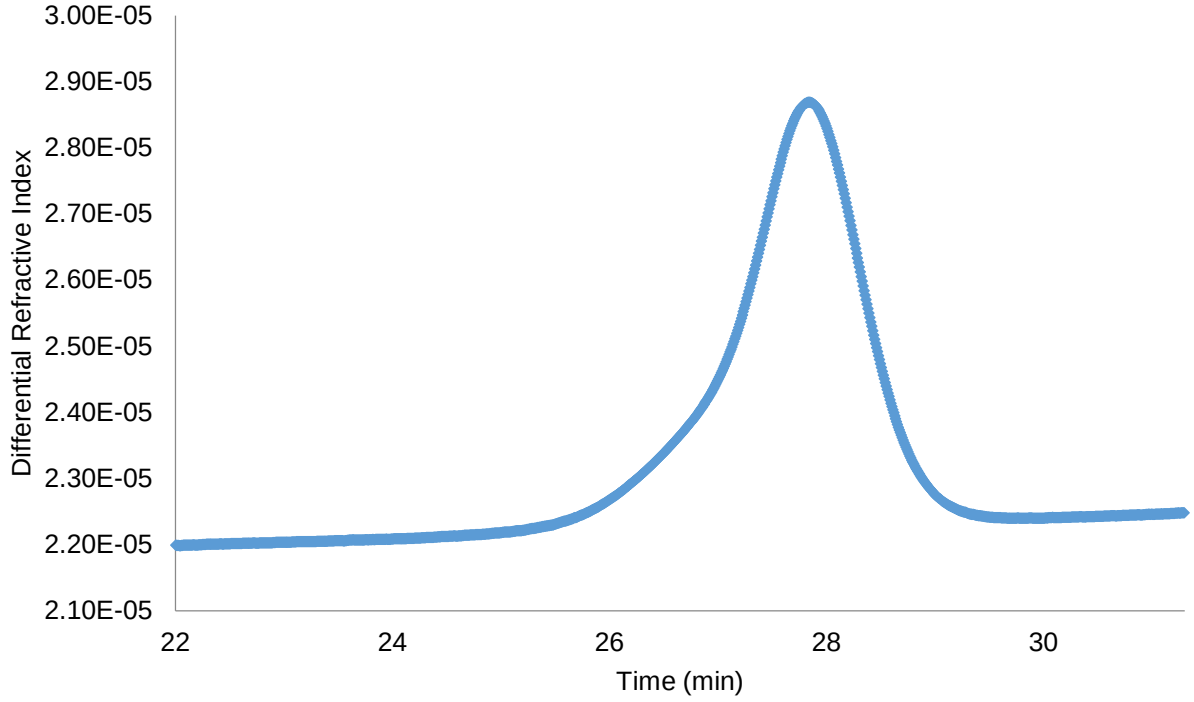

Figure S82. GPC trace of PLA-PCL formed in an one-pot red-ox polymerization starting with (thiolfan*)Ti(O^iPr)$_2$ (Table 3, Entry 1).

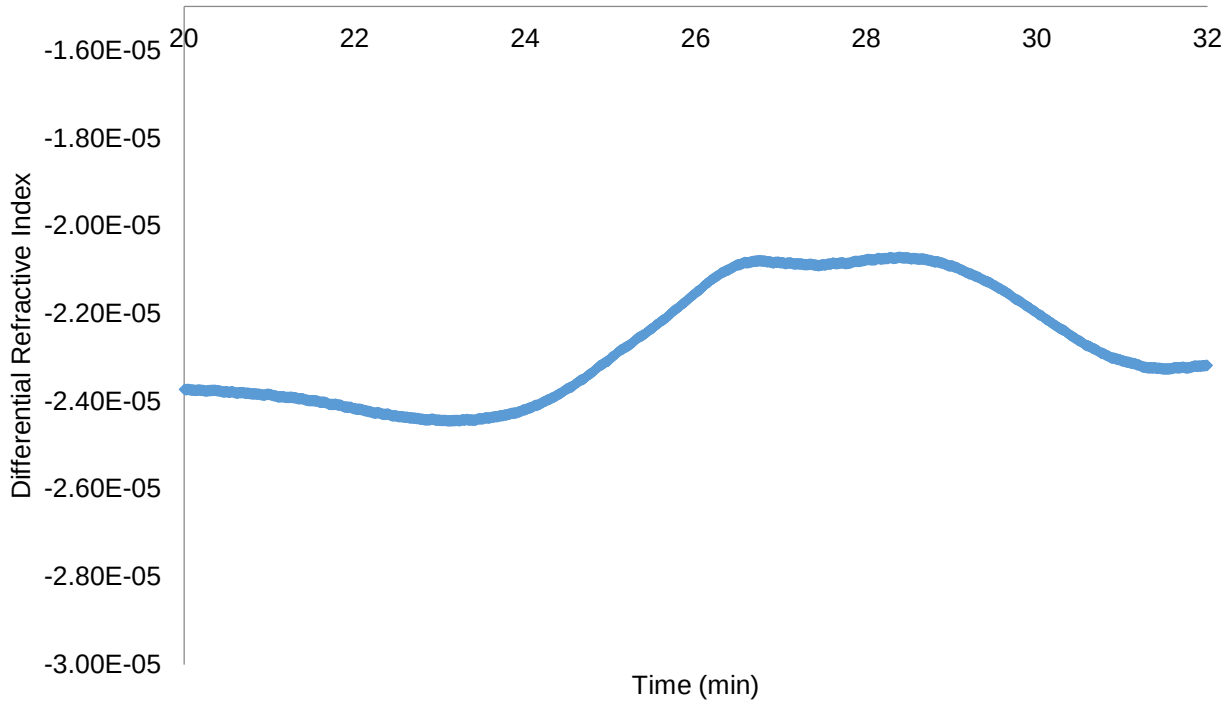

Figure S83. GPC trace of PLA-PCHO from an one-pot red-ox polymerization process starting with the reduced species, (thiolfan*)Ti(O^iPr)$_2$ (Table 3, Entry 2).

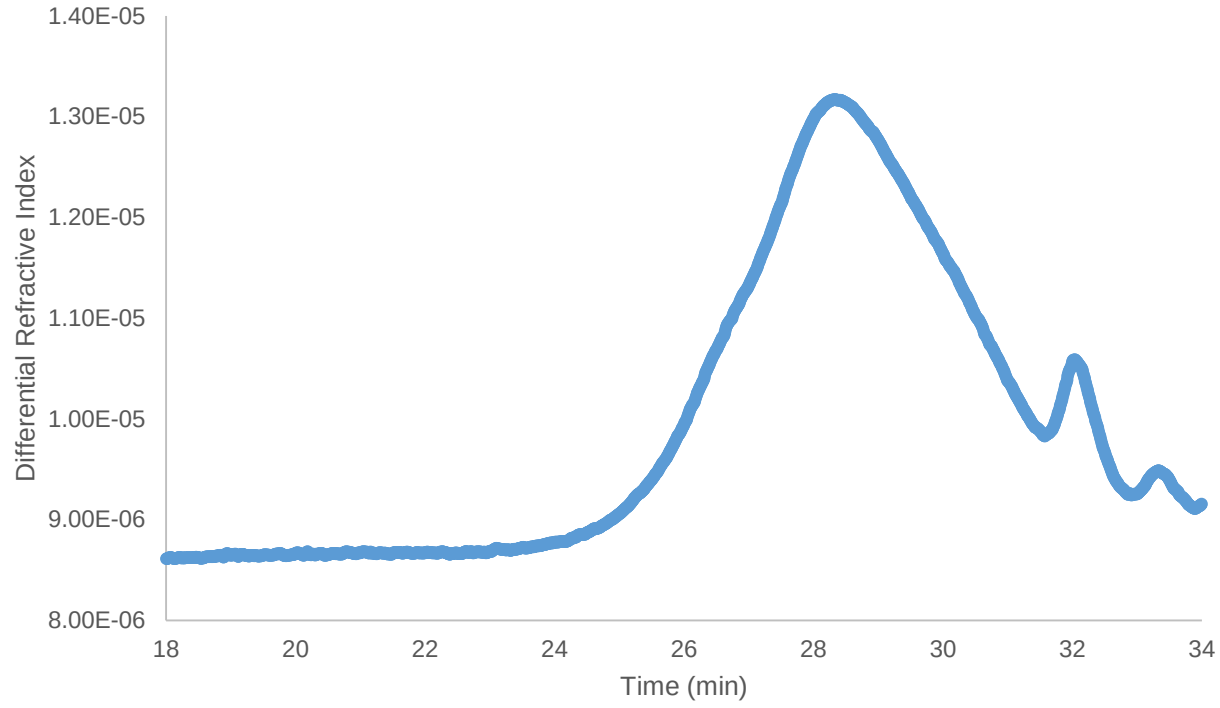

Figure S84. GPC trace of PCHO-PLA formed in an one-pot ox-red polymerization starting with [(thiolfan*)Ti(O^iPr)$_2$][BAr^F] (Table 3, Entry 3).

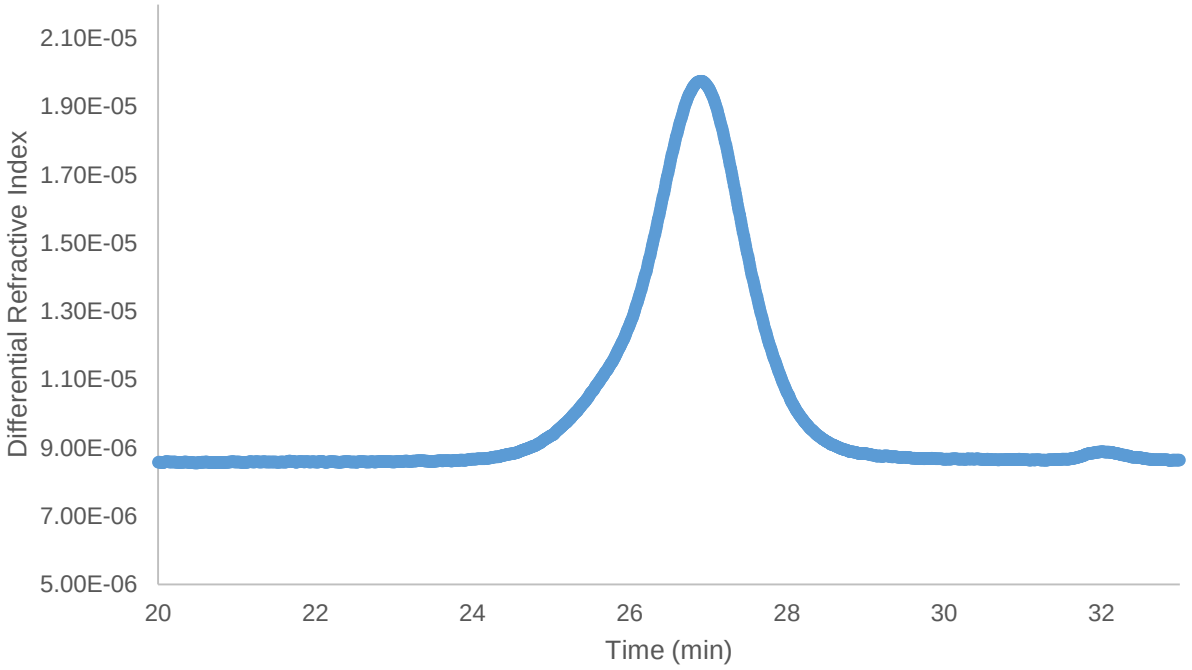

Figure S85. GPC trace of PLA-PCL-PLA from an one-pot red-ox-red polymerization process starting with the reduced species, (thiolfan*)Ti(O^iPr)$_2$ (Table 3, Entry 4).

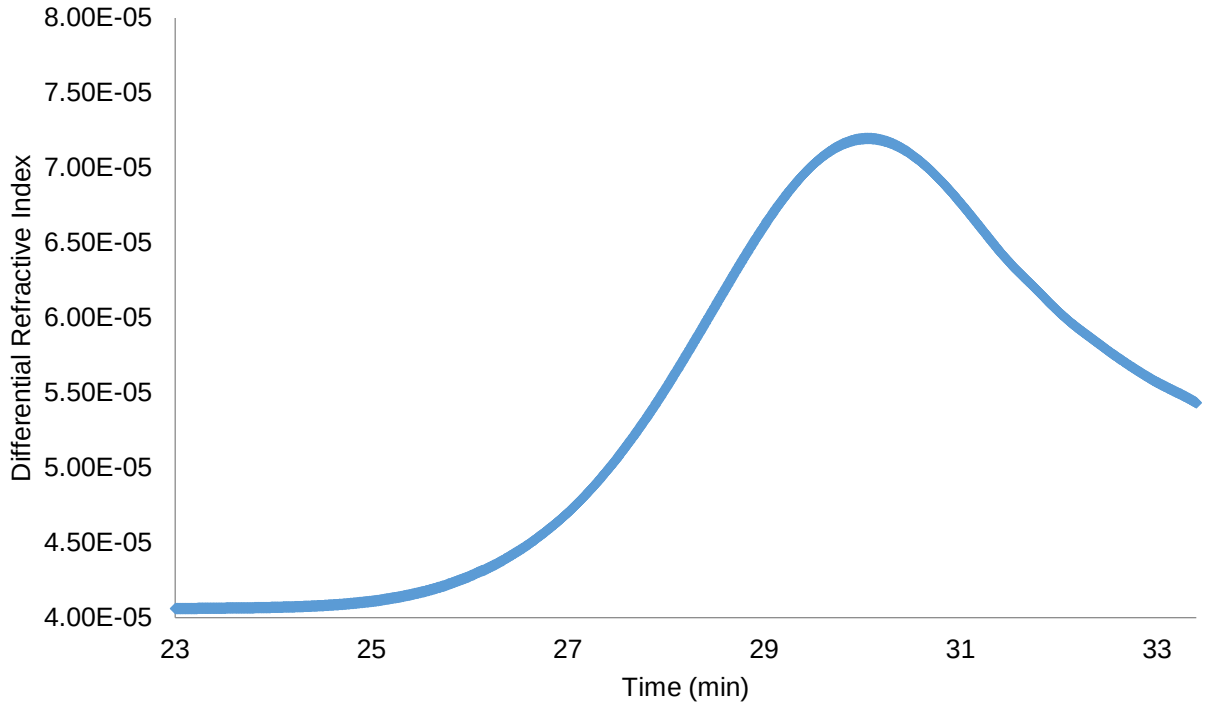

Figure S86. GPC trace for the polymerization of 100 equivalents of ε-caprolactone at 100 ºC by ^{Ac}FcBAr^F (Table S1, Entry 2).

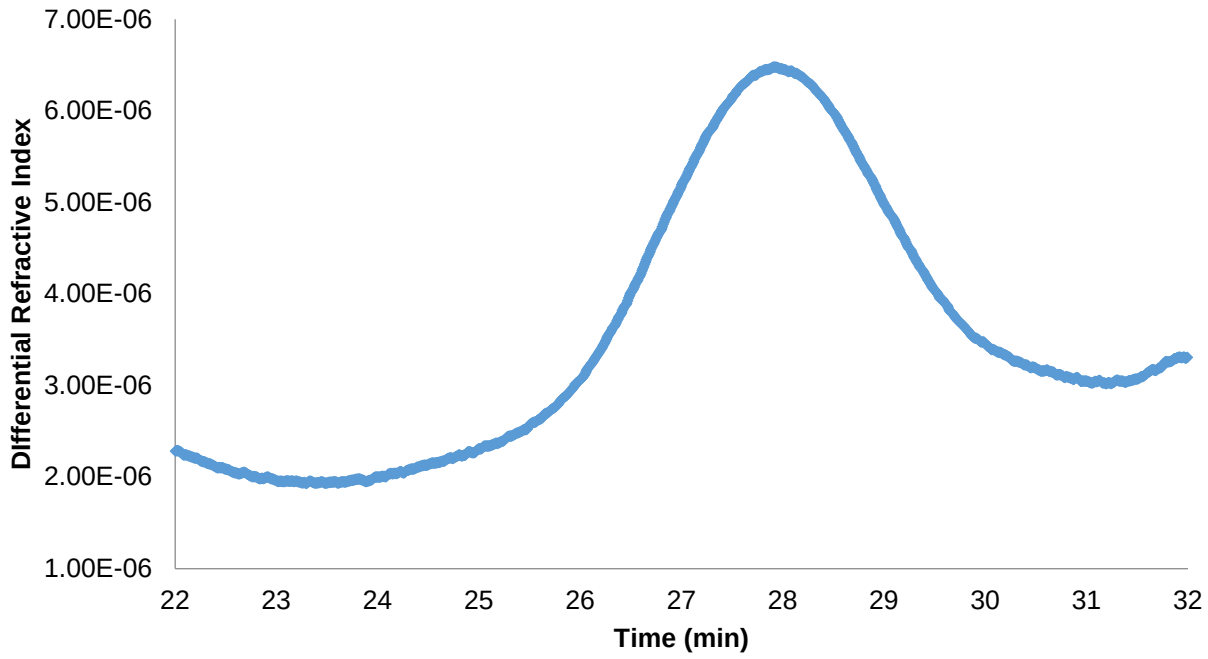

Figure S87. GPC trace for the polymerization of 100 equivalents of δ-valerolactone at 100 ºC by ^{Ac}FcBAr^{F} (Table S1, Entry 3).

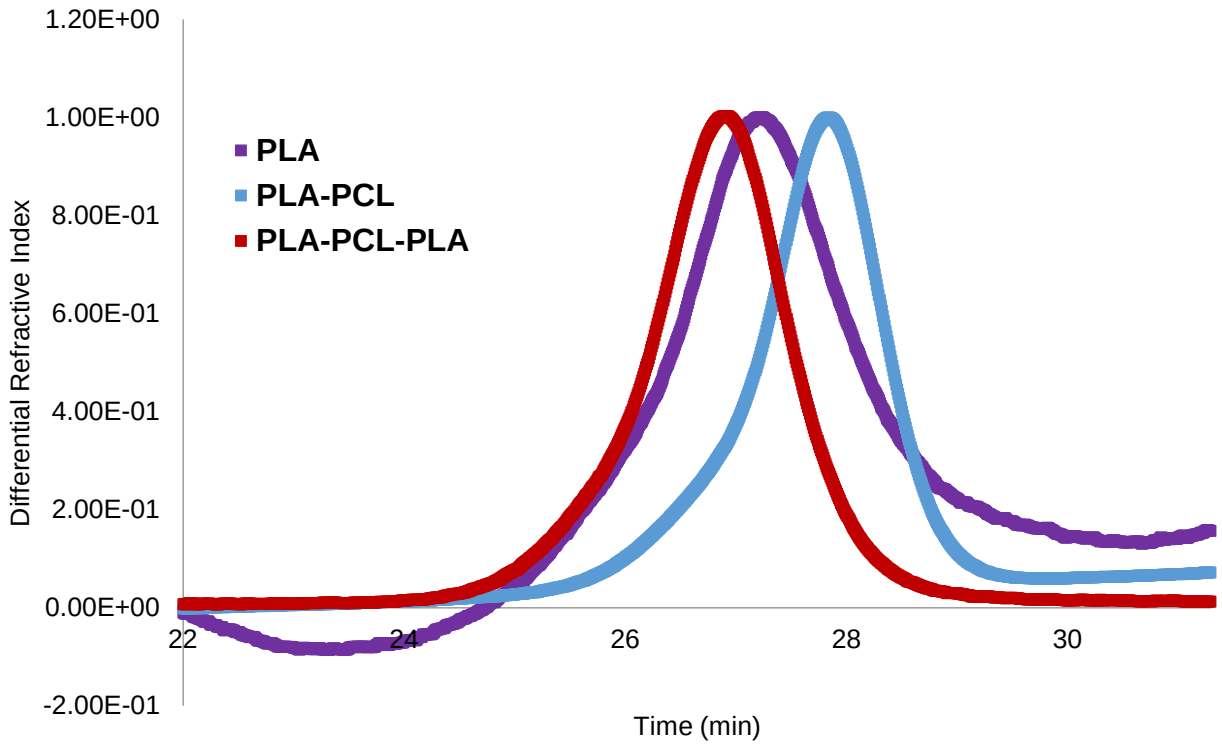

Figure S88. GPC traces for each step of the polymerization to form the PLA-PCL-PLA copolymer (Table S3, entries 1ac).

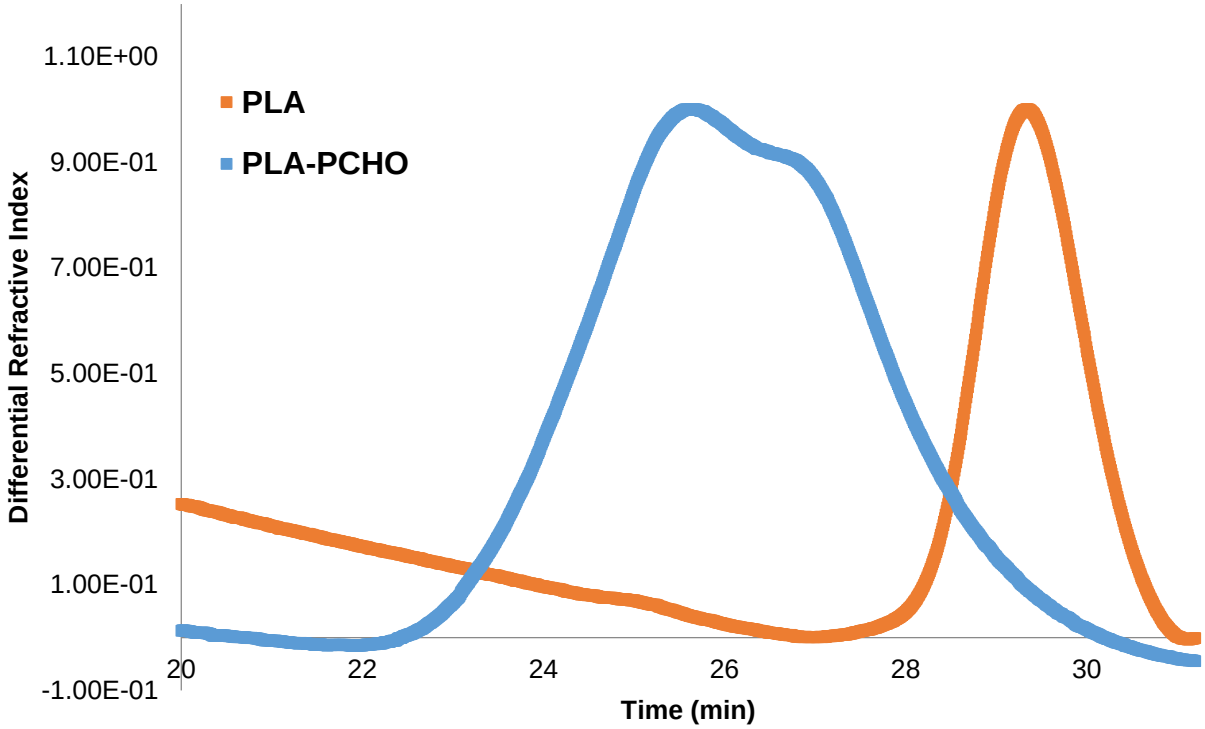

Figure S89. GPC traces for each step of the polymerization to form the PLA-CHO copolymer (Table S3, entries 2ab).

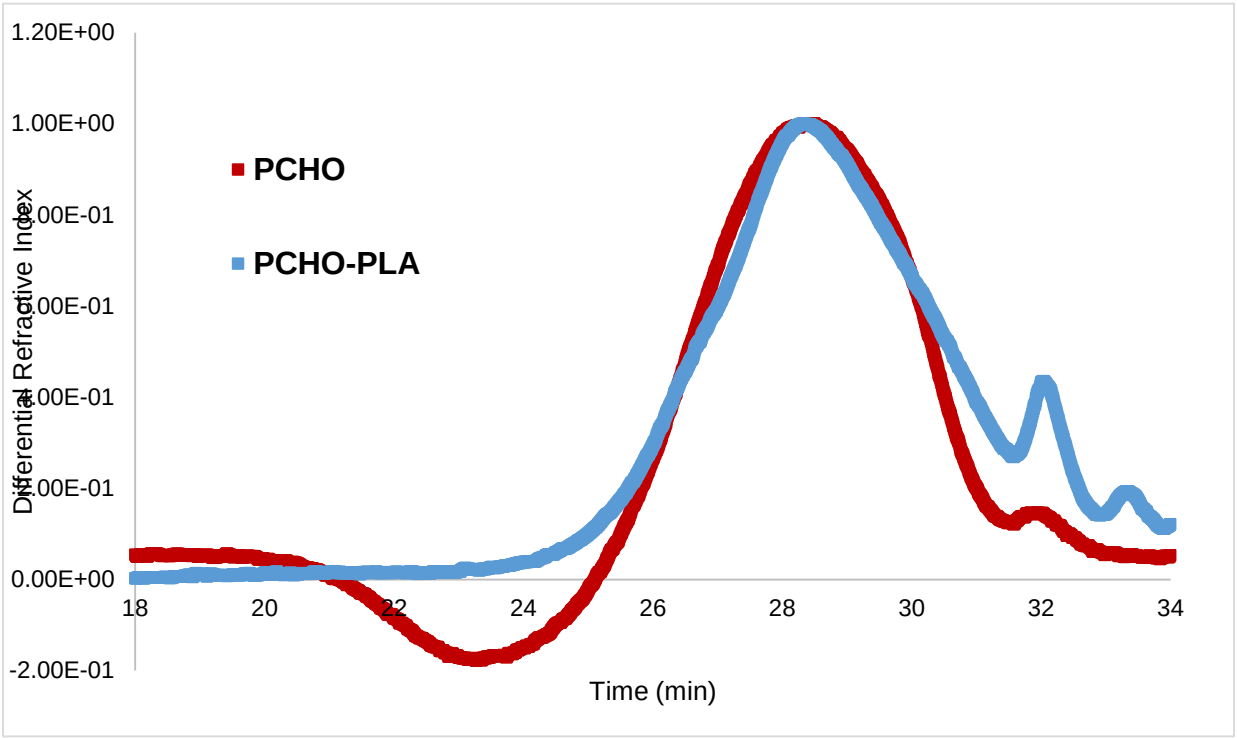

Figure S90. GPC traces for each step of the polymerization to form the PCHO-PLA copolymer (Table S3, entries 3ab).